

UNIVERSITY OF GAZİANTEP
GRADUATE SCHOOL OF
NATURAL & APPLIED SCIENCES

CRYSTALLIZATION BEHAVIORS OF MILK FAT BY
SEASONS

M.Sc. THESIS

IN

FOOD ENGINEERING

BY

TUĞBA ELBİR

NOVEMBER 2012

Crystallization Behaviors of Milk Fat by Seasons

M.Sc. Thesis

in

Food Engineering

University of Gaziantep

Supervisor

Prof. Dr. Ahmet KAYA

Co-Supervisor

Assist. Prof. Dr. Oya ÖZKANLI

by

Tuğba ELBİR

November 2012

©2012 [Tugba ELBIR]

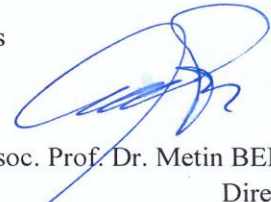
T.C.
UNIVERSITY OF GAZİANTEP
GRADUATE SCHOOL OF
NATURAL & APPLIED SCIENCES
FOOD ENGINEERING

Name of the thesis: Crystallization Behaviors of Milk Fat by Seasons

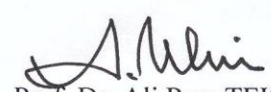
Name of the student: Tuğba ELBİR

Exam date: 19.11.2012


Approval of the Graduate School of Natural and Applied Sciences

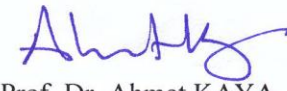

Assoc. Prof. Dr. Metin BEDİR
Director

I certify that this thesis satisfies all the requirements as a thesis for the degree of Master of Science.


Prof. Dr. Ali Rıza TEKİN
Head of Department

This is to certify that we have read this thesis and that in opinion it is fully adequate, in scope and quality, as a thesis for the degree of Master of Science.



Assist. Prof. Dr. Oya ÖZKANLI
Co-Supervisor


Prof. Dr. Ahmet KAYA
Supervisor

Examining Committee Members

Signature

Prof. Dr. Ahmet KAYA



Assoc. Prof. Dr. Metin BEDİR



Assist. Prof. Dr. K. Bülent BELİBAĞLI



I hereby declare that all information in this document has been obtained and presented in accordance with academic rules and ethical conduct. I also declare that, as required by these rules and conduct, I have fully cited and referenced all material and results that are not original to this work.



Tuğba ELBİR

ABSTRACT
CRYSTALLIZATION BEHAVIORS OF MILK FAT BY SEASONS

ELBIR, Tugba
M.Sc. in Food Engineering
Supervisor: Prof.Dr. Ahmet KAYA
Co-Supervisor: Assist.Prof.Dr. Oya OZKANLI
November 2012, 110 pages

In this study, thermal profiles (heating-cooling curves, isothermal crystallization), rheological properties (flow curves), crystal size and shape, crystal polymorphic type and solid fat content of milk fats produced at each season were investigated. Two different cooling rates (2 and 10°C/min) and different crystallization temperatures (5, 10, 14, 17 and 20°C) were studied by using differential scanning calorimetry (DSC), X-ray diffractometer (XRD), rheometer, polarized light microscope (PLM), nuclear magnetic resonance (NMR). Fatty acid composition and color properties were determined by using gas chromatography (GC) and spectrophotometer.

Fatty acid compositions and color values revealed that seasonal differences had significant effect on these parameters of milk fat. Milk fat had the highest value of stearic acid and oleic acid at summer. Higher values for saturated fatty acids were recorded in autumn and winter. It was found that cooling rate affected the crystallization and melting behavior, size and morphology of the milk fat crystals. In contrast to that, type and formation time of polymorphs were not affected by cooling rate and seasonal difference. It was shown that, at 0°C, highest solid fat content (SFC) belonged to autumn milk fat and all of the milk fat melted at about 35°C.

Keywords: Milk fat, isothermal crystallization, rheology, XRD, polymorphic type.

ÖZ

SÜT YAĞININ MEVSİMLERE GÖRE KRİSTALLENME DAVRANIŞLARI

ELBİR, Tuğba

Yüksek Lisans Tezi, Gıda Mühendisliği Bölümü

Tez Yöneticisi: Prof.Dr. Ahmet KAYA

Yardımcı Tez Yöneticisi: Yrd.Doç. Dr. Oya ÖZKANLI

Kasım 2012, 110 sayfa

Bu çalışmada, her mevsim üretilen süt yağlarının ısı profilleri (ısıtma-soğutma grafikleri, izotermal kristallenme), reolojik özellikleri (akış eğrileri), kristal boyutu ve şekli, kristalin polimorfik tipi ve süt yağının katı yağ içeriği araştırıldı. İki farklı soğutma hızı (2 ve 10°C/dk) ve farklı kristallenme sıcaklıkları (5,10,14,17 ve 20°C)'nin etkisi, diferansiyel taramalı kalorimetri (DSC), X-ışını difraktometresi (XRD), reometre, polarize ışık mikroskobu (PLM), nükleer manyetik rezonans cihazı (NMR) kullanılarak çalışıldı. Gaz kromatografisi (GC) ve renk tayin cihazı kullanılarak, yağ asidi bileşimi ve renk özellikleri belirlendi.

Yağ asidi bileşimleri ve renk değerleri, mevsimsel farklılıkların süt yağının bu parametreleri üzerinde anlamlı derecede etkili olduğunu açığa çıkarmıştır. Süt yağının, en yüksek stearik asit ve oleik asit değerlerine yaz mevsiminde sahip olduğu gözlenmiştir. Yüksek miktardaki doymuş yağ asidi değeri ise sonbahar ve kış mevsimlerinde kaydedilmiştir. Soğutma hızlarının, süt yağının kristallenme ve erime davranışlarını ve süt yağı kristallerinin boyut ve şeklini etkilediği bulunmuştur. Bunun aksine, polimorfik tipler ve bunların oluşma zamanları soğutma hızından ve mevsimsel farklılıklardan etkilenmemiştir. 0°C'de en yüksek katı yağ içeriğinin sonbahara ait olduğu ve bütün süt yağlarının yaklaşık 35°C'de eridiği görülmüştür.

Anahtar Kelimeler: Süt yağı, izotermal kristallenme, reoloji, XRD, polimorfik tip.

To my family

ACKNOWLEDGEMENT

I would like to express my deepest sense of gratitude to my supervisor , Professor Dr. Ahmet KAYA for his continuous support ,patience guidance and encouragement throughout my thesis study. I have been extremely lucky to have a supervisor who cared so much about my work, and who responded to my questions and queries so promptly.

I am also very grateful to my co-supervisor Assist. Prof. Dr. Oya ÖZKANLI, Instructor Gülten ŞEKEROĞLU and Research Assist. Dilek BÜYÜKBEŞE for their supports, interests and valuable hints.

I share the credit of my work with my dear fiance Erhan HORUZ. I am grateful to him for his constant support, encouragement and patience.

I wish to thank my friends Tuğba İNANÇ, Hülya ÖZDEMİR and Tuba ÖZKARA for helping me get through the difficult times, and for all the emotional support, continuous help and friendship.

Finally, and most importantly, my special thanks go to my parents and sister for their love and continuous support- both spiritually and materially.

CONTENTS

	Page
ABSTRACT.....	v
ÖZ.....	vi
ACKNOWLEDGEMENTS.....	viii
CONTENTS.....	ix
LIST OF FIGURES.....	xii
LIST OF TABLES.....	xix
NOMENCLATURE.....	xx
CHAPTER I: INTRODUCTION.....	1
1.1. Definition and Composition of Milk.....	1
1.1.1. Water.....	1
1.1.2. Fat.....	1
1.1.3. Protein.....	2
1.1.4. Carbohydrates.....	2
1.1.5. Minerals.....	2
1.2. Chemical Properties of Milk Fat.....	2
1.3. Physical Properties of Milk Fat.....	5
1.3.1. Fractionation.....	5
1.3.2. Polymorphism.....	7
1.3.3. Crystallization.....	10
1.3.3.1. Milk Fat Nucleation.....	11
1.3.3.2. Crystal Growth.....	11
1.3.3.3. Crystallization Kinetics of Fats.....	12
1.3.3.4. Parameters Affecting Crystallization.....	13
1.3.4. Solid Fat Content (SFC).....	14
1.3.5. Rheological and Textural Properties of Milk Fat.....	14

1.3.5.1. The Factors Affecting Visco-elastic Properties of Milk Fat.....	14
1.3.5.2. Chemical Composition.....	15
1.3.5.3. Process Conditions.....	15
1.3.5.4. Solid Fat Content.....	15
1.3.5.5. Microstructure- Fat Crystal Network.....	15
CHAPTER II: LITERATURE REVIEW.....	16
2.1. Summaries of the Recent Studies.....	16
2.1.1. X-Ray Diffractometer (XRD).....	16
2.1.2. Differential Scanning Calorimeter (DSC).....	18
2.1.3. Pulsed Nuclear Magnetic Resonance (pNMR).....	20
2.1.4. Polarized Light Microscope (PLM).....	21
2.1.5. Rheometer.....	21
2.2. Aim of the Study.....	22
CHAPTER III: MATERIALS & METHODS.....	23
3.1. Materials.....	23
3.1.1. Samples.....	23
3.1.2. Chemicals.....	23
3.2. Methods.....	23
3.2.1. Fatty Acis Composition.....	23
3.2.2. Color Determination.....	24
3.2.3. Thermal Profile Analysis.....	24
3.2.4. XRD Experiments.....	25
3.2.5. Rheological Measurements.....	25
3.2.6. Solid Fat Content Determination (SFC).....	25
3.2.7. Microstructure Analysis.....	26
3.2.8. Statistical Analysis of Results.....	26
CHAPTER IV: RESULTS & DISCUSSIONS.....	27
4.1. Fatty Acid Composition.....	27
4.2. Color Determination.....	29
4.3. Thermal Profile Analysis.....	31

4.3.1. Heating-Cooling Curve.....	31
4.3.2. Isothermal Crystallization.....	36
4.4. Rheological Properties.....	40
4.4.1. Heating-Cooling Curves.....	40
4.4.2. Isothermal Crystallization.....	44
4.4.3. Flow Curve.....	48
4.5. XRD Measurements.....	51
4.5.1. Isothermal Crystallization.....	51
4.6. Solid Fat Content Determination.....	56
4.7. Polarized Light Microscopy.....	58
CHAPTER V: CONCLUSION.....	60
REFERENCES.....	61
APPENDIX A.....	68
APPENDIX B.....	108

LIST OF FIGURES

	Page
Figure 1.1. Crystal structures of fats.....	8
Figure 1.2. Lateral packing types.....	9
Figure 1.3. Longitudinal arrangement of triglyceride.....	9
Figure 4.1. Seasonal changes in SFA/UFA of milk fat.....	28
Figure 4.2. Seasonal changes in yellowness index of milk fats.....	30
Figure 4.3. Seasonal changes in b* values of milk fats.....	30
Figure 4.4. Thermal profile of autumn milk fat at 2°C/min cooling and heating rate..	31
Figure 4.5. DSC cooling curves of milk fats at 2°C/min rate.....	32
Figure 4.6. DSC cooling curves of milk fats at 10°C/min rate.....	33
Figure 4.7. DSC heating curves of milk fats at 2°C/min rate.....	34
Figure 4.8. DSC heating curves of milk fats at 10°C/min rate.....	35
Figure 4.9. Isothermal crystallization of autumn milk fat at 17°C.....	37
Figure 4.10. Isothermal crystallization of milk fats at 10°C.....	37
Figure 4.11. Isothermal crystallization of milk fats at 14°C.....	38
Figure 4.12. Isothermal crystallization of milk fats at 17°C.....	38
Figure 4.13. Isothermal crystallization of milk fats at 20°C.....	39
Figure 4.14. Viscosity change of spring milk fat at different shear rates and 2°C/min cooling-heating rate.....	40
Figure 4.15. Viscosity change of spring milk fat at different shear rates and 10°C/min cooling-heating rate.....	41
Figure 4.16. Viscosity change of summer milk fat at different shear rates and 2°C/min cooling-heating rate.....	41
Figure 4.17. Viscosity change of summer milk fat different shear rates and 10°C/min cooling-heating rate.....	42
Figure 4.18. Viscosity change of autumn milk fat at different shear rates and 2°C/min cooling-heating rate.....	42
Figure 4.19. Viscosity change of autumn milk fat at different shear rates and 10°C/min cooling-heating rate.....	43

Figure 4.20. Viscosity change of winter milk fat at different shear rates and 2°C/min cooling-heating rate.....	43
Figure 4.21. Viscosity change of winter milk fat at different shear rates and 10°C/min cooling-heating rate.....	44
Figure 4.22. Viscosity changes of milk fat with time at isothermal crystallization at shear rate with 25 1/s and 14°C after cooling from 70°C with 2°C/min cooling rate.....	45
Figure 4.23. Viscosity changes of milk fat with time at isothermal crystallization at shear rate with 50 1/s and 14°C after cooling from 70°C with 2°C/min cooling rate.....	45
Figure 4.24. Viscosity changes of milk fat with time at isothermal crystallization at shear rate with 100 1/s and 14°C after cooling from 70°C with 2°C/min cooling rate.....	46
Figure 4.25. Viscosity changes of milk fat with time at isothermal crystallization at shear rate with 25 1/s and 14°C after cooling from 70°C with 10°C/min cooling rate.....	46
Figure 4.26. Viscosity changes of milk fat with time at isothermal crystallization at shear rate with 50 1/s and 14°C after cooling from 70°C with 10°C/min cooling rate.....	47
Figure 4.27. Viscosity changes of milk fat with time at isothermal crystallization at shear rate with 100 1/s and 14°C after cooling from 70°C with 10°C/min cooling rate.....	47
Figure 4.28. Flow curve of spring milk fat.....	49
Figure 4.29. Flow curve of summer milk fat.....	49
Figure 4.30. Flow curve of autumn milk fat.....	50
Figure 4.31. Flow curve of winter milk fat.....	50
Figure 4.32. Wide angle X-ray diffraction pattern of the isothermal crystallization after fast cooling (10°C/min) of the autumn milk fat from 70 to 5°C.....	52
Figure 4.33. 3D plots of X-ray diffraction pattern of the isothermal crystallization after fast cooling (10°C/min) of the autumn milk fat from 70 to 5°C.....	53
Figure 4.34. Wide angle X-ray diffraction pattern of the isothermal crystallization after slow cooling (2°C/min) of the autumn milk fat from 70 to 5°C.....	53
Figure 4.35. 3D plots of X-ray diffraction pattern of the isothermal crystallization after slow cooling (2°C/min) of the autumn milk fat from 70 to 5°C.....	54
Figure 4.36. Wide angle X-ray diffraction pattern of the isothermal crystallization after fast cooling (10°C/min) of the autumn milk fat from 70 to 20°C....	55
Figure 4.37. 3D plots of X-ray diffraction pattern of the isothermal crystallization after fast cooling (10°C/min) of the autumn milk fat from 70 to 20°C....	55

Figure 4.38. Solid fat content profile of milk fat samples by NMR.....	56
Figure 4.39. SFC curves of milk fat sample heating at 2°C/min by DSC.....	57
Figure 4.40. SFC curves of milk fat sample heating at 10°C/min by DSC.....	57
Figure 4.41. Images of milk fat crystals at different temperatures and cooling rates..	59
Figure A.1. Melting profile of milk fat samples cooling at 2°C/min (A) winter milk fat, (B) summer milk fat, (C) spring milk fat.....	69
Figure A.2. Melting profile of milk fat samples cooling at 10°C/min (A) winter milk fat, (B) spring milk fat, (C) summer milk fat, (D) autumn milk fat.	70
Figure A.3. Wide angle X-ray diffraction pattern of the isothermal crystallization after slow cooling (2°C/min) of the autumn milk fat from 70 to 10°C...	71
Figure A.4. 3D plots of X-ray diffraction pattern of the isothermal crystallization after slow cooling (2°C/min) of the autumn milk fat from 70 to 10 °C...	71
Figure A.5. Wide angle X-ray diffraction pattern of the isothermal crystallization after slow cooling (2°C/min) of the autumn milk fat from 70 to 14°C...	72
Figure A.6. 3D plots of X-ray diffraction pattern of the isothermal crystallization after slow cooling (2°C/min) of the autumn milk fat from 70 to 14 °C...	72
Figure A.7. Wide angle X-ray diffraction pattern of the isothermal crystallization after slow cooling (2°C/min) of the autumn milk fat from 70 to 17°C...	73
Figure A.8. 3D plots of X-ray diffraction pattern of the isothermal crystallization after slow cooling (2°C/min) of the autumn milk fat from 70 to 17 °C...	73
Figure A.9. Wide angle X-ray diffraction pattern of the isothermal crystallization after slow cooling (2°C/min) of the autumn milk fat from 70 to 20°C...	74
Figure A.10. 3D plots of X-ray diffraction pattern of the isothermal crystallization after slow cooling (2°C/min) of the autumn milk fat from 70 to 20 °C...	74
Figure A.11. Wide angle X-ray diffraction pattern of the isothermal crystallization after fast cooling (10°C/min) of the autumn milk fat from 70 to 10°C..	75
Figure A.12. 3D plots of X-ray diffraction pattern of the isothermal crystallization after fast cooling (10°C/min) of the autumn milk fat from 70 to 10 °C	75
Figure A.13. Wide angle X-ray diffraction pattern of the isothermal crystallization after fast cooling (10°C/min) of the autumn milk fat from 70 to 14°C..	76
Figure A.14. 3D plots of X-ray diffraction pattern of the isothermal crystallization after fast cooling (10°C/min) of the autumn milk fat from 70 to 14 °C.	76
Figure A.15. Wide angle X-ray diffraction pattern of the isothermal crystallization after fast cooling (10°C/min) of the autumn milk fat from 70 to 17°C..	77
Figure A.16. 3D plots of X-ray diffraction pattern of the isothermal crystallization after fast cooling (10°C/min) of the autumn milk fat from 70 to 17 °C.	77
Figure A.17. Wide angle X-ray diffraction pattern of the isothermal crystallization after slow cooling (2°C/min) of the winter milk fat from 70 to 5°C.....	78

Figure A.18. 3D plots of X-ray diffraction pattern of the isothermal crystallization after slow cooling (2°C/min) of the winter milk fat from 70 to 5 °C....	78
Figure A.19. Wide angle X-ray diffraction pattern of the isothermal crystallization after slow cooling (2°C/min) of the winter milk fat from 70 to 10°C...	79
Figure A.20. 3D plots of X-ray diffraction pattern of the isothermal crystallization after slow cooling (2°C/min) of the winter milk fat from 70 to 10 °C...	79
Figure A.21. Wide angle X-ray diffraction pattern of the isothermal crystallization after slow cooling (2°C/min) of the winter milk fat from 70 to 14°C...	80
Figure A.22. 3D plots of X-ray diffraction pattern of the isothermal crystallization after slow cooling (2°C/min) of the winter milk fat from 70 to 14 °C...	80
Figure A.23. Wide angle X-ray diffraction pattern of the isothermal crystallization after slow cooling (2°C/min) of the winter milk fat from 70 to 17°C...	81
Figure A.24. 3D plots of X-ray diffraction pattern of the isothermal crystallization after slow cooling (2°C/min) of the winter milk fat from 70 to 17 °C...	81
Figure A.25. Wide angle X-ray diffraction pattern of the isothermal crystallization after slow cooling (2°C/min) of the winter milk fat from 70 to 20°C...	82
Figure A.26. 3D plots of X-ray diffraction pattern of the isothermal crystallization after slow cooling (2°C/min) of the winter milk fat from 70 to 20 °C...	82
Figure A.27. Wide angle X-ray diffraction pattern of the isothermal crystallization after fast cooling (10°C/min) of the winter milk fat from 70 to 5°C.....	83
Figure A.28. 3D plots of X-ray diffraction pattern of the isothermal crystallization after fast cooling (10°C/min) of the winter milk fat from 70 to 5°C.....	83
Figure A.29. Wide angle X-ray diffraction pattern of the isothermal crystallization after fast cooling (10°C/min) of the winter milk fat from 70 to 10°C...	84
Figure A.30. 3D plots of X-ray diffraction pattern of the isothermal crystallization after fast cooling (10°C/min) of the winter milk fat from 70 to 10°C...	84
Figure A.31. Wide angle X-ray diffraction pattern of the isothermal crystallization after fast cooling (10°C/min) of the winter milk fat from 70 to 14°C...	85
Figure A.32. 3D plots of X-ray diffraction pattern of the isothermal crystallization after fast cooling (10°C/min) of the winter milk fat from 70 to 14°C...	85
Figure A.33. Wide angle X-ray diffraction pattern of the isothermal crystallization after fast cooling (10°C/min) of the winter milk fat from 70 to 17°C...	86
Figure A.34. 3D plots of X-ray diffraction pattern of the isothermal crystallization after fast cooling (10°C/min) of the winter milk fat from 70 to 17°C...	86
Figure A.35. Wide angle X-ray diffraction pattern of the isothermal crystallization after fast cooling (10°C/min) of the winter milk fat from 70 to 20°C...	87
Figure A.36. 3D plots of X-ray diffraction pattern of the isothermal crystallization after fast cooling (10°C/min) of the winter milk fat from 70 to 20°C...	87

Figure A.37. Wide angle X-ray diffraction pattern of the isothermal crystallization after slow cooling (2°C/min) of the spring milk fat from 70 to 5°C.....	88
Figure A.38. 3D plots of X-ray diffraction pattern of the isothermal crystallization after slow cooling (2°C/min) of the spring milk fat from 70 to 5°C.....	88
Figure A.39. Wide angle X-ray diffraction pattern of the isothermal crystallization after slow cooling (2°C/min) of the spring milk fat from 70 to 10°C....	89
Figure A.40. 3D plots of X-ray diffraction pattern of the isothermal crystallization after slow cooling (2°C/min) of the spring milk fat from 70 to 10°C...	89
Figure A.41. Wide angle X-ray diffraction pattern of the isothermal crystallization after slow cooling (2°C/min) of the spring milk fat from 70 to 14°C...	90
Figure A.42. 3D plots of X-ray diffraction pattern of the isothermal crystallization after slow cooling (2°C/min) of the spring milk fat from 70 to 14°C...	90
Figure A.43. Wide angle X-ray diffraction pattern of the isothermal crystallization after slow cooling (2°C/min) of the spring milk fat from 70 to 17°C...	91
Figure A.44. 3D plots of X-ray diffraction pattern of the isothermal crystallization after slow cooling (2°C/min) of the spring milk fat from 70 to 17°C...	91
Figure A.45. Wide angle X-ray diffraction pattern of the isothermal crystallization after slow cooling (2°C/min) of the spring milk fat from 70 to 20°C...	92
Figure A.46. 3D plots of X-ray diffraction pattern of the isothermal crystallization after slow cooling (2°C/min) of the spring milk fat from 70 to 20°C...	92
Figure A.47. Wide angle X-ray diffraction pattern of the isothermal crystallization after fast cooling (10°C/min) of the spring milk fat from 70 to 5°C.....	93
Figure A.48. 3D plots of X-ray diffraction pattern of the isothermal crystallization after fast cooling (10°C/min) of the spring milk fat from 70 to 5°C.....	93
Figure A.49. Wide angle X-ray diffraction pattern of the isothermal crystallization after fast cooling (10°C/min) of the spring milk fat from 70 to 10°C...	94
Figure A.50. 3D plots of X-ray diffraction pattern of the isothermal crystallization after fast cooling (10°C/min) of the spring milk fat from 70 to 10°C...	94
Figure A.51. Wide angle X-ray diffraction pattern of the isothermal crystallization after fast cooling (10°C/min) of the spring milk fat from 70 to 14°C...	95
Figure A.52. 3D plots of X-ray diffraction pattern of the isothermal crystallization after fast cooling (10°C/min) of the spring milk fat from 70 to 14°C...	95
Figure A.53. Wide angle X-ray diffraction pattern of the isothermal crystallization after fast cooling (10°C/min) of the spring milk fat from 70 to 17°C...	96
Figure A.54. 3D plots of X-ray diffraction pattern of the isothermal crystallization after fast cooling (10°C/min) of the spring milk fat from 70 to 17°C...	96
Figure A.55. Wide angle X-ray diffraction pattern of the isothermal crystallization after fast cooling (10°C/min) of the spring milk fat from 70 to 20°C...	97

Figure A.56. 3D plots of X-ray diffraction pattern of the isothermal crystallization after fast cooling (10°C/min) of the spring milk fat from 70 to 20°C...	97
Figure A.57. Wide angle X-ray diffraction pattern of the isothermal crystallization after slow cooling (2°C/min) of the summer milk fat from 70 to 5°C...	98
Figure A.58. 3D plots of X-ray diffraction pattern of the isothermal crystallization after slow cooling (2°C/min) of the summer milk fat from 70 to 5°C...	98
Figure A.59. Wide angle X-ray diffraction pattern of the isothermal crystallization after slow cooling (2°C/min) of the summer milk fat from 70 to 10°C.	99
Figure A.60. 3D plots of X-ray diffraction pattern of the isothermal crystallization after slow cooling (2°C/min) of the summer milk fat from 70 to 10°C.	99
Figure A.61. Wide angle X-ray diffraction pattern of the isothermal crystallization after slow cooling (2°C/min) of the summer milk fat from 70 to 14°C.	100
Figure A.62. 3D plots of X-ray diffraction pattern of the isothermal crystallization after slow cooling (2°C/min) of the summer milk fat from 70 to 14°C.	100
Figure A.63. Wide angle X-ray diffraction pattern of the isothermal crystallization after slow cooling (2°C/min) of the summer milk fat from 70 to 17°C.	101
Figure A.64. 3D plots of X-ray diffraction pattern of the isothermal crystallization after slow cooling (2°C/min) of the summer milk fat from 70 to 17°C.	101
Figure A.65. Wide angle X-ray diffraction pattern of the isothermal crystallization after slow cooling (2°C/min) of the summer milk fat from 70 to 20°C.	102
Figure A.66. 3D plots of X-ray diffraction pattern of the isothermal crystallization after slow cooling (2°C/min) of the summer milk fat from 70 to 20°C.	102
Figure A.67. Wide angle X-ray diffraction pattern of the isothermal crystallization after fast cooling (10°C/min) of the summer milk fat from 70 to 5°C...	103
Figure A.68. 3D plots of X-ray diffraction pattern of the isothermal crystallization after fast cooling (10°C/min) of the summer milk fat from 70 to 5°C...	103
Figure A.69. Wide angle X-ray diffraction pattern of the isothermal crystallization after fast cooling (10°C/min) of the summer milk fat from 70 to 10°C.	104
Figure A.70. 3D plots of X-ray diffraction pattern of the isothermal crystallization after fast cooling (10°C/min) of the summer milk fat from 70 to 10°C.	104
Figure A.71. Wide angle X-ray diffraction pattern of the isothermal crystallization after fast cooling (10°C/min) of the summer milk fat from 70 to 14°C.	105
Figure A.72. 3D plots of X-ray diffraction pattern of the isothermal crystallization after fast cooling (10°C/min) of the summer milk fat from 70 to 14°C.	105
Figure A.73. Wide angle X-ray diffraction pattern of the isothermal crystallization after fast cooling (10°C/min) of the summer milk fat from 70 to 17°C.	106
Figure A.74. 3D plots of X-ray diffraction pattern of the isothermal crystallization after fast cooling (10°C/min) of the summer milk fat from 70 to 17°C.	106

- Figure A.75. Wide angle X-ray diffraction pattern of the isothermal crystallization after fast cooling ($10^{\circ}\text{C}/\text{min}$) of the summer milk fat from 70 to 20°C . **107**
- Figure A.76. 3D plots of X-ray diffraction pattern of the isothermal crystallization after fast cooling ($10^{\circ}\text{C}/\text{min}$) of the summer milk fat from 70 to 20°C . **107**

LIST OF TABLES

	Page
Table 1.1. Fatty acid composition of milk fat.....	3
Table 4.1. Fatty acid composition of milk fats.....	28
Table 4.2. Color properties of milk fat.....	29
Table 4.3. DSC crystallization onset (OT) and peak (PT) temperatures, enthalpy and area of milk fats.....	34
Table 4.4. DSC end (ET), peak (PT) temperatures, clear point (CP), enthalpy and area of milk fats.....	36
Table 4.5. DSC isothermal crystallization parameters of milk fats.....	39
Table 4.6. Viscosity and activation energy values of milk fats.....	51
Table B.1. ANOVA results of myristic acid content of milk fat by seasons.....	109
Table B.2. ANOVA results of palmitic acid content of milk fat by seasons.....	109
Table B.3. ANOVA results of stearic acid content of milk fat by seasons.....	109
Table B.4. ANOVA results of oleic acid content of milk fat by seasons.....	109
Table B.5. ANOVA results of L* value of milk fats by seasons.....	110
Table B.6. ANOVA results of a* value of milk fats by seasons.....	110
Table B.7. ANOVA results of b* value of milk fats by seasons	110
Table B.8. ANOVA results of yellowness index of milk fats by seasons.....	110
Table B.9. ANOVA results of activation energies of milk fats by seasons.....	110

NOMENCLATURE

a^*	Redness-greenness value
α	Alpha
Å	Angstrom
AMF	Anhydrous milk fat
ANOVA	Analysis of variance
AOCS	American oil chemists` society
b^*	Yellowness-blueness value
β	Beta
β'	Beta prime
CP	Clear point
DAG	Diacylglycerol
ΔH	Enthalpy
DSC	Differential scanning calorimeter
DTA	Differential thermal analysis
E_a	Activation energy
ET	End temperature
FA	Fatty acid
FID	Flame ionization detector
γ	Gamma
GC	Gas chromatography
HMF	High melting fraction
ISO	International organization for standardization
L^*	Lightness-darkness value
LMF	Low melting fraction
MAG	Monoacylglycerol

MMF	Middle melting fraction
NMR	Nuclear magnetic resonance
OT	Onset temperature
PLM	Polarized light microscope
pNMR	Pulsed nuclear magnetic resonance
PT	Peak temperature
r^2	Correlation coefficient
SFA	Saturated fatty acid
SFC	Solid fat content
τ	Shear stress
TAG	Triacylglycerol
TCU	Temperature control unit
Θ	Theta
3L	Triple chain
UFA	Unsaturated fatty acid
X	Fraction of crystals transformed
XRD	X-Ray diffraction
YI	Yellowness index

CHAPTER I

INTRODUCTION

1.1. Definition and Composition of Milk

Milk is a fluid secreted by the female of all mamalian species, of which there are more than 4000 for the primary function of meeting the complete nutritional requirements of the neonate of the species (Fox and McSweeney, 1998). According to physical chemistry, milk is a nontransparent, whitish nonhomogeneous liquid where several components are kept in multidispersed state of emulsion, colloidal suspension, or solution.

On the authority of Food and Drug Administration of the US, milk indicates cows' milk. Milk from different animals must be identified to imply the animals. For example, milk from goats must be named goats' milk (Hui, 2007).

The main componenet of milk is water, but depend on animals, milk has different amount of lipids, proteins and carbohydrates which are produced within the mammal gland. Lesser amounts of minerals and different fat-soluble and water-soluble compounds reproduced from blood plasma, specific blood proteins and intermediates of mammal (Varnam and Sutherland, 2001).

1.1.1. Water

Water is a suitable component where different ingredients of milk (total solids) are dissolved or suspended. Water portion of milk changes from 85.4 to 87.7 % according to various species of cows. A little amount of the water in milk is hydrated to the lactose and salts and certain amounts are connected with the proteins.

1.1.2 Fat

The bulk of the fat is seen like little globules in the milk, its average nearly 2 to 5 microns in size. The form is an example of oil-in-water type emulsion. The fat globules surfaces are covered with an adsorbed layer of substance generally called as

the fat globule membrane which has phospholipids and proteins in the form of a complicated and fixed the fat emulsion (Sri and Vishweshwar, 2005). Milk fat is generally regarded as being of complex composition. Triacylglycerols are dominant and constitute 98 % of milk fat, together with little quantities of di- and monoacylglycerols and free fatty acids. Measurable quantities of phospholipids, cholesterol and cholesterol esters and cerebrosides are also present (Varnam and Sutherland, 2001).

1.1.3. Protein

Milk proteins are classified into two major types, casein and whey protein, both of which are heterogeneous. Milk contains about 3.3 % total protein, of which about 2.5 % is casein and 0.6 % is whey protein. The remaining 0.2 % comprises a number of nitrogenous compounds referred to as the non-protein nitrogen content (Ranken, 1988).

1.1.4. Carbohydrates

Lactose which is milk sugar exists only in milk. Lactose exists in solution in the milk serum. During crystallization, lactose becomes harsh sandy crystals. Its sweetness is less 6 times than sucrose. It is liable for the failure called as grittiness in ice-cream or condensed milk. Lactic acid and different organic acids are formed by fermentation of lactose by bacteria. It is significant both in fermented milk products and in the deformation of milk and milk products by souring (Sri and Vishweshwar, 2005).

1.1.5. Minerals

The mineral substance or salts of milk despite exist in little amounts; exert significant effect on the physicochemical attributes and nutritive value of milk. The main salt ingredients i.e. those exist in significant amounts, contains potassium, sodium, magnesium, calcium, phosphate, citrate, chloride, sulphate and bicarbonate (Sri and Vishweshwar, 2005).

1.2. Chemical Properties of Milk Fat

Natural fats are mainly composed of triacylglycerols (TAG), which determine their physical and thermal properties. Milk fat is one of the most complex fats found in nature (Lopez et al., 2001). Milk fat is consisted of 98 % TAG, which are triesters of

fatty acids and glycerol. The remaining part composed of minor ingredients mainly polar lipids mostly di- and mono-acylglycerols, cholesterol, phospholipids and traces of free fatty acids (Lopez et al., 2006; Mazzanti et al., 2009). Above 400 fatty acids and 200 TAG have been recognized with a large variety of chain lengths, number of unsaturation, branching and position on the glycerol (Lopez et al., 2006; Lopez et al., 2007). Table 1.1 shows fatty acid composition of milk fat.

Table 1.1. Fatty acid composition of milk fat (Creamer and MacGibbon, 1996).

	Common Name	Composition		
		Typical (% w/w)	mol %	Range (% w/w)
C4:0	Butyric	3.9	10.1	3.1-4.4
C6:0	Caproic	2.5	4.9	1.8-2.7
C8:0	Caprylic	1.5	2.4	1.0-1.7
C10:0	Capric	3.2	4.3	2.2-3.8
C12:0	Lauric	3.6	4.1	2.6-4.2
C14:0	Myristic	11.1	11.1	9.1-11.9
C14:1	Myristoleic	0.8	0.8	0.5-1.1
C15:0	-	1.2	1.1	0.9-1.4
C16:0	Palmitic	27.9	24.9	23.6-31.4
C16:1	Palmitoleic	1.5	1.4	1.4-2.0
C18:0	Stearic	12.2	9.8	10.4-14.6
C18:1 <i>cis</i>	Oleic	17.2	13.9	14.9-22.0
C18:1 <i>trans</i>		3.9	3.2	
C18:2	Linoleic	1.4	1.1	1.2-1.7
C18:2 <i>conj</i>	Conjugated Linoleic acid	1.1	0.9	0.8-1.5
C18:3	α Linoleic	1.0	0.8	0.9-1.2
	Minor acids	6.0	5.1	4.8-7.5

A greater part of these acids consist a very small amounts (>0.01 %). However, there are nearly 15 fatty acids that are found at or above 1.0 % concentration (Fox and McSweeney, 2006). Percentages for these fatty acids are given in table. Milk fat is constituted by triglycerides that compose short (C4-C10), medium (C12-C16) and long (C18-C20) chain fatty acids. The long chain fatty acids are came from fatty acids of the blood plasma, the short chain fatty acids are biosynthesized in the

mammal gland and the medium chain are biosynthesized both ways (Alonso et al., 2004).

Milk fat contains significant amounts of saturated fatty acids which are molecules with unbranched hydrocarbon chains, they change in length from 4 to 18 carbon atoms. The most important saturated fatty acid from a quantitative viewpoint is palmitic acid (16:0), which exist about 25 to 30 % of the total, while two other fatty acids, 14:0 and 18:0 have values from 10 to 13 %. Oleic acid (cis 9-18:1) is the primary cis-monounsaturated fatty acid, exist around 15–21% of the total. Cis-polyenoic acids exist at dilute concentrations in milk fat, because of the biohydrogenation reactions that occur in the forestomach. These acids are consisted approximately just linoleic acid (cis 9, cis 12-18:2), nearly 1.2 to 1.7 % and α -linolenic acid (cis 9, cis 12, cis 15-18:3), nearly 0.9 to 1.2%. These two fatty acids are essential fatty acids and which cannot be produced by the body and must be obtained by the diet (Fox and McSweeney, 2006).

Vaccenic acid (trans 11-18:1) is the primary significant trans isomer with values ranging from nearly 30 to 60 % of the total trans-18:1. The concentration of trans-18:1 types substantially from nearly 2.0 to 6.0 %. The higher values of vaccenic acid for milk fat are observed in milk fat from cows fed on summer pasture, whereas the lower values are related to the feed concentration and ensilage to cows in the winter (Fox and McSweeney, 2006).

Fatty acids are also classified as volatile and non-volatile. Butyric, caproic, caprylic, capric, lauric and small quantities of others are volatile. Non-volatiles are myristic, palmitic, oleic, stearic and small quantities of the others. Volatile acids are responsible for the characteristic flavor of butter and cream. Butyric acid is the most important volatile acid. Butyric acid gives to butter its characteristic taste and is largely responsible for the rancid flavor which sometimes occurs in dairy products (Ozbayram, 2000).

The fatty acid content of milk fat is not stable. A lot of factors affect the fatty acid composition. Factors may be of animal origin such that breed of cow, stage of lactation, mastitis and ruminal fermentation, or they may related to feed, i.e. type

(silage or grass) , quality and quantity of feed, related to fibre and energy intake, season of production and production region (Ozbayram, 2000).

1.3. Physical Properties of Milk Fat

1.3.1. Fractionation

Milk fat consists of a lot of triglycerides which vary due to differences between the fatty acid residues and triglycerides determine the physical properties of milk fat (Ozbayram, 2000; Van Aken et al., 1999). These variations affect melting characteristic and cause broad melting range and span from -40 to 40°C (Breitschuh and Windhab, 1998; Van Aken et al., 1999). They also are resulting in broad crystallization. Because of these varieties milk fat has some disadvantages. Using milk fat as ingredients in food and nonfood product is restricted in those thermal and physical attributes of milk fat. Such as, addition of milk fat develops softening in chocolate and causes poor spreadability of butter. And milk fat can not be used in pastry production because hardness and plasticity of milk fat is not proper for pastries (Lopez and Ollivon, 2009).

The benefit range of milk fat can be extended by modification of milk fat (Van Aken et al., 1999). Alteration of milk fat enhances its nutritional and functional properties (Fatouh et al., 2003). There are many modification techniques that is dietary, chemical and physical (Van Aken et al., 1999). Dietary manipulation by means of feeding protected fats to dairy animals can produce milk fat with a high content of polyunsaturated fatty acids. It is not popular because of high cost of the supplement. Hydrogenation or enzymatic interesterification is methods using in chemical modification (Fatouh et al., 2003). Chemical modification is not favourable because chemical treatment undesirable process for consumer. Physical alteration of milk fat is categorized into two parts according to alteration of chemical composition.

(i) Fractionation methods and mixing with vegetable oils that change the chemical content

(ii) Texturisation and cream tempering treatments that do not alter the chemical composition (Lopez et al., 2006).

Supercritical fluid extraction is used for fractionated of milk fat, short-path distillation, solvent fractionation and dry fractionation (Fox and McSweeney, 2006).

Supercritical fluid extraction benefits from the solubility of constituents close to the critical point of CO₂ and change of solubility using small alterations in temperature and pressure. In this technique, milk fat is fractionated into three streams enriched in short-chain, medium-chain or long-chain triacylglycerols. A benefit of supercritical CO₂ fractionation is that six or more fractions are obtained in one single step.

Crystallization technique is applied for fractionation of milk fat at different melting points with using an organic solvent. Acetone, ethanol or other solvents also hexane, pentane, ethylacetate and isopropanol is used as solvent (Fox and McSweeney, 2006). However this method is more efficient in the separation, it is not preferred in food applications because removing procedure of solvent is expensive. Also some flavor and toxicological problems may be appeared in solvent residue and fractions may be lost flavor compounds during deodorization (Fatouh et al., 2003).

In short-path distillation method, substances are volatilized into a vacuum and milk fat can be separated into fractions with individual chemical and physical properties. Short-path distillation is nonpopular method because of high cost (Fox and McSweeney, 2006; Fatouh et al., 2003).

Popular technique for fractionation of milk fat is melt crystallization or simply dry fractionation. The aim of dry fractionation is the separation of triglycerides on the basis on their melting points. Some advantages of dry fractionation are; there is no organic solvents or process auxiliary, reasonable processing cost, a comparatively basic equipment and protection of flavour of milk fat. Crystallization and separation are two basic parts for dry fractionation (Lopez et al., 2006). In crystallization step, milk fat is melted, cooled by controlled and molten milk fat is crystallized during cooling or at desired temperature. Then the crystals are separated from the liquid phase in separation step (Fox and McSweeney, 2006).

Milk fat is generally separated in three major fractions with dissimilar melting points. These are low melting fraction (LMF), middle melting fraction (MMF) and high melting fraction (HMF) (Van Aken et al., 1999). These main fractions crystallize individually and each of them has different melting broad. The melting profile of

milk fat obtained from differential scanning calorimeter (DSC) shows three main peaks due to three main fractions : LMF from -25 to +10 °C, MMF from +10 to +19°C with definite peak at 17°C and HMF from +19 to +34°C. (Deffense, 1993) HMF is composed of three long chain saturated fatty acid, MMF consists of two long chain saturated fatty acids and one short chain or long chain cis-unsaturated fatty acid and LMF have one long chain unsaturated fatty acid and two short or cis-unsaturated fatty acids (Timms, 1980; Vanhoutte, 2002).

Milk fat fraction and recombination of the fractions improve the thermal and physical properties of milk fat and allow the improvement of new products. The high melting fractions can be used as shortening in puff pastry, fat bloom inhibitors in chocolate, cocoa butter replacing in confectionary products, edible films and frozen desserts. Low melting fractions are used in biscuits, short breads, cold spreadable butter, pourable frying oils (Lopez et al., 2006).

1.3.2. Polymorphism

Natural fats include a wide range of TAG species with fatty acids of various chain length and degree of unsaturation. Milk fat is made up hundreds of different TAG species with no single species exhibit at greater than about 5%. Due to this wide range crystallization of milk fat is complex. In a crystal lattice, properties of TAG molecules appear in multiple forms. In other words, same molecule can crystallize into different crystalline forms. This event called as polymorphism (Shahidi, 2005).

Polymorphism is the aptitude of a molecule to take more than one crystalline form depending on its arrangement within the crystal lattice (Shahidi, 2005). Crystal polymorphism is supplementary explanation of the crystalline behaviour of milk fat (Heyen et al., 1999). The crystallization behavior of TAG, on condition that rate of crystallization, size of crystal, morphology and total crystallinity, temperature, cooling rate, fat purity, rate of crystallization and shear rate are affected by polymorphism.

Opportunity of variations in hydrocarbon chain packing gives rise to polymorph. The subcell concept can describe the mode of packing of the hydrocarbon chains. During fat crystallization, triacylglycerol molecules take in a particular formation and

packing arrangement for optimize intramolecular and intermolecular interactions and carry out an efficient packing. Unit cell is the smallest building of a crystal. Crystal lattice arises from the repetition of unit cell in its three axial directions. Unit cell contains smaller repeating unit that is subcell (McGauley, 2001). A crystal structure is shown in Figure 1.1 (Fox and McSweeney, 2006).

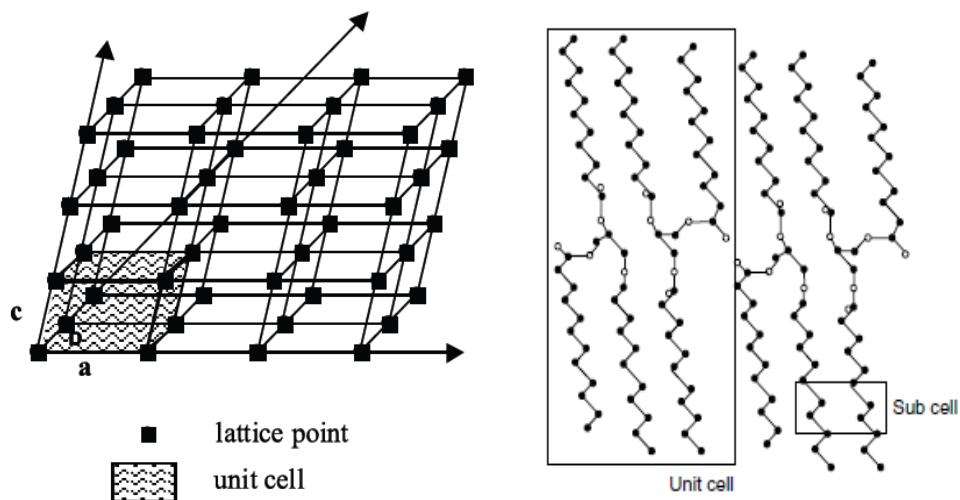


Figure 1.1. Crystal structures of fats

In fats and oils, polymorphism is related to different packing of the hydrocarbon chains and their angle of tilt (Shahidi, 2005). Three typical subcell structures are hexagonal (H), orthorhombic perpendicular (O) and triclinic paralel (T) (Figure 1.2). In the triclinic packing there is one ethylene group per subcell, and all zigzag planes are paralel. There is also one ethylene group per subcell in orthorombic packing but the difference between two packing is that the crystal planes are perpendicular to their adjacent planes. The hexagonal packing appears at just below melting point of the acyl chains.

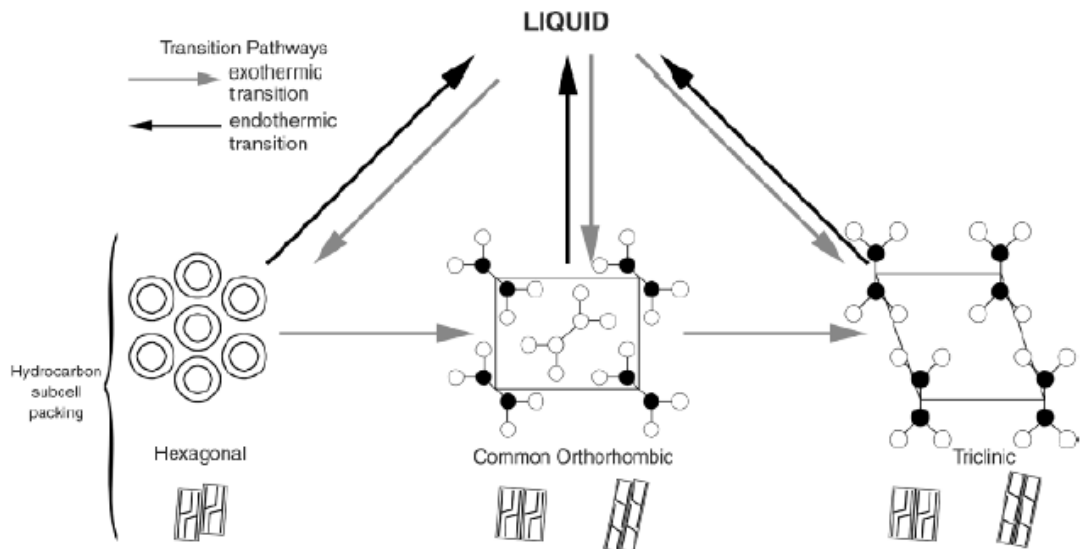


Figure 1.2. Lateral packing types

TAGs are oriented in chair a chair or tuning fork configuration in the crystalline lattice. X-ray spectra is used for finding the height of these chair structures as long spacings and the distance between the molecules in the chair structures as long spacings (Shahidi, 2005). The TAG can take either a double or triple chain-length structure as seen in Figure 1.3. There are three main polymorphic forms of fats that are α (alpha), β' (beta prime), β (beta). These polymorphs have hexagonal, orthorhombic and triclinic subcell structure respectively. Sometimes a form γ (gamma) is reported, but this is not a basic form (Timms, 1994; Vanhoutte, 2002).

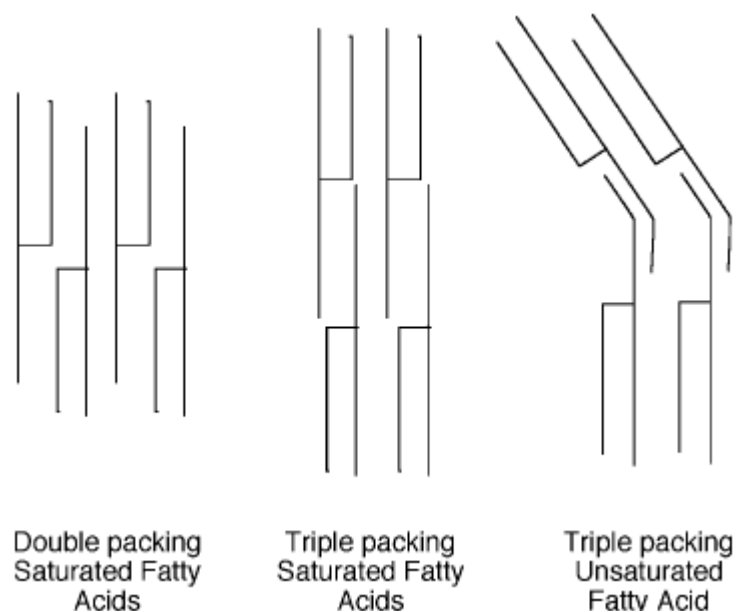


Figure 1.3. Longitudinal arrangement of triglyceride

Fats show monotropic polymorphism that is the less-stable polymorphs form first but then transform into more stable forms. The γ , α , β' and β represents increasing order of stability, density, melting point and enthalpy of fusion. α and β' polymorphs form primarily in milk fat because of the complexity of molecular composition (Garti and Sato, 2001). When temperature is raised slightly, the less stable α polymorph transforms to the more stable β' .

Some information about the lateral packing and the longitudinal stacking is required for describing the crystalline structure (Mazzanti et al., 2009). The longitudinal stacking and lateral packing are worked by X-ray diffraction at small and wide angles, respectively (Lopez and Ollivon, 2009).

1.3.3. Crystallization

Melting and crystallization of milk fat is complex phenomena because of its very wide range of different triglycerides (Vanhoutte, 2002; Walstra and Jenness, 1984). Crystallization is changing in phase from liquid to a solid state. This is an exothermic process. Edible fats are crystallized for many causes, such as (1) fractionation into definite groups of triglycerides with variable melting and physical properties, (2) to gain certain texture to food product such as chocolates, confectionary coatings, cream, butter and margarines (Foubert et al., 2008). Thermodynamic and kinetic factors effect the crystallization. Thermodynamic parameters are surface-melt interfacial free energy and crystallization temperature. Aggregation of substances, molecular adsorption, diffusion, solvation/desolvation and conformational rearrangements are kinetic factors (Vanhoutte, 2002). Milk fat crystallization is also affected by compositional and processing conditions. Milk fat composition affects of region, season and animal lineage. Processing conditions are churning type, cooling rate, scale of operation, agitation and storage condition (Shi et al., 2001; Herrera and Hartel, 2000).

Crystallization of milk fat affects many properties such as,

- rheological properties,
- the susceptibility of globules to churning
- globule resistance to disruption
- the consistency and mouth feel of high-fat products (Lopez et al., 2002).

Crystallization contains three steps that are nucleation, crystal growth and crystal rearrangements.

1.3.3.1. Milk Fat Nucleation

Nucleus is a very small crystal that can appear in a solution at definite temperature and concentration (Vanhoutte, 2002). Nucleation began when milk fat cooled at temperature below melting point. When temperature of fat decreased to under its melting point, the substances become supercooled. Supercooling is equal to supersaturation and is the thermodynamic driving force for crystallization to take place. At that point, molecules start to agglomerate into cluster. This cluster indicates the nucleus.

Three kinds of nucleation are mentioned for fats. They are primary homogenous, primary heterogenous and secondary nucleation. For homogenous nucleation, pure solution in the absence of foreign substances and interfaces are required. Milk fat nucleation generally is not homogeneous due to the presence of catalytic impurities such as water, dirt, monoacylglycerols, diacylglycerols, phospholipids and proteins. Heterogeneous nucleation is the widespread process in milk fat crystallization. Heterogeneous nucleation is accelerated by existence of foreign substances and interfaces. Secondary nucleation is the formation of new nuclei in the presence of existing crystals. In this process, crystal slurry is shaken in a container and crystals contact with other crystal, container wall and consequently secondary nuclei are formed. Secondary nucleation is much significant in milk fat crystallization (Fox and McSweeney, 2006; Shahidi, 2005).

1.3.3.2. Crystal Growth

Degree of supersaturation, the rate of molecular diffusion and the time necessary for TAG molecules to fit into the forming crystal lattice can determine the rate of crystal growth. Crystal growth occurs because of combination of nuclei and other TAG molecules from the liquid phase. A molecule gets the crystal surface after it diffused from the liquid phase, at this point there are two choices. These are depends on configuration of crystal lattice. It can attach into crystal lattice or diffuse back to the supersaturated system. Growth continues as long as there is a driving force for

crystallization. Finally crystal growth stops when the system reaches phase equilibrium or the whole system is crystallized.

Growth of TAG is generally is very slow. There may be several reasons for slow growth rate of TAG crystals:

1. During the incorporation of a TAG molecule into the crystal lattice, very large loss in conformational entropy is required so a long time is required for incorporation of TAG into the crystal lattice.
2. In a multicomponent fat, similar molecules compete with each other for unoccupied site in crystal lattice. At the same crystallization driving force, crystallization rate of multicomponent fat is slower than pure TAG. But formation of compound crystals which generally occur in α or β' forms and infrequently in the β form may increase the crystal growth in multicomponent fat (Fox and McSweeney, 200; Shahidi, 2005; Vanhoutte, 2002).

1.3.3.3. Crystallization Kinetics of Fats

Kinetics of fat crystallization is important for controlling operations in the food industry to produce the desired product features (Herrera and Hartel, 2000). The most general approach for description of isothermal phase transformation kinetics is the Avrami equation. Avrami kinetics is related with the overall crystallization process, involving nucleation and growth. The Avrami equation is given:

$$(1-X) = \exp (-kt^n)$$

Where X is fraction of crystal transformed at time t during crystallization, k is crystallization rate constant which depends primarily on crystallization temperature, and n is the Avrami exponent which is a constant correlating to the dimensionality of the transformation. The Avrami exponent (n) is a function of the number of dimensions and shows the details of nucleation and growth processes. The crystallization rate constant (k) is a combination of nucleation and growth rate constants and is a strong function of temperature. Arrhenius equation usually explains the temperature dependency (Shahidi, 2005).

1.3.3.4. Parameters Affecting Crystallization

Crystallization of milk fat can be influenced by several factors such as, source and nature of milk fat, minor components, rate of agitation, operation scale, temperature and cooling rate (Grall and Hartel, 1992).

Nature of Milk fat: The fatty acid composition of milk fat has wide range not like other fats. If induction times of milk fat and cocoa butter (limited fatty acid broad) are compared, induction time of milk fat for nucleation is faster. This may shows higher driving force or capable of TAG in milk fat come together into crystal structure more readily (Shahidi, 2005).

Minor Components: Triacylglycerols generally contain minor constituents such as diacylglycerol (DAG), monoacylglycerol (MAG), free fatty acids, phospholipids, These trace component can affect the crystallization (Shahidi, 2005). For example, addition of 1 % milk fat MAG to milk fat TAG enhances the spreadability of fat (Wright et al., 2000).

Rate of Agitation: The velocity of mixing probably stimulates the nucleation and crystal growth. In nucleation, there is a mechanical disturbance that provides energy to overcome the energy barrier for nucleation and because of this reason agitation rate may promotes the crystallization (Shahidi, 2005). Solid fraction yields increases with increasing agitation speed. Small crystal size and higher crystallization rate were also obtained by higher agitation speed (Herrera and Hartel, 2000).

Operation Scale: The size of operation may affect the crystallization rate. For instance, crystallization from an emulsion needs lower temperature than crystallization from bulk fat. Nucleation in an emulsion occurs at low temperature because of broad spreading area of the catalyzing nucleation sites (Shahidi, 2005).

Crystallization temperature: Formation of the polymorphs, crystals size, solid fat composition and the physical properties of fractions are affected by crystallization temperature (Herrera and Hartel, 2000). Nucleation rate increases and induction time for crystallization decreases with increasing in subcooling. When the subcooling is low, crystallization rate is slow and only the more stable polymorph form. At high

subcoolings, molecules incorporate into the crystal faster so TAG molecules attached to the surface imperfectly.

Cooling rate: Cooling rate is the important factor which affects the crystallization. At low temperature, rapid cooling generally influences the nucleation positively. During slow cooling, the temperature is higher for a longer time and the TAG have more opportunity to rearrange into a crystal lattice. Cooling rate also influence the rate of nucleation. Higher nucleation rate is achieved using rapid cooling rate at low temperature. Because rapid cooling at low temperature causes formation of various small crystals. Slow cooling leads to formation of large crystals (Shahidi, 2005).

1.3.4. Solid Fat Content (SFC)

Percentage of solid fat in a milk fat sample at a definite temperature defines the solid fat content of milk fat (Kaylegian and Lindsay, 1995). Solid fat content of milk fat is a function of temperature (Fox and McSweeney, 2006). On the other hand, solid fat content is a very important parameter to describe the texture of milk fat (Heyen et al., 1999). Macroscopic characteristics of milk fat crystal system are affected by SFC (Campos et al., 2002). Solid fat content is a significant property for estimating the fat functionality at various part of processing. Moreover, the solid fat content provides informations about hardness and spreadability (Fatouh et al., 2003).

1.3.5. Rheological and Textural Characteristics of Milk Fat

There are a lot of significant rheological characteristics of milk fat. Hardness, spreadability, thixotrophy and work softening are affected by milk fat rheology. Also milk fat has two considerable properties; hardness and spreadability because they are related with consumer acceptableness. Solid fat content of milk fat can change drastically between 10 and 20°C and at high temperatures milk fat shows less viscous flow. These features cause narrow temperature range for spreadability of milk fat. Work-softening indicate that when a shearing force is performed to milk fat, sample softens (Fox and McSweeney, 2006).

1.3.5.1. The Factors Affecting Visco-elastic Properties of Milk Fat

The macroscopic textural properties of milk fat are decided by following constituents:

- Chemical composition
- Processing conditions
- SFC
- Microstructure

1.3.5.2. Chemical Composition

The fatty acid composition is strongly related with for firmness of milk fat. Determination of firmness based not only on fatty acid remains, but also on triglyceride molecules and crystals.

1.3.5.3. Process Conditions

Final texture of fat can be affected by processing condition and texturation. Both cooling rate and the temperature to which milk fat is cooled, affect the physical properties of milk fat and milk fat product. Rapid cooling rate gives many small crystals but a few large crystals are obtained by slow cooling (Vanhoutte, 2002).

1.3.5.4. Solid Fat Content

Solid fat content also affects to macroscopic attributes of milk fat. For example, higher solid fat contents cause an increase in butter hardness (DeMan, 1963; Parkinson et al., 1970).

1.3.5.5. Microstructure-Fat Crystal Network

All levels of structure, especially microstructure, can influence the textural properties of a fat. The microstructure contains the spatial distribution of mass, particle size, interparticle separation distance, particle shape, and interparticle interaction forces (Narine and Marangoni, 1999; Marangoni, 2002).

CHAPTER II

LITERATURE REVIEW

2.1. Summaries of the Recent Studies

In this part, the summaries of studies in literature were categorized as instruments used.

2.1.1. X-Ray Diffractometer (XRD)

X-ray diffraction (XRD) method determines the forms of crystals which is a method where a collimated X-ray beam is operated at a one crystal of the substance under examination or, like is more common technique in the research of fat crystals, a milk fat including many randomly directed crystals. The second modification is called powder diffraction which is most frequently used. Both of them give the basic information about the structure of crystals.

A crystalline sample transmits the important amount of emitted X-radiation. A little amount is scattered in every directions by all pattern in the substance. The planes of patterns in a crystal behave basically as diffraction gratings. Diffraction of electromagnetic radiation by crystals can take place only when the wavelength of the radiation is of the equal order of magnitude as the regular repeat distance between patterns. The phenomenon is show the using of X-rays to decide crystal form (Fox and McSweeney, 2006). X-ray diffraction is a device which is commonly used to decide the crystal form of fats (Wiking et al., 2009).

In the literature, there are many works relevant with determination of polymorphic structure by X-ray diffractometry. Woodrow and deMan (1968) obtained the X-ray diffraction pattern with milk fat solidified at room temperature. The X-ray diffracton pattern showed short spacings of 4.64, 4.17 and 3.78 Å. The short spacing of 4.17 and 3.78 Å indicate the existence of the β' form and 4.64 Å spacing is related with the β form. Ten Grotenhuis et al. (1999) studied the various cooling rates changing

from 0.5 to 20°C/min with cooling procedure from 70 to -70°C/min. They obtained a typical XRD pattern at 5°C with cooling rate of 5°C/min. At the same cooling rate, two peaks were observed at -30 and -70°C with d-spacing 3.7 and 4.2 Å for the γ form. At cooling rate 1.67°C/min only α crystals were obtained. Wright et al. (2000) observed identical X-ray diffraction pattern of milk fat at 5 and 25°C. Short spacing at 3.8 Å was observed at both temperatures. Lopez et al. (2001) examined the polymorphic form of milk fat temperature range 50 to -15°C with slow cooling at 0.1°C/min cooling rate. At small angle four different lamellar structures were detected with double chain (2L) length of 41.5, 48.3 and 39.2 Å and a triple chain (3L) length of 62.2 Å. For temperature smaller than 13°C triacylglycerols crystallize in α form which is detected until -15°C. Wide angle X-ray patterns were obtained at 4.3 Å ($q= 1.46 \text{ \AA}^{-1}$) and 3.88 Å ($q=1.6 \text{ \AA}^{-1}$) which are related to β' form at about 23°C. At about 13°C, second diffraction line occurred at 4.22 Å ($q= 1.49 \text{ \AA}^{-1}$) corresponds to α form. And a weak line at 4.58 Å ($q= 1.37 \text{ \AA}^{-1}$) is obtained. They thought that this line might be related to the traces of β form.

Lopez et al. (2002) studied the crystallization and polymorphic evolutions of triacylglycerols of milk fat at 4°C. Sample was quenched from 60 to 4°C. At isothermal conditions at 4°C, two crystalline structures were initially formed with double chain length of 47 Å and triple chain length of 70.5 Å which corresponds to α form. For time longer than 15 minutes, short spacing displaced the formation of β' form coexistence with α form. At time longer than 100 hours, crystalline structures at 40.5 Å (2L) and 54.2 Å (3L) were recorded. In the studies of Lopez et al. (2005), crystallizations were controlled at cooling rates of 3 and 1°C/min from 60 to -10°C to determine the triacylglycerol organizations formed. At 2°C/min, triacylglycerols crystallize in 3 kinds lamellar forms with double-chain length of 46 and 38.5 Å and a triple-chain length of 72 Å stackings of a α type that are related to 2 peaks at 17.2 and 13.2°C.

In another studies of Lopez et al. (2006), crystallization attributes of milk fat was analyzed on cooling at 1°C/min at wide and small angles. Two 2L (47.3 and 41.6 Å) and one 3L (72.1 Å) lamellar structures with α form were formed at small angle. At wide angle single peak was observed at 4.16 Å ($q= 1.51 \text{ \AA}^{-1}$). Wiking et al. (2009) applied the following time-temperature program, isothermal at 65°C for 5 min,

cooling to 20°C by 10°C/min and holding at this temperature for 60 min. First peak with double-chain length appeared at 47.4 Å ($q= 0.021 \text{ \AA}^{-1}$) at isothermal temperature and disappeared after 35 min. This peak was related with α form. The second peak was observed at 41.5 Å ($q= 0.024 \text{ \AA}^{-1}$) which corresponded to double spacing and was related to β' form.

In studies of Fredrick et al. (2011), milk fat was heated to 65°C, holded at that temperature for 10 minutes, then cooled to 5°C by 25°C/min, holded at 5°C for 120 minutes and heated to 65°C by 5°C/min. X-ray patterns were obtained at small and wide angle. 3 individual peaks were observed. A small peak appeared at 46.5 Å (2L) ($q= 0.022 \text{ \AA}^{-1}$) at time 0 minute and disappeared during the first minutes of isothermal crystallization. The other two peaks was obtained at 71.4 Å ($q= 0.014 \text{ \AA}^{-1}$) and 35.7 Å ($q= 0.028 \text{ \AA}^{-1}$) at beginning of isothermal period. In wide angle X-ray diffraction pattern two sharp peaks were observed at 3.8 Å and 4.15 Å which were related with β' and α form respectively.

2.1.2. Differential Scanning Calorimeter (DSC)

Differential scanning calorimeter measures the thermal behaviour of substances. In differential scanning calorimeter, the difference between the heat flow of sample and reference material is measured as a function of temperature or time. In differential scanning calorimeter, the difference between the heat flow (J/s or W) to or from a test piece and a reference substance is tested depend on temperature or time while the test piece and the reference substance are operated together to a controlled temperature-time programme. Differential scanning calorimeter is thus a kind of DTA (Fox and McSweeney, 2006). DSC is the most common method to study crystallization of milk fat. This method provides the some information about the thermodynamic of the primary crystallization, but not about the evolution of structure of crystals (Wiking et al., 2009). The time temperature shedule used in these examination generally contains three steps: first of all the materials are heated and held at a high temperature for definite time to damage every homogenous crystal nuclei, secondly the materials are cooled at a certain rate to the isothermal crystallization temperature and eventually the materials are held at that temperature until crystallization is finish (Foubert et al., 2008).

From typical DSC melting curves, three overlapped endotherms are existed and their temperatures and enthalpies change according to the thermal treatment applied and the TAG content of milk fat. These three endotherms are associated with the presence of three fractions of milk fat (Timms, 1980; Lopez and Ollivon, 2009).

Ten Grotenhuis et al. (1999) observed that the figure of the DSC cooling curve of milk fat depended on the cooling rate. The temperature at which the milk fat started to crystallize decreased with increasing cooling rate. DSC curves of milk fat obtained during heating at a rate of 5°C/min after the milk fat had been cooled at various cooling rates depending from -0.2 to -20°C/min. Curves of milk fat cooled at rate of -1, -2.5, -5 and -10°C/min were similar and showed three distinctive endothermic peaks. First peak started at about 40°C and ended at 8°C. The temperature of second peak was between 8 and 20°C. Third peak started at 20°C and ended at clear point of 35°C.

Other investigation was carried out by Lopez et al. (2001) to obtain crystallization and melting curve. Crystallization curve was obtained at temperature from 60 to -15°C/min at 0.1°C/min. Samples were heated from -15 to 60°C at 2°C/min for melting behavior. Three exothermal peaks were observed with an initial crystallization temperature is 24.1°C.

In another studies of Lopez et al. (2005), various cooling rates (0.5, 1, 2, 3 and 5°C/min) were used for examination of crystallization behavior at temperatures from 60 to -8°C. Melting curves were followed from -8 to 60°C at 2°C/min. Results indicated that initial crystallization temperature decreased with increasing cooling rate and cooling rate affected the shape of the crystallization and melting curve. Results showed the three exotherms in contrast to general crystallization curve.

Wiking et al. (2009) studied the isothermal DSC experiment. Samples were cooled from 65°C to any crystallization temperature at rates of 0.1 and 10°C/min. DSC curves indicated that the slow cooling resulted in crystallization to start before the temperature was lowered to 20°C. Two step crystallization occurred at the rapid cooling. First crystallization occurred at 2.0 min and second one was at 18.5 min.

Smet et al. (2010) studied the isothermal crystallization of milk fat using DSC. Milk fat with increased unsaturated fatty acid content (UMF) and anhydrous milk fat (AMF) were compared. Samples were held at 65°C for 10 min, then cooled to the suitable crystallization temperature at 10°C/min and held at this temperature for definite time and finally heated to 65°C at 20°C/min. According to results, onset temperature of crystallization for UMF (13.9°C) was lower than for AMF (15.3°C).

2.1.3. Pulsed Nuclear Magnetic Resonance (pNMR)

Pulsed nuclear magnetic resonance is the most commonly technique used for SFC determination. The NMR method for SFC determination is based on the principal that nuclear spins align in a magnetic field. In a pNMR measurement, the realignment of the nuclear spins of ^1H atoms after a strong electromagnetic pulse is measured. Application of a short 90° radio frequency electromagnetic pulse provides excitation to the ^1H atoms, causing them to leave their equilibrium, aligned state. The pulse is then withdrawn leading to the relaxation of the ^1H atoms and a return to the aligned, equilibrium state. Differences in the time scale for the relaxation process of the solid and liquid protons are used to determine the SFC. Protons, in general, have less mobility in the solid phase than in the liquid phase, therefore leading to large differences in the relaxation times of the ^1H atoms (Shahidi, 2005).

NMR method was used for determination of solid fat content in most of studies. Fatouh et al. (2003) determined the solid fat content of milk fat and milk fat fractions. Samples were tempered at 100°C for 15 minutes and put in a water bath at 60°C for 15 minute and then 60 minutes at 0°C and eventually 35 minutes at every worked temperature between 0 and 55°C at 5°C intervals. They showed that solid fat content decreased with increasing temperature at all temperatures and solid fat content increased in the sequence order: LMF, MMF and HMF.

Campos et al. (2002) studied the effect of cooling rate on SFC. Samples heated to 80°C for 30 minutes and then immersed in water bath at different temperatures. They found that higher cooling rates and degrees of undercooling was concluded a higher SFC.

Wiking et al. (2009) heated samples to 65°C and hold at that temperature for 15 minutes and then cooled to 20°C using two different cooling rates: 10°C/min and 0.1°C/min. They found that the milk fat which was subjected to slow cooling had a 6.4 % SFC when the temperature reached 20°C and increased to 16.3 % at 80 minutes but the rapid cooling of milk fat resulted in 0.1 % SFC at the beginning of the incubation at 20°C, which increased to 15.7 % at 88 minutes.

2.1.4. Polarized Light Microscopy (PLM)

Polarized light microscopy is used to investigate crystal network properties of milk fat during nucleation and crystal growth, and over time as a result of the processing conditions and storage time (Shahidi, 2005). In many studies, size and shape of the milk fat crystals were defined by polarized light microscope. Wright et al., (2001); Campos et al., (2002) and Lopez et al., (2005) observed the milk fat crystals at different crystallization temperatures and different cooling rates. They reported that fast cooling shows a lot of little crystals and slow cooling yield wide spherulitic particle. Other investigation was carried out by Lopez & Ollivon (2009) to compare the crystal shape of milk fat and milk fat fractions. Crystals were obtained cooling at 1°C/min corresponded to spherulites for milk fat and the stearin fraction while the olein fraction coincide with needle-shape crystals.

2.1.5. Rheometer

Rheology is a macroscopic method which gives information about behavior of materials under given conditions (Oldörp, 2007). Rheology is used widely in researching and identifying the nature and microstructure of milk fat and fat-originated dairy products. The essential rheological property of a substance needs the experimental consideration of a basic relationship (a rheological equation of state) that mathematically concerned stress and strain, or stress and strain rate. The essential operational data must be observed with using rheometers which provide values of stress, and either strain or strain rate, which are relevanted just by the rheological property of the material (Fox and McSweeney, 2006). Melting or crystallization temperatures can also easily be determined with rheometers (Oldörp, 2007).

2.2. Aim of the Study

Milk fat is one of the main constituents of milk fat and determines the specific properties of butter and cream. It is also an important in many bakery and confectionary industry applications. The various applications require different properties of milk fat, which in turn requires improved functionality control. The functional properties of milk fat are strongly related to the amount and the type milk fat crystals at the temperature of application. The crystalline part of the fat determines the firmness of products in which fat is present as the continuous phase, such as butter and butter oil, and the stability of products containing an emulsion of milk fat, such as cream. So knowledge about crystallization behavior of milk fat is very important.

The aim of this work is to investigate the relationship between the kinetics of milk fat crystallization and the development of crystal size and rheological properties of milk fat. To achieve this, the temperature, solid fat content, crystal forms, heating-cooling curves and firmness was monitored on samples taken simultaneously from the crystallization setup. In addition, the structure of the fat crystals was visualized by microscopy.

CHAPTER III

MATERIALS & METHODS

3.1. Materials

3.1.1. Samples

Cow milk was obtained every season through a year from a local (Gaziantep) farm. Milk samples were pasteurized by heating at 65°C. Pasteurized milk was separated at 40°C. The cream was churned at low temperature and high rpm for produce butter. After churning step, water bath was used at 70 °C for melting of produced butter. The melted butter was regularly stirred and the oil part on the serum part was led to separate for 3 h. Then filtration was applied by using thick layer cheese cloth for clarification of oil part and put into amber glass bottles.

3.1.2. Chemicals

Fatty acid methyl esters and other chemicals used were supplied from Merck and Sigma Chemical Companies.

3.2. Methods

3.2.1. Fatty Acid Composition

The fatty acid composition of milk fat was determined after conversion of fatty acids into the corresponding methylesters. Transesterification of milk fats were prepared according to method 5509 of the ISO (2000). 100 µL milk fat samples were put into centrifuge tube then 0.5 mL KOH/CH₃OH solution at room temperature was added. This mixture was completed to 100 mL with heptane. Then it was mixed on vortex tube stirrer for 10 min. Finally, the mixture centrifuged at high rpm for 15 min. After centrifuge, sample was put into vial and analyzed by GC.

A 7890A gas chromatography system (Agilent Technologies, USA) equipped with a flame ionisation detector (FID), a split/spitless injector (operated with a split ratio of 1:50), and a capillary column HP-88 (88 % Cianopropylaryl 60 m × 0.250 mm

ID \times 0.20 μm) was used. Helium was used as the carrier gas. The injection temperature was 250°C. The oven temperature was kept at 120°C for 1 min, then programmed from 120°C to 175°C for 10 min at 10°C/min, from 175°C to 210°C for 5 min at 5°C/min, finally, 230°C for 5 min. FAs were identified by comparison of retention times to known standards (Anonymous, 2008). The results were expressed as g fatty acid/100 g total fatty acids (%). Fatty acid compositions were evaluated at different fractionation conditions in relation to the original AMF.

3.2.2. Color Determination

The color values of milk fats were measured by HunterLab Colorflex Model Spectrocolorimeter (HunterLab, Reston, VA, USA). Before the test, the instrument was standardized with standard black glass and white tile as specified by the manufacturer. The color values were expressed as L^* (whiteness or brightness/darkness), a^* (redness/greenness), b^* (yellowness/blueness) and YI (yellowness index) values according to the CIELAB system.

3.2.3. Thermal Profile Analysis

Crystallization and melting profiles were obtained with a DSC4000 model differential scanning calorimeter (DSC) (Perkin-Elmer, USA), equipped with an Intracooler-SP. The DSC was calibrated with an indium standard. Approximately 10 mg of samples were measured in aluminum pans and they were closed and put to calorimeter. An empty closed pan was taken for reference. AMF samples were analyzed at 70°C for 5 min to erase thermal history, cooled to -55°C at 10°C/min, held at that temperature for 5 min, and heated to 70°C at 10°C/min.

For isothermal crystallization 10 mg milk fat was analysed using following program: Firstly milk fats were held at 70°C for 5 min to delete thermal history, then cooled to 20, 17, 14 and 10°C at 10 and 2°C/min, samples were held at each crystallization temperature for 120 min. and finally heated to 70°C at 10 and 2°C/min. Thermograms of both experiments were analyzed to determine temperatures of various features on the DSC curves by the pyris data analysis software provided with the instrument.

3.2.4. XRD Experiments

XRD patterns were recorded with a PanAnalytical X'Pert Pro Diffractometer (Philips, Netherlands), equipped with a TCU 110 Anton Paar temperature control unit. Monochromated CuK α radiation with a wavelength of 1.5418 Å was used to observe diffraction patterns in the 2 Θ range 5.0 and 30.1° which corresponds to d-spacing 17.5 and 2.9 Å. Potassium iodide was used for calibration of the equipment. The melted substances were put into sample holder with dimensions 1x10x15 mm³. The sample handle was adjusted in a vacuum measuring room. The temperature of the sample handle was checked by at the same time cooling with water or liquid nitrogen and heating using Anton Paar TTK-450 air cooling. Isothermal crystallization was performed using XRD at wide angle. Samples were held at 70°C for 5 min, cooled to 20, 17, 14, 10 and 5°C at rates of 2 and 10°C/min. Samples were held at each crystallization temperature for 120 min.

3.2.5. Rheological Measurements

Isothermal crystallization, cooling-melting profiles and flow curves of AMF were carried out at 25, 50 and 100 1/s shear rates using a controlled stress/strain rheometer (Thermoscientific-MARSII model) equipped with a TCP/P peltier temperature controller unit and a thermostat. A cone and plate configuration was used (diameter=35 mm and angle=1°). For isothermal crystallization the following program was used : milk fats were held at 70°C for 2 min then cooled to 14°C at 2 and 10°C and held at this temperature for 120 min under three different shear rate; 25, 50 and 100 1/s.

Cooling-heating curves were obtained cooled from 70 to 13°C and then heated to 70°C at 2 and 10°C/min at shear rate of 25, 50 and 100 1/s. For flow curves, program contained 5 temperature; 70, 60, 50, 40 and 30°C respectively. Samples were held at each temperature for 5 min at 10 1/s then shear rates of samples were increased from 0 to 200 1/s. Flow curves were shown as shear rate vs shear stress.

3.2.6. Solid Fat Content Determination (SFC)

Minispec mq 20 model pulsed Nuclear Magnetic Resonance (Bruker, Germany) was used to determine the solid fat content (SFC) of AMF, according to AOCS method Cd 16-81 (AOCS, 1989). Molten fat at 80°C were held at 60°C for 30 min. Then

samples were transferred to water bath at 26.7°C and 0°C for 15 min for each temperature respectively. Finally samples were put water bath at crystallization temperature that was 35, 30, 25, 20, 15, 10, 5 and 0°C for 30 min. After that solid fat contents were measured.

3.2.7. Microstructure Analysis

The microstructures of crystallized sample were observed using Leica DM5200 P model polarized light microscopy (PLM) (Leica, Germany). One droplet of melted milk fat samples was placed on glass slide and glass cover slip was placed over the sample. The prepared slides were placed on microscope. The following time-temperature schedule, checked by a Linkam Scientific Instrument hot stage, was used. The samples were held at 50°C for 1 min, then milk fats were cooled 20, 17, 14, 10 and 5°C at cooling rate of 0.1, 2 and 10°C then held at these temperatures for 120 min. Images were examined by 10x objective and recorded every minutes during the experiment.

3.2.8. Statistical Analysis of Results

The results were compared by analysis of variance (ANOVA) to test for significant differences between milk fats produced in each season at 5% significance level using SPSS 16.0 program. Trends were considered significant when means of compared pairs differed at $p < 0.05$ level.

CHAPTER IV

RESULTS & DISCUSSIONS

4.1. Fatty Acid Composition

The fatty acid composition of milk fats produced at each season was defined in Table 4.1. According to the result, myristic, palmitic, stearic and oleic acid were the main fatty acids of milk fat samples. As shown in table, myristic acid was maximum value for autumn milk fat like as palmitic acid. Milk fat had highest values of stearic acid and oleic acid at summer. These fatty acids showed that there were significant differences among the seasons ($p < 0.05$) (Table B.1, B.2, B.3 and B.4). Higher values for saturated fatty acids were observed in autumn and winter, on the contrary spring and summer milk fat had higher values for unsaturated fatty acids with lesser magnitude. The same results were found by Alonso et al. (2004).

Also, ratio of saturated to unsaturated fatty acids and trend of this ratio according to the seasons were given Table 4.1 and Figure 4.1, respectively. Spring and summer milk fat had lowest ratio of saturated vs unsaturated because the content of saturated fatty acid is lowest in summer and spring when the cows feed with grass. On the other hand, higher ratio was observed at autumn and winter due to indoor feeding at winter and autumn (Månsson, 2008). These results are accordance in some studies such as Frelich et al., 2009.

Table 4.1. Fatty acid composition of milk fats (% w/w).

Fatty Acids		Spring	Summer	Autumn	Winter
Saturated					
C4:0	Butyric acid	2.4	2.1	2.3	2.7
C6:0	Caproic acid	1.7	1.4	1.7	2.0
C8:0	Caprylic acid	1.1	0.9	1.2	1.3
C10:0	Capric acid	2.5	2.1	2.7	2.7
C12:0	Lauric acid	3.1	2.8	3.5	3.3
C14:0	Myristic acid	9.7	8.8	12.3	10.9
C15:0	Pentadecanoic acid	0.9	1.0	1.1	1.0
C16:0	Palmitic acid	26.7	30.1	34.6	29.3
C17:0	Margaric acid	0.6	0.8	0.5	0.5
C18:0	Stearic acid	10.4	10.5	7.0	9.2
Total saturated (SFA)		59.1	60.5	66.9	62.9
Unsaturated					
C14:1	Myristoleic acid	1.2	0.8	2.1	1.6
C16:1	Palmitoleic acid	1.6	0.8	2.3	0.7
C17:1	Margaroleic acid	0.3	0	0.2	0.2
C18:1 trans	Oleic acid	1.9	0.6	0.5	1.4
C18:1 cis	Oleic acid	27.1	28.3	21.5	23.9
C18:2 cis	Linoleic acid	3.6	3.0	2.1	3.8
C20:0	Gadoleic acid	0.7	0.5	0.2	0.7
Total unsaturated (UFA)		36.4	34	28.9	32.3
SFA/UFA		1.62	1.78	2.31	1.95

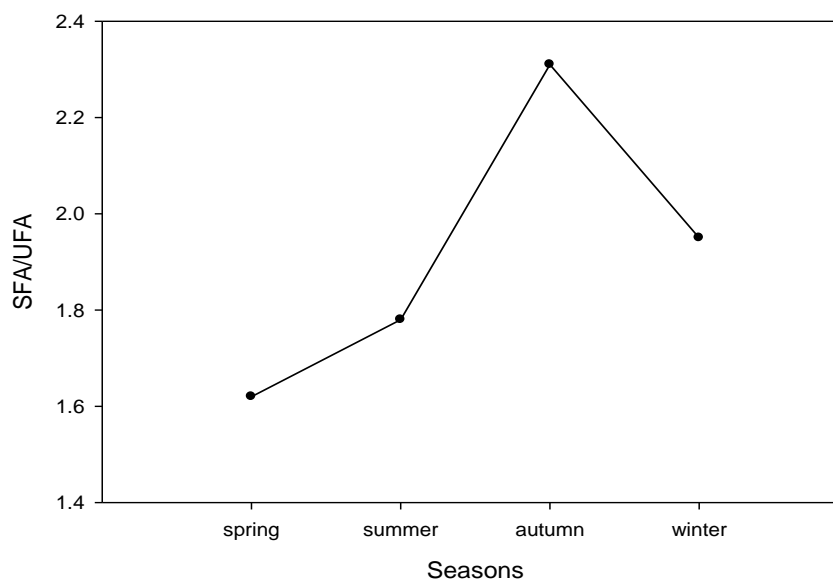


Figure 4.1. Seasonal changes in SFA/UFA of milk fat

4.2. Color Determination

The color of dairy product varies from white to yellow according to fat-soluble pigments especially carotenoids. Carotenoids are obtained from plant sources in diet; they are not synthesized by the animal. For that reason, feeding differences is responsible for the variation in color of the products (Bylund, 2003; Fox and McSweeney, 1998).

L*, a*, b* and YI values of milk fat samples were given in Table 4.2. L*, a*, b* and YI of milk fat samples were different significantly each other among seasons ($p < 0.05$) (Table B.5, B.6, B.7 and B.8). Most important parameter for color is yellowness index. As shown in table and graph, summer milk fat had highest yellowness index means that milk fat in summer had yellowest color among the seasons. In summer, cows fed on grass and produced more yellow-colored. In contrast that, lowest yellowness index belonged to winter due to indoor feeding (Fox and McSweeney, 1998). It was shown that b* value result showed parallelism with yellowness indexes. Positive b* value expresses the yellowness degree of sample. Summer milk fat had maximum b* value and winter milk fat had minimum b* value. L* value indicates the whiteness or darkness. In contrast to these result, highest value of L* was found at winter because of winter milk fat had light yellow color and so closed to white.

Table 4.2. Color properties of milk fats

Samples	L*	a*	b*	YI
Spring	67.0	-2.6	22.1	44.7
Summer	65.2	-1.7	37.1	69.5
Autumn	66.9	-2.7	14.7	30.4
Winter	68.4	-2.2	9.4	19.5

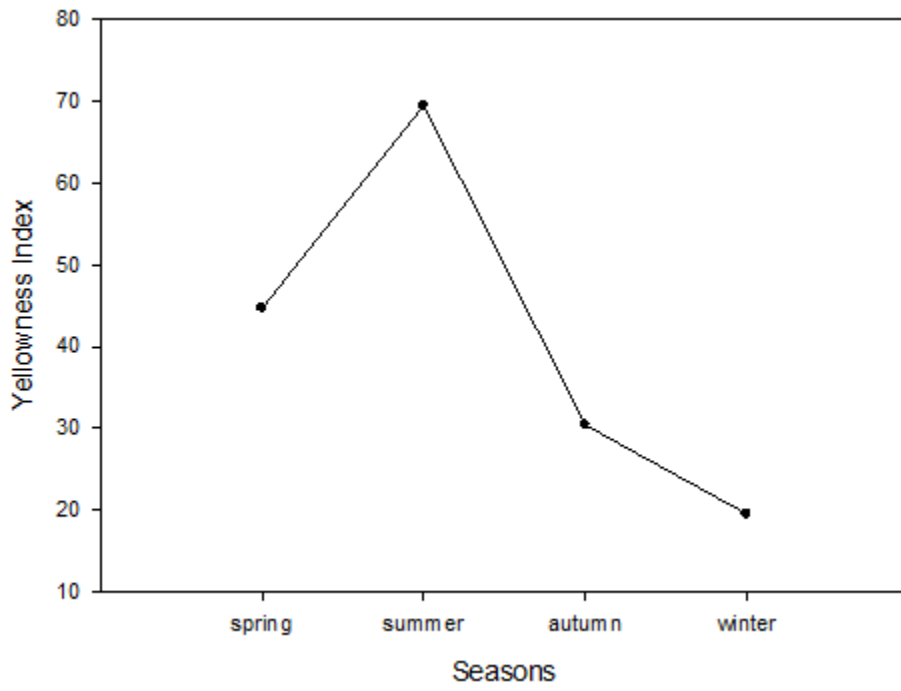


Figure 4.2. Seasonal changes in yellowness index of milk fats

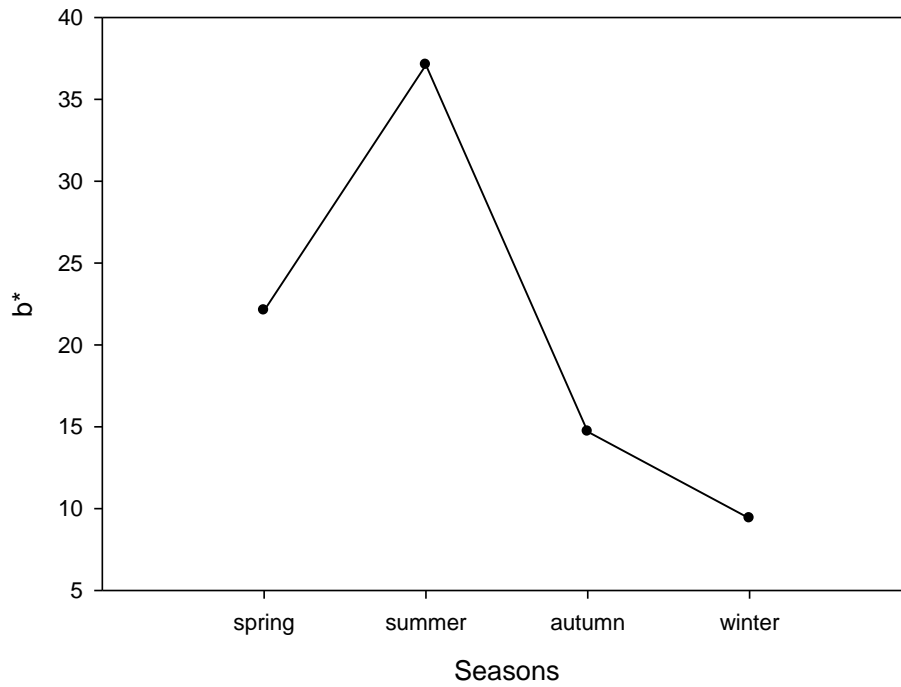


Figure 4.3. Seasonal changes in b* values of milk fats

4.3. Thermal Profile Analysis

4.3.1. Heating-Cooling Curve

Figure 4.4 shows the cooling-heating curve of autumn milk fat. As shown in Figure 4.4, c_1 and c_2 were two exothermic peaks during cooling; h_1 , h_2 and h_3 were three endothermic peaks during heating. This curve was confirmed by Ten Grotenhuis et al. (1999) who mentioned the typical DSC cooling and heating cycle of milk fat. Similar heating cooling curve was obtained by Lopez et al. (2007) at 2°C/min. Deffense (1993) interpreted DSC melting profile. According to Deffense (1993), h_1 corresponded to low-melting fraction from -25 to +10°C, middle-melting fraction from +10 to +19°C showed as h_2 and h_3 indicated the high-melting fraction from +19 to +34°C. Height of peaks and temperature at peak appeared in melting profile were different among the milk fat samples produced each season. Because thermal history and triglyceride composition of fats affects the relative size and position of peaks. Heating-cooling curves of other season milk fats at rapid and slow cooling were given in Appendix A.

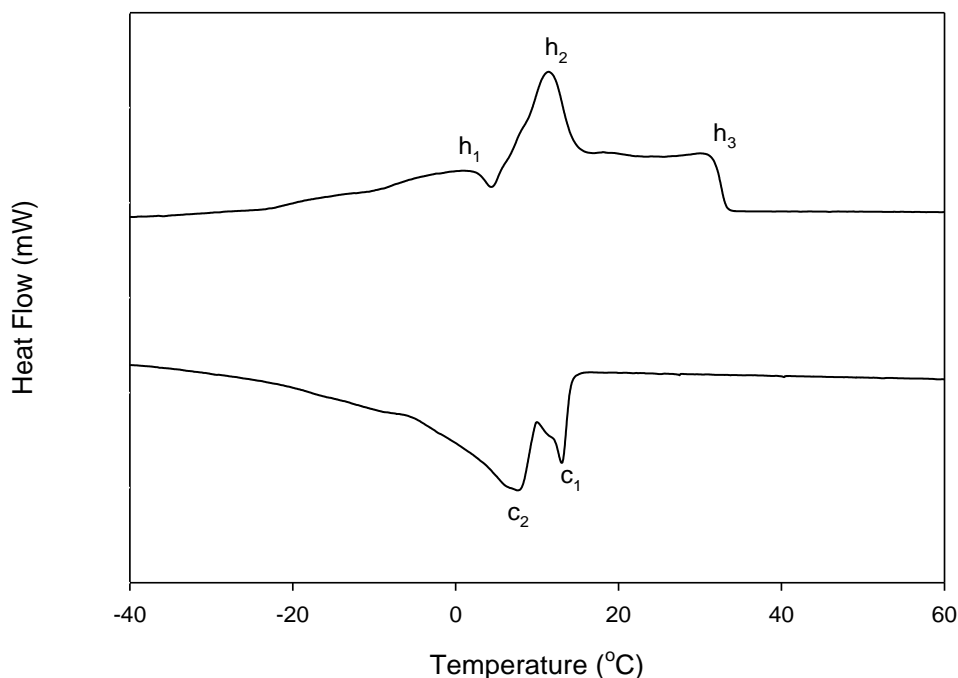


Figure 4.4. Thermal profile of autumn milk fat at 2°C/min cooling and heating rate

Figure 4.5 and 4.6 showed the seasonal change in cooling profiles of milk fat samples at different cooling rates ($2^{\circ}\text{C}/\text{min}$ and $10^{\circ}\text{C}/\text{min}$). The crystallization and melting behaviour of a fat is also affected by the cooling rate (Campos et al., 2002). The effect of cooling rate on crystallization of milk fat is shown in Fig 4.5 and 4.6. When the sample is cooled at a slow rate ($2^{\circ}\text{C}/\text{min}$), two different crystallization peaks are observed. Similar results were obtained in some studies. Campos et al. (2002) studied at four different cooling rates and they observed two peaks at $1^{\circ}\text{C}/\text{min}$ and $5^{\circ}\text{C}/\text{min}$ while one peak was obtained at $12^{\circ}\text{C}/\text{min}$ and $20^{\circ}\text{C}/\text{min}$. Ten Grotenhuis et al. (1999) showed the same results in their studies. Their DSC curves had one peak at $20^{\circ}\text{C}/\text{min}$ and two different peaks were examined at $1^{\circ}\text{C}/\text{min}$ and $5^{\circ}\text{C}/\text{min}$. This may be because of slow process of the crystallization kinetics. At slow cooling, long time allows the combine with each other of similar chain lengths TAGs, co-crystallize and fractionate. So first peak in cooling curves may indicate the crystallization of higher melting TAGs and the other is lower one (Campos et al., 2002).

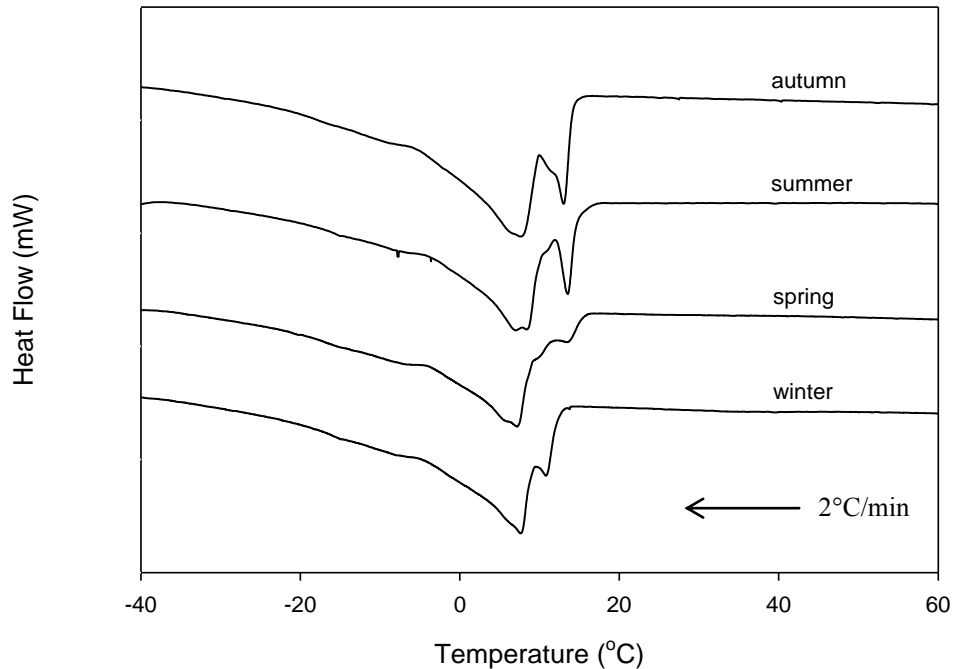


Figure 4.5. DSC cooling curves of milk fats at $2^{\circ}\text{C}/\text{min}$ rate

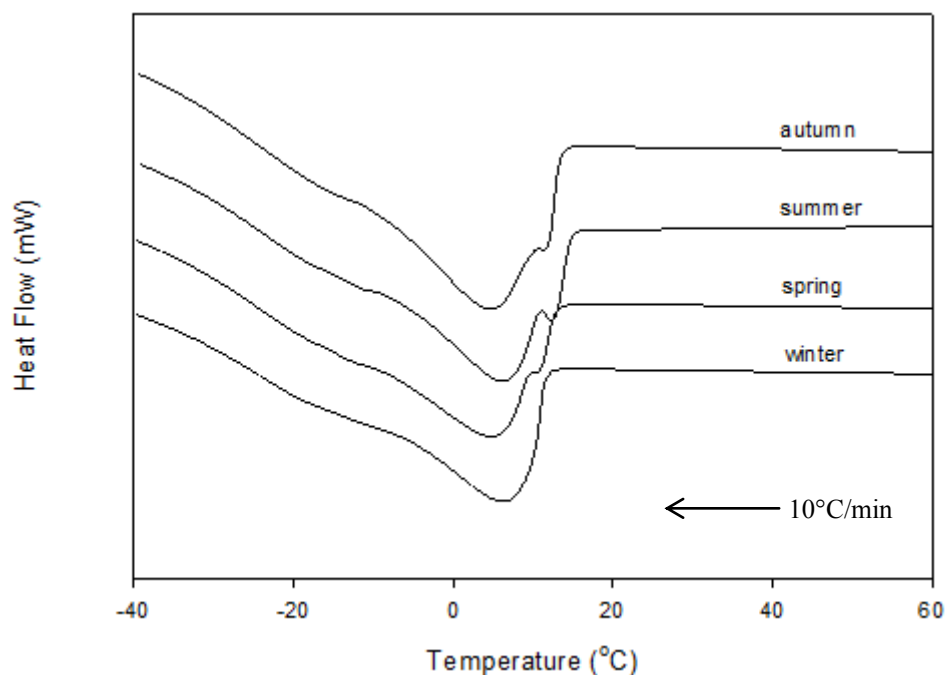


Figure 4.6. DSC cooling curves of milk fats at 10°C/min rate

Onset and peak temperature of each exotherms and enthalpies of crystallization were given in Table 4.3. For slow cooling, onset temperature of first exotherms varied from 12.24 to 15.30. Winter milk fat crystallized firstly but spring milk fat had maximum onset temperature. In second exotherms, peak of winter milk fat appeared firstly and summer milk fat crystallized finally. In rapid cooling profile, only summer milk fat showed two peaks. Winter milk fat had minimum onset temperature contrary of summer milk fat. The temperature at which the milk fat started to crystallize decreased with increasing cooling rate. These trends were in good agreement with many studies in literature. Ten Grotenhuis et al. (1999) studied with six different cooling rates and they found inverse proportion between cooling rates and onset temperature. Same results were observed by Lopez et al. (2005).

The enthalpy of crystallization (ΔH) and the temperature at which the milk fat started to crystallize (onset temperature) decreased with increasing cooling rate. Ten Grotenhuis et al. (1999) found the same result.

Table 4.3. DSC crystallization onset (OT) and peak (PT) temperatures, enthalpy and area of milk fats.

Samples	dT/dt (°C/min)	1st crystallization		2nd crystallization		ΔH (J/kg)	Area (mJ)
		OT (°C)	PT (°C)	OT (°C)	PT (°C)		
Spring	2	14.89	13.45	9.27	7.02	-60.3	641.0
	10	13.59	4.32	-	-	-50.9	541.0
Summer	2	15.30	13.30	10.47	7.57	-60.3	669.6
	10	16.25	4.91	-	-	-51.4	570.4
Autumn	2	14.65	12.63	9.76	7.27	-67.1	738.2
	10	15.44	3.72	-	-	-57.9	637.3
Winter	2	12.24	10.70	9.02	7.50	-54.4	592.4
	10	11.48	6.18	-	-	-51.0	519.3

The DSC heating curves of milk fats were recorded during heating at rates of 2 and 10°C/min after the milk fats had been cooled at the same rates (Figures 4.7 and 4.8). The curves of milk fat samples are similar and show the three characteristic endothermic peaks. Table 4.4 shows the clear points, peak temperatures and enthalpies of melting peaks.

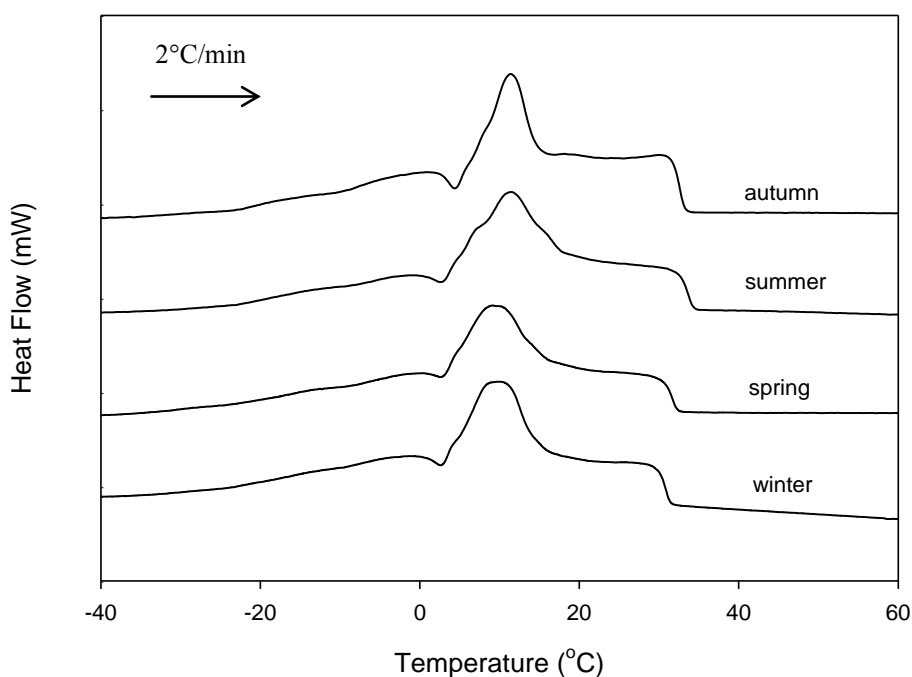


Figure 4.7. DSC heating curves of milk fats at 2°C/min rate

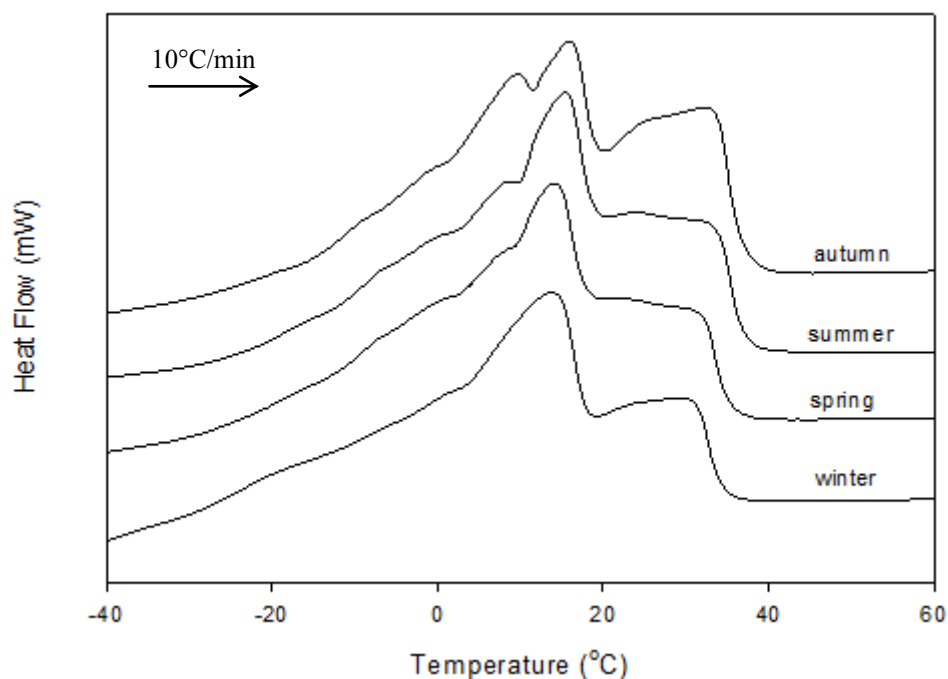


Figure 4.8. DSC heating curves of milk fats at 10°C/min rate

Smet et al. (2010) reported that melting temperature of the fraction of low melting triglycerides was smaller than 10°C, middle melting fractions melted between 10 and 20°C and high melting fractions melted at a temperature above 20°C. Results found in this study were supported by Smet et al. (2010). According to Table 4.4 winter milk fat had lowest melting point and summer milk fat had highest one. These differences related to the unsaturated triglyceride composition. Shi et al. (2001) found that rapid crystallization rate resulted in higher content of higher melting triglycerides for AMF. Similar behavior was found in present study. All milk fat samples had higher clear point at rapid crystallization rate (10°C/min).

Table 4.4. DSC end (ET), peak (PT) temperatures, clear point (CP), enthalpy and area of milk fats

Samples	dT/dt (°C/min)	1st melting		2nd melting		3rd melting		ΔH (J/kg)	Area (mJ)
		ET (°C)	PT (°C)	ET (°C)	PT (°C)	CP (°C)	PT (°C)		
Spring	2	2.18	0.29	14.70	9.26	32.34	28.76	69.2	735.8
	10	-	-	17.59	14.18	34.92	31.67	58.6	622.9
Summer	2	2.08	-0.66	16.82	11.43	34.51	31.13	60.1	667.1
	10	-	-	18.54	15.43	36.72	33.17	59.4	659.2
Autumn	2	3.97	0.97	14.69	11.39	33.00	30.36	70.1	771.4
	10	11.08	9.75	18.81	15.93	36.69	32.31	63.2	695.7
Winter	2	2.29	-0.51	14.49	10.06	31.46	28.65	59.7	649.8
	10	-	-	17.74	13.73	34.15	30.35	56.5	575.3

4.3.2. Isothermal Crystallization

Isothermal crystallization at 10, 14, 17 and 20°C after cooled from 70°C at 10°C/min was performed with DSC. The isothermal DSC curves for each season milk fat at 10, 14, 17 and 20°C were given in Figures 4.10-4.13. It was clear that the first crystallization occurred during cooling or during stabilization interval between cooling and isothermal period. But this peak was not much visible to integrate in curves of milk fats. The second crystallization appeared at later time (Figure 4.9). The same curve was obtained by Foubert et al. (2008). Onset, end, peak times and enthalpies of second crystallization peaks were given in Table 4.5. The clearest peak belonged to autumn milk fat which had the highest enthalpy. The curves at 10 and 20°C had different peak time for each milk fat samples between 33 and 46 minutes and between 18 and 30 minutes respectively. Peak times were closer 14 and 17°C.

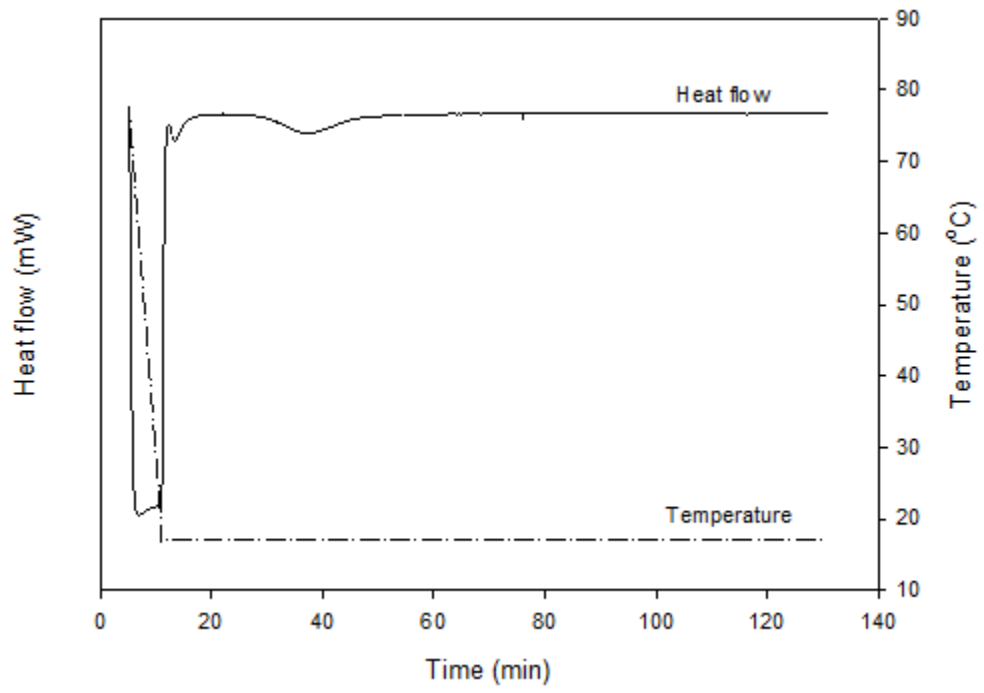


Figure 4.9. Isothermal crystallization of autumn milk fat at 17°C

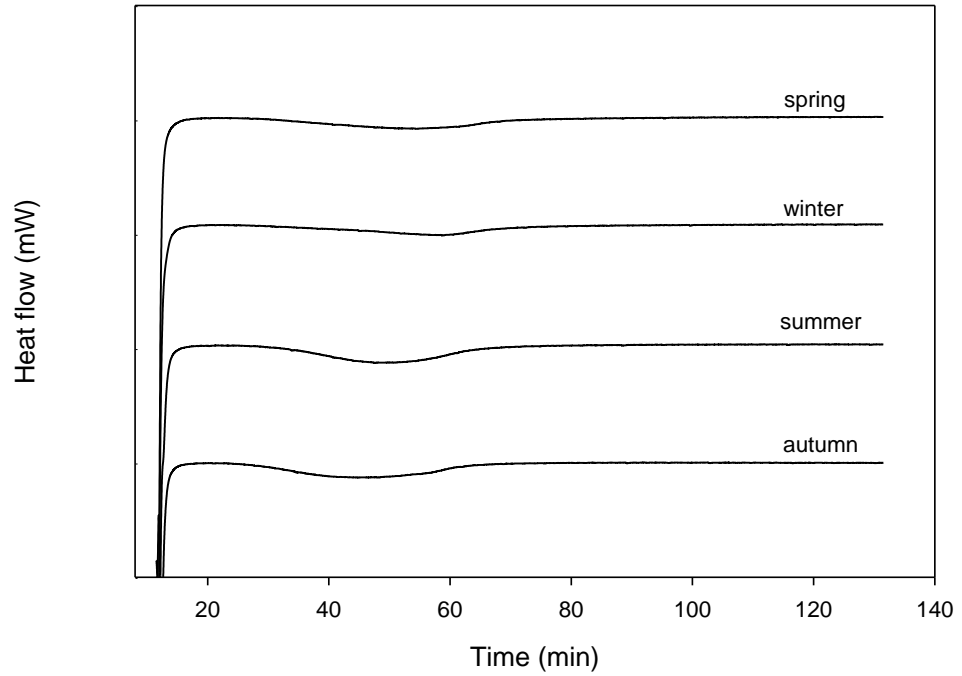


Figure 4.10. Isothermal crystallization of milk fats at 10°C

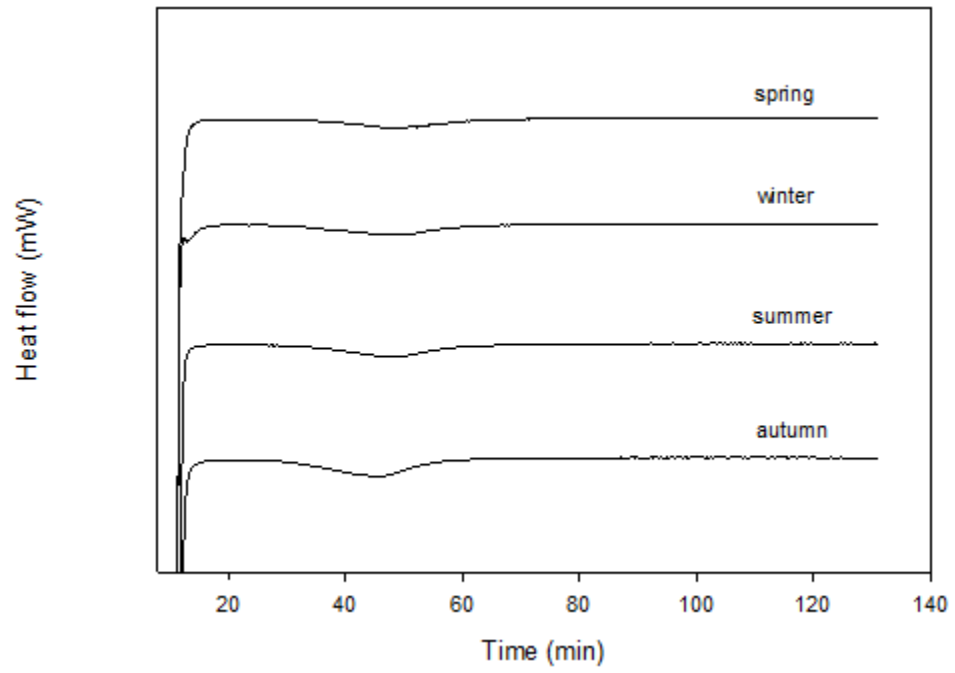


Figure 4.11. Isothermal crystallization of milk fats at 14°C

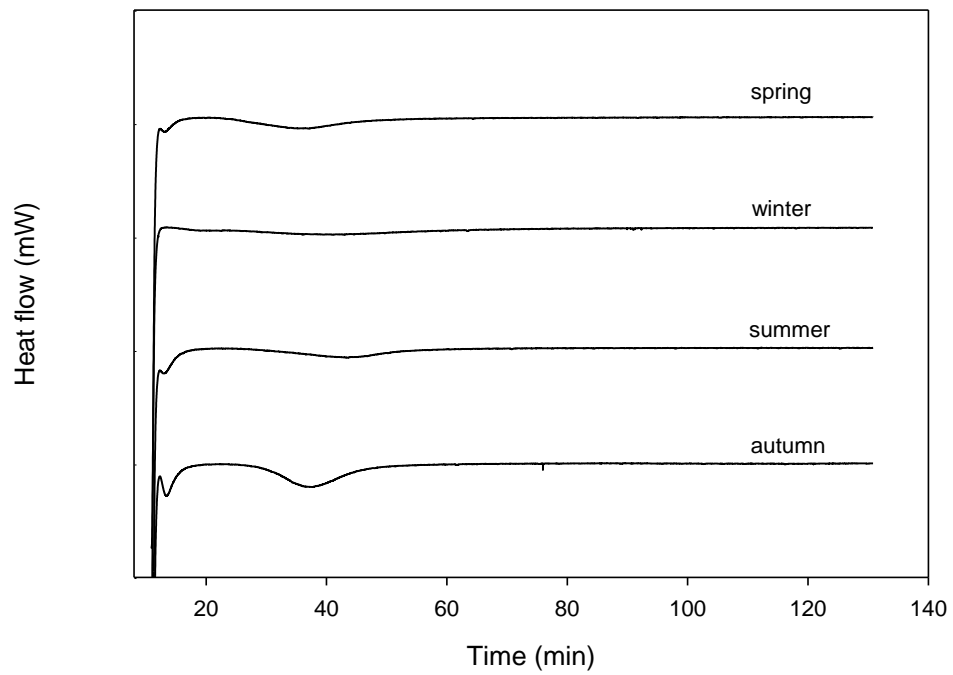


Figure 4.12. Isothermal crystallization of milk fats at 17°C.

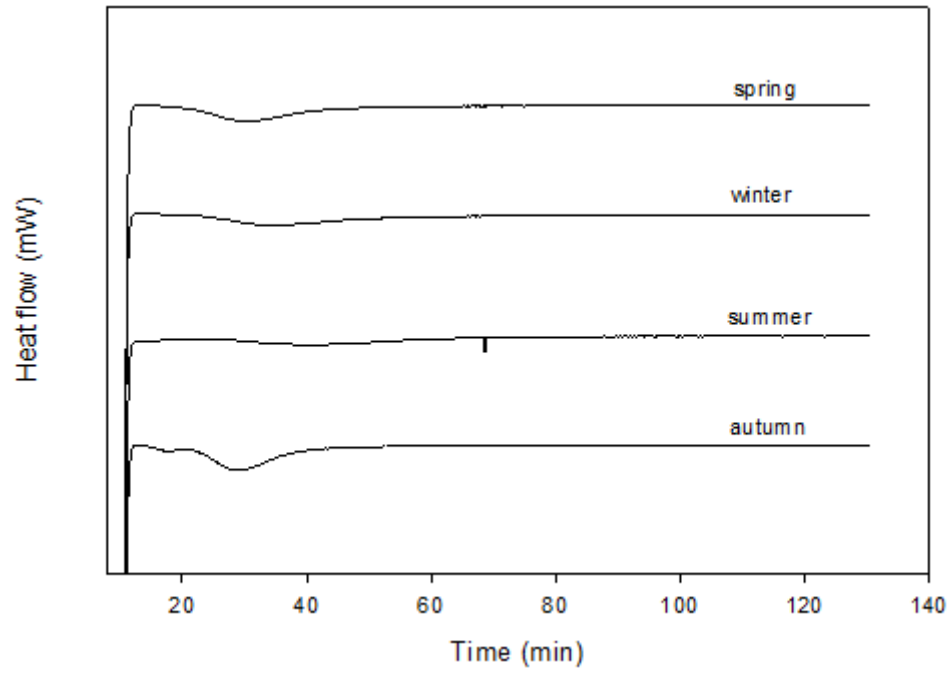


Figure 4.13. Isothermal crystallization of milk fats at 20°C

Table 4.5. DSC isothermal crystallization parameters of milk fats

Samples	T (°C)	Onset time (min)	End time (min)	Peak time (min)	ΔH (J/kg)	Area (mJ)
Spring	10	24.0	56.8	43.0	9.9	105.3
	14	24.8	50.8	37.1	7.5	80.1
	17	12.5	37.1	26.0	8.9	94.4
	20	11.1	29.7	19.9	8.8	107.7
Summer	10	20.2	53.3	36.3	17.4	192.8
	14	23.4	47.5	36.3	8.7	96.7
	17	19.2	42.7	32.6	7.1	78.8
	20	17.3	47.0	30.8	6.3	74.1
Autumn	10	17.2	51.8	33.3	17.3	191.3
	14	19.5	43.5	34.4	12.9	141.7
	17	18.6	36.1	26.5	13.3	146.8
	20	12.1	26.6	18.6	9.2	101.8
Winter	10	29.6	56.3	47.0	8.0	81.4
	14	22.6	47.3	37.8	6.6	67.0
	17	14.9	45.7	30.3	4.3	43.8
	20	14.0	39.0	24.9	7.5	78.6

4.4. Rheological Properties

4.4.1. Heating-Cooling Curves

Heating cooling curves of milk fats were also recorded by rheometer (Figures from 4.14 to 4.21). Two cooling rates (2 and 10°C/min), three shear rates (25, 50 and 100 1/s) were used for heating cooling curves between 13 and 70°C. Viscosity vs temperature curves gave the melting point of the milk fats. Temperature corresponded to intersection of heating and cooling curve was melting point. For cooling at 2°C/min, melting point of milk fat samples were about 34.7, 35.6, 35.3 and 33.4°C for spring, summer, autumn and winter milk fat respectively. For rapid cooling (10°C/min), values were approximately 25, 26.6, 33.5 and 25.9°C for the same sequence of milk fat. Highest melting point belonged to summer milk fat for slow cooling and for rapid cooling autumn milk fat had maximum value. These results matched up with melting points determined from DSC curves.

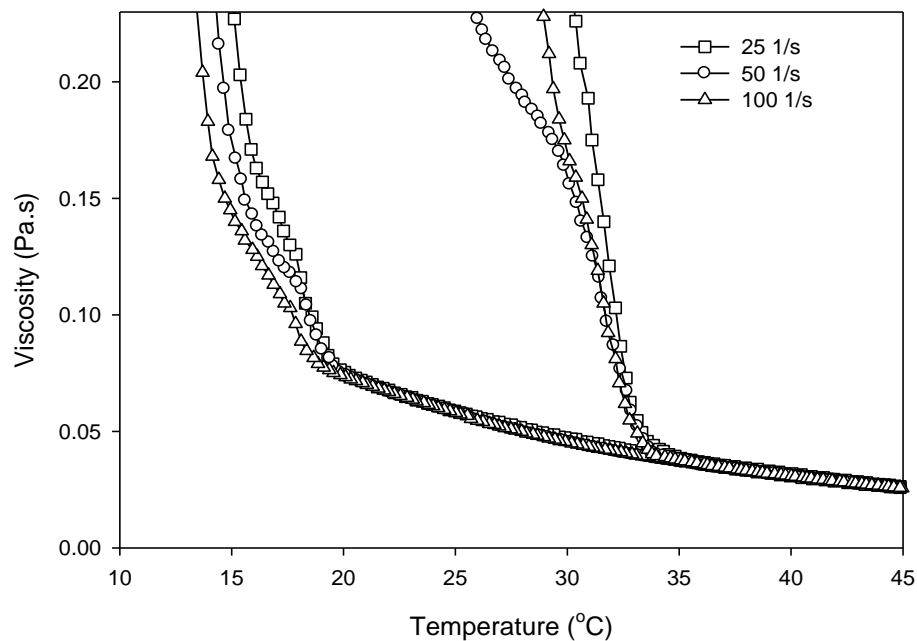


Figure 4.14. Viscosity change of spring milk fat at different shear rates and 2°C/min cooling-heating rate

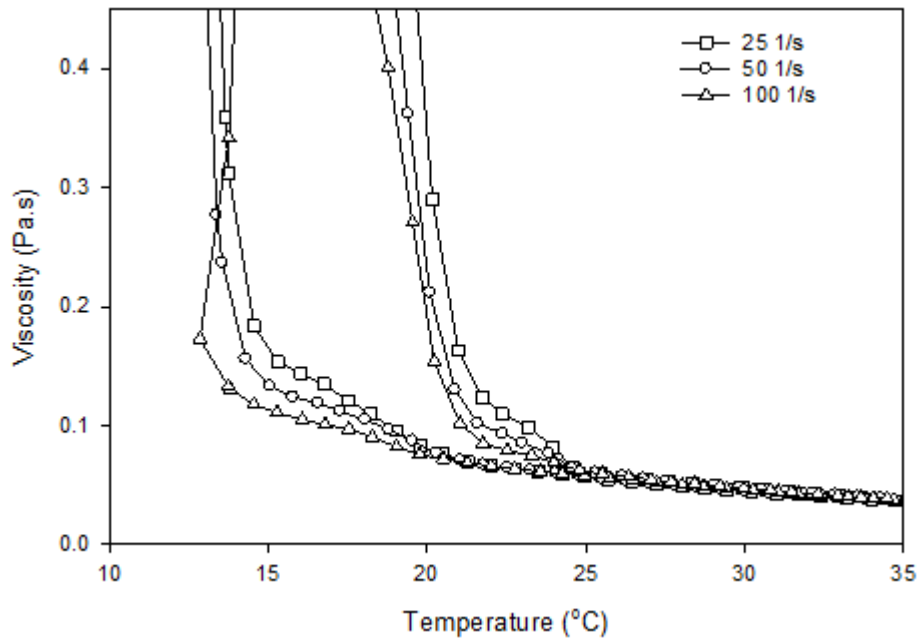


Figure 4.15. Viscosity change of spring milk fat at different shear rates and 10°C/min cooling-heating rate

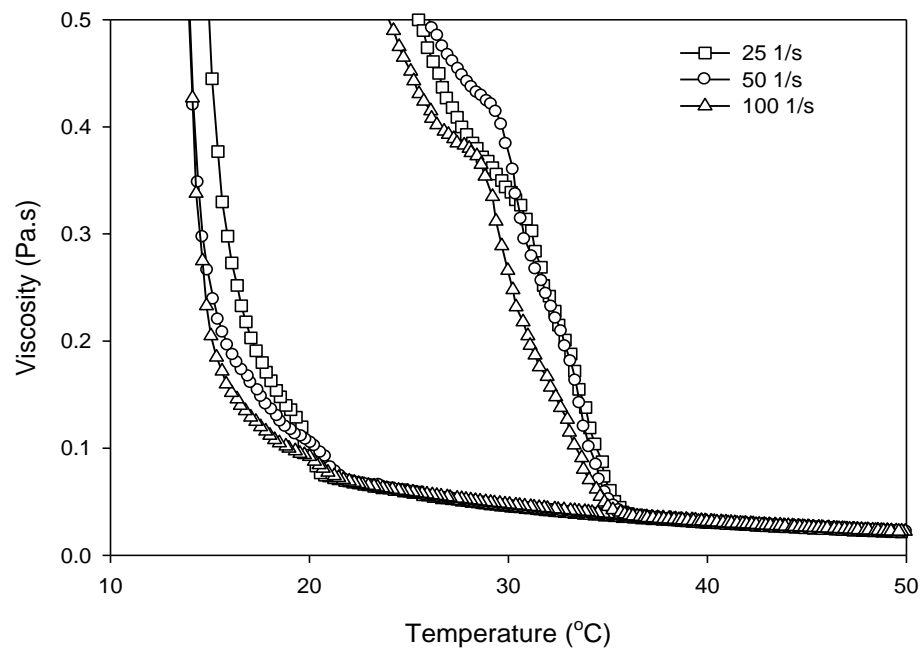


Figure 4.16. Viscosity change of summer milk fat at different shear rates and 2°C/min cooling-heating rate

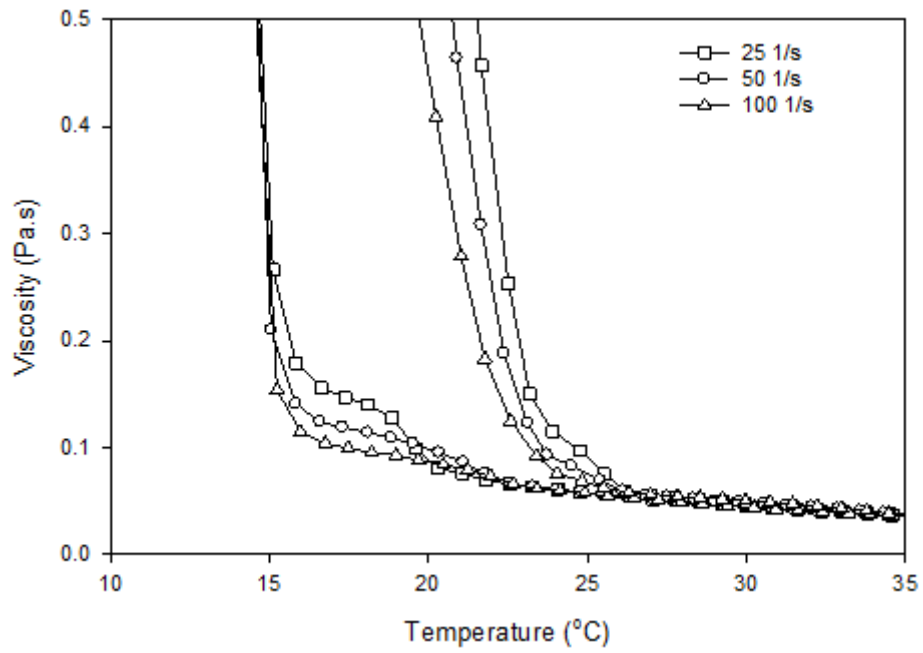


Figure 4.17. Viscosity change of summer milk fat at different shear rates and 10°C/min cooling-heating rate

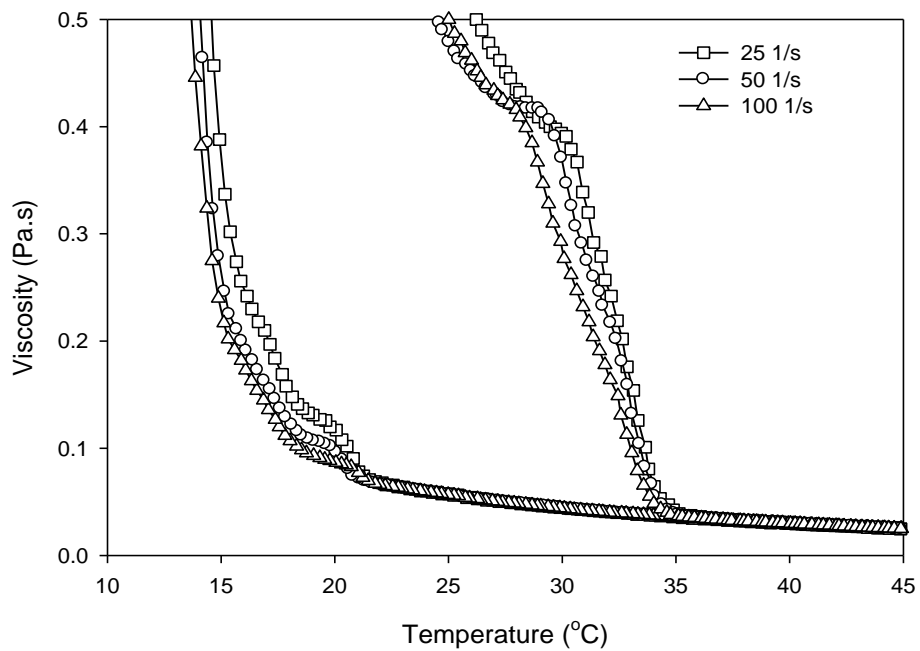


Figure 4.18. Viscosity change of autumn milk fat at different shear rates and 2°C/min cooling-heating rate

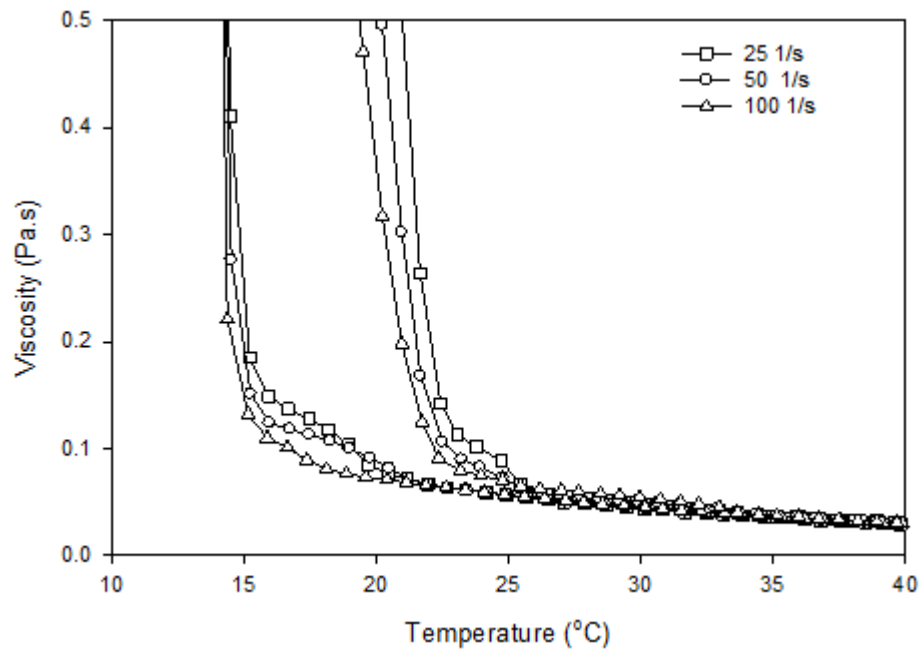


Figure 4.19. Viscosity change of autumn milk fat at different shear rates and 10°C/min cooling-heating rate

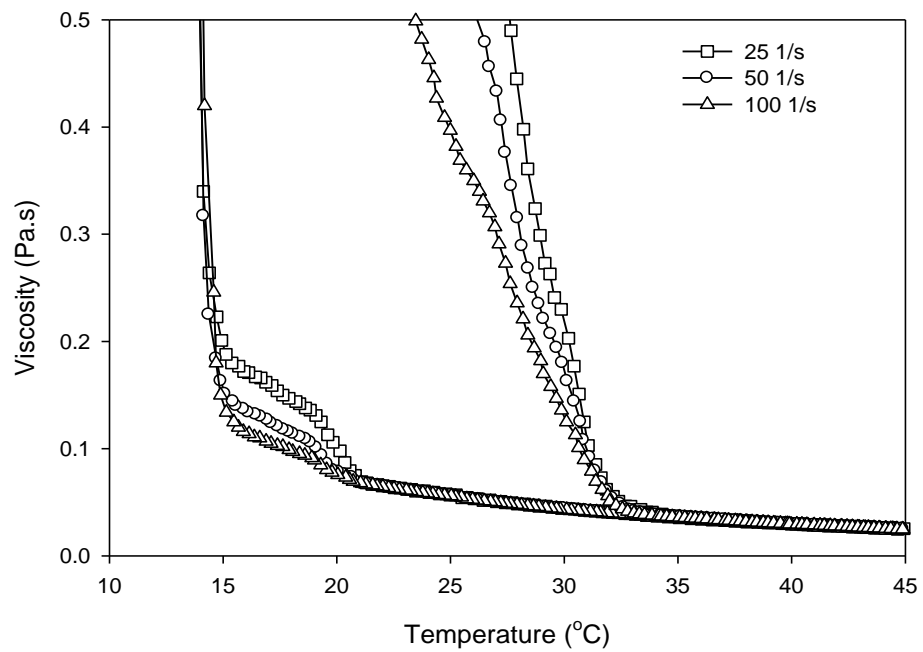


Figure 4.20. Viscosity change of winter milk fat at different shear rates and 2°C/min cooling-heating rate

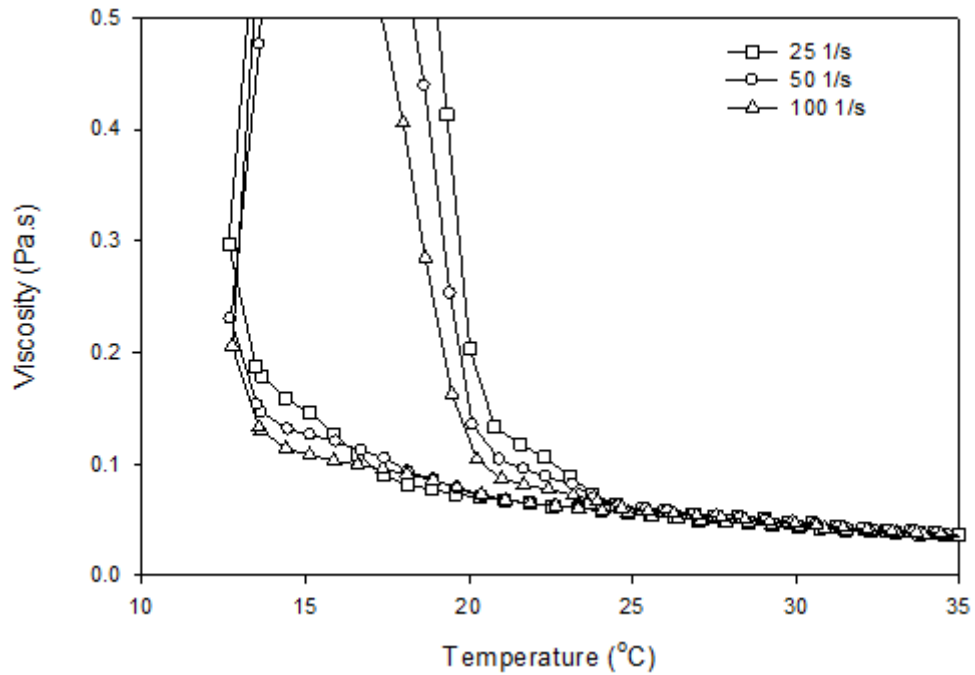


Figure 4.21. Viscosity change of winter milk fat at different shear rates and 10°C/min cooling-heating rate

4.4.2. Isothermal Crystallization

Isothermal crystallization was examined by the viscosity changes vs time in rheometer which provided well-defined shear flow conditions for crystallization (Breitschuh and Windhab, 1998; Breitschuh and Windhab, 1996). Viscosity-time curves of milk fat samples were obtained isothermal crystallization process at 14°C after cooled from 70°C at three different shear rate; 25, 50 and 100 1/s and two cooling rate; 2 and 10°C/min (Figures 4.22 - 4.27). The rheological profiles of all milk fats showed that weak structures formed during early stage of crystallization. Weak structures developed into semi-solid form on further crystallization. Viscosity increased with the crystallization progress. When crystallization finished, a constant viscosity was reached. Breitschuh & Windhab (1998) found similar result for crystallization of milk fat under shear. It was clear that from graphs, autumn milk fat had highest viscosity in contrast to winter milk fat. For both cooling rate, viscosities decreased with increasing shear rate.

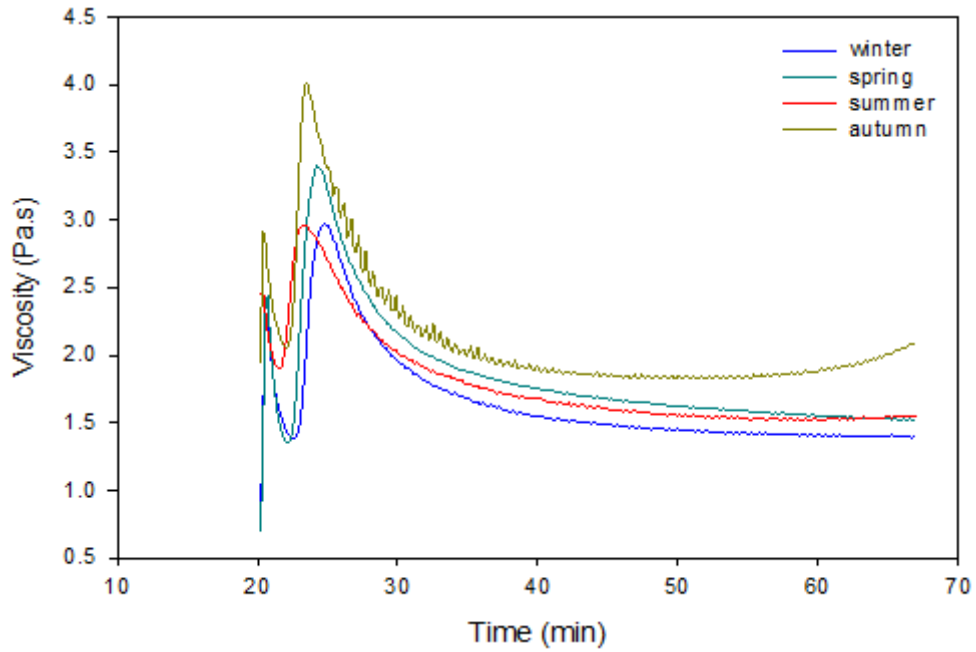


Figure 4.22. Viscosity changes of milk fat with time during isothermal crystallization at shear rate with 25 1/s and 14°C after cooling from 70°C with 2°C/min cooling rate

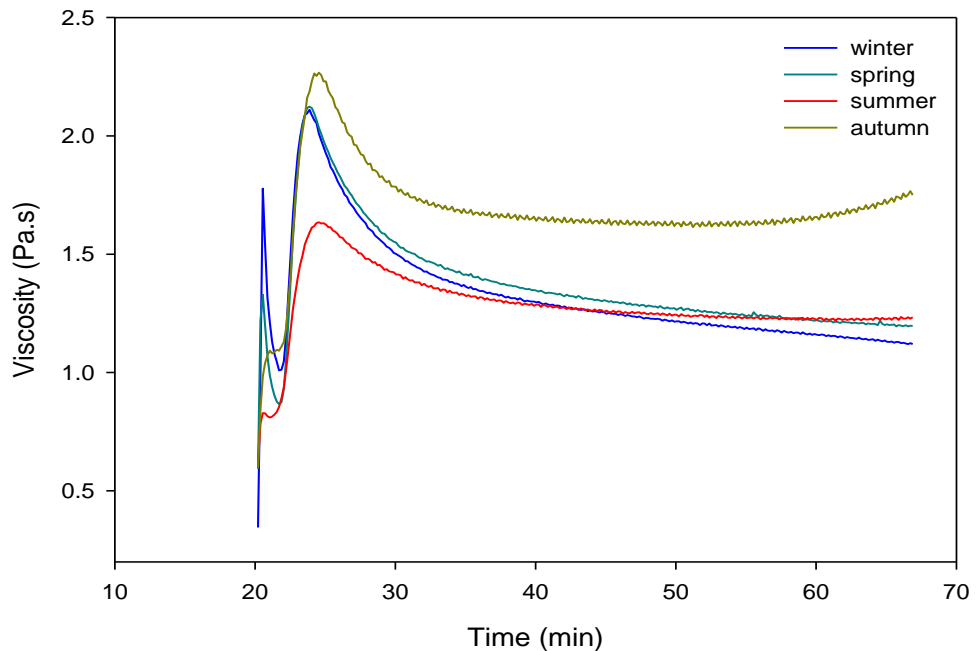


Figure 4.23. Viscosity changes of milk fat with time during isothermal crystallization at shear rate with 50 1/s and 14°C after cooling from 70°C with 2°C/min cooling rate

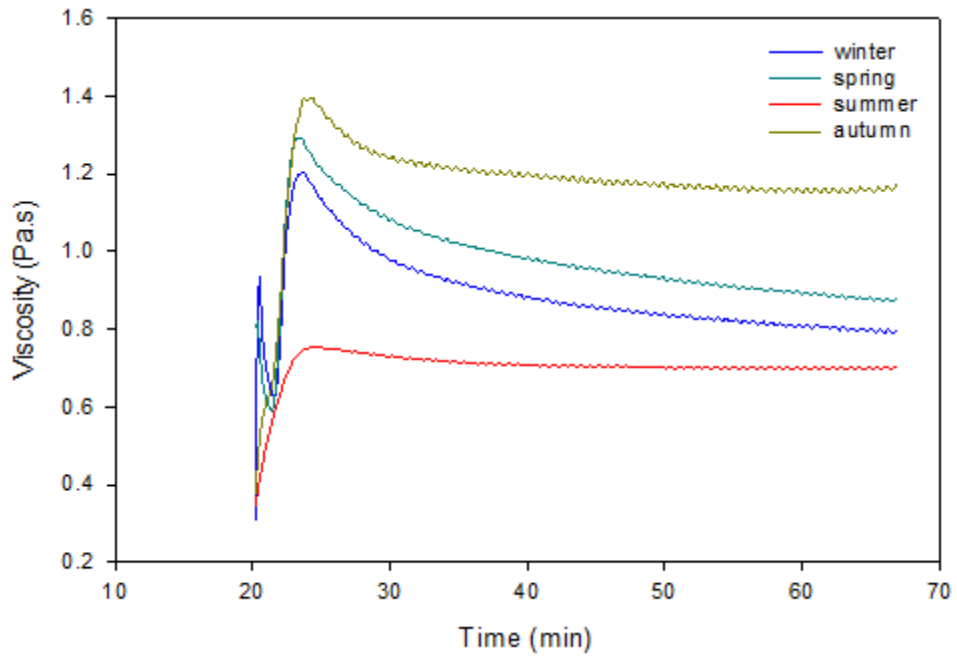


Figure 4.24. Viscosity changes of milk fat with time during isothermal crystallization at shear rate with 100 1/s and 14°C after cooling from 70°C with 2°C/min cooling rate

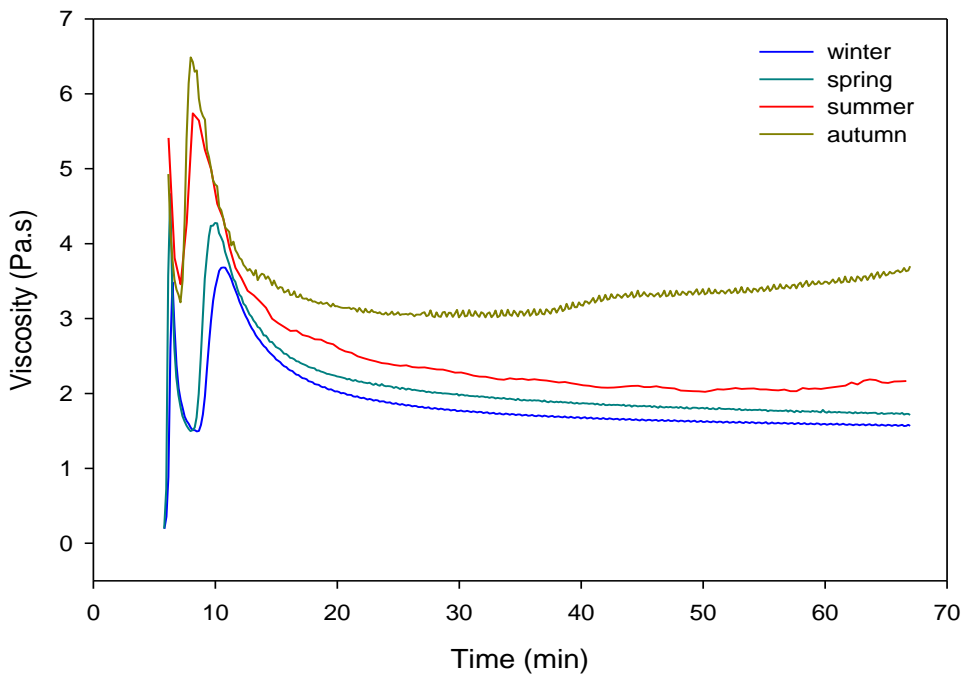


Figure 4.25. Viscosity changes of milk fat with time during isothermal crystallization at shear rate with 25 1/s and 14°C after cooling from 70°C with 10°C/min cooling rate

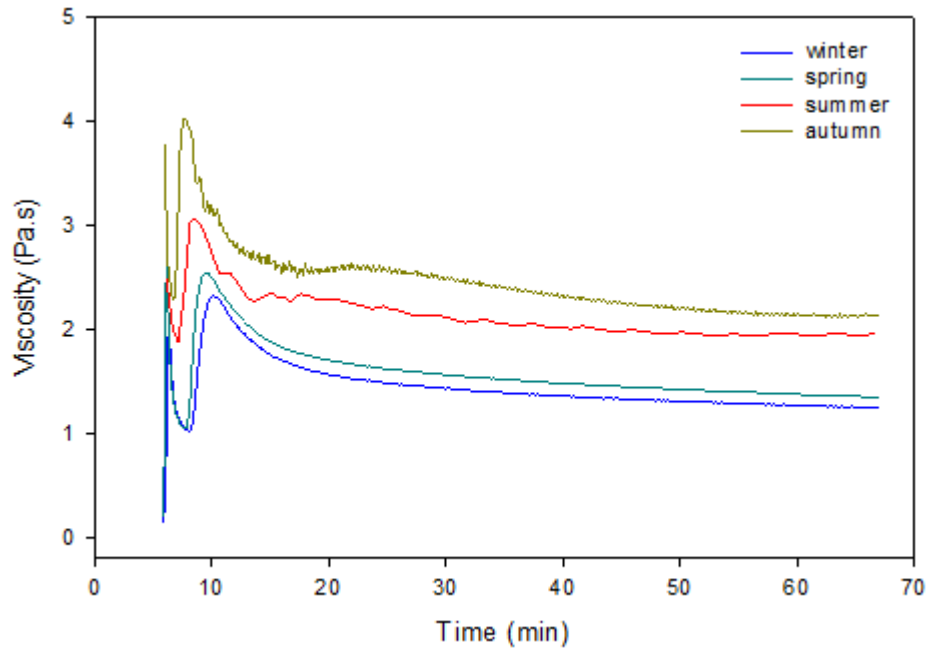


Figure 4.26. Viscosity changes of milk fat with time during isothermal crystallization at shear rate with 50 1/s and 14°C after cooling from 70°C with 10°C/min cooling rate

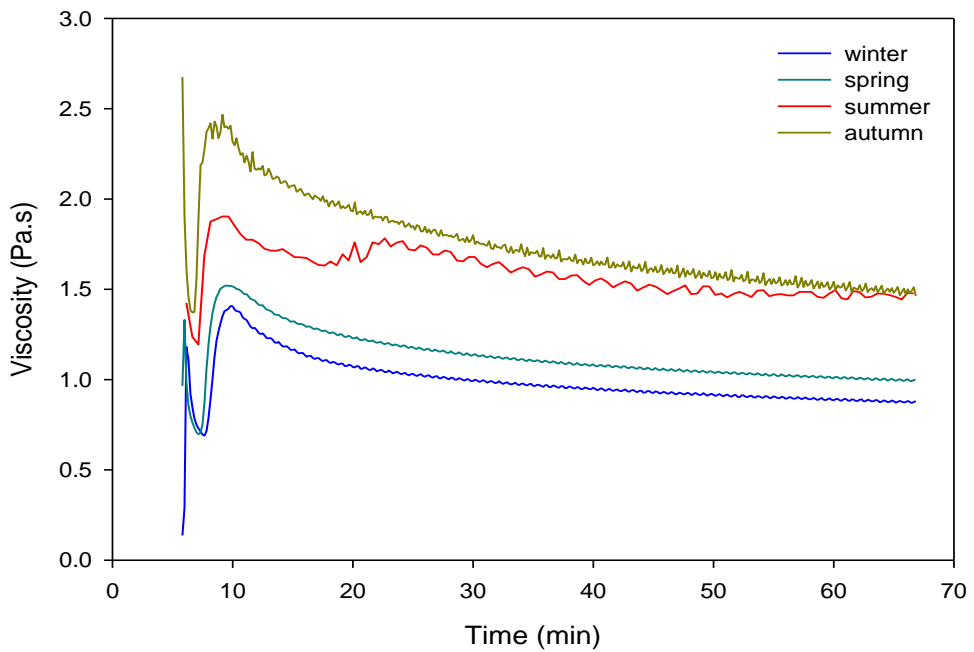


Figure 4.27. Viscosity changes of milk fat with time during isothermal crystallization at shear rate with 100 1/s and 14°C after cooling from 70°C with 10°C/min cooling rate

Campos et al. (2002) reported that rapid cooling is accompanied by a rapid increase in viscosity, thus severely limiting mass transfer. Our result was supported by them. At rapid cooling (10°C/min), time of viscosity increase was below 10 minute while time at slow cooling was about 20 min.

4.4.3. Flow Curve

Flow curve of milk fat samples were recorded by rheometer for five temperatures that were 70, 60, 50, 40 and 30°C. (Figures 4.28-4.31). All milk fat samples were exhibited the similar behavior. At above crystallization temperature, milk fats flowed as Newtonian. Viscosities were calculated from Newtonian equation (4.1) result of modeling of the flow curves and activation energies were calculated from the Arrhenius equation (4.2). Viscosities, activation energies and their R-square values were given in Table 4.6.

$$\text{Newtonian model: } \tau = \eta * \gamma \quad (4.1)$$

$$\text{Arrhenius model: } \eta = \eta_o + E_a/R*T \quad (4.2)$$

where; τ : shear stress, γ : shear rate, η : viscosity, E_a : activation energy,

R: universal gas constant (8.314 J/mol*K), T: temperature (Kelvin)

For each temperature, the maximum viscosity belonged to summer milk fat. Activation energy of milk fat samples was between 28 and 30 kj/mol. Results were shown that there were no significantly differences between milk fat samples produced at each seasons ($p>0.05$) (Table B.9).

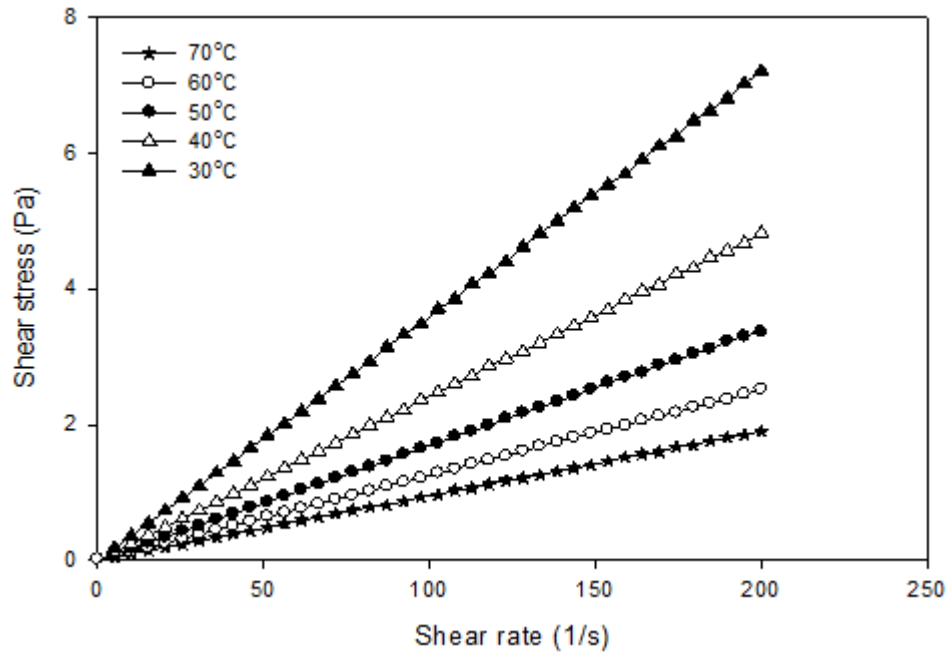


Figure 4.28. Flow curve of spring milk fat

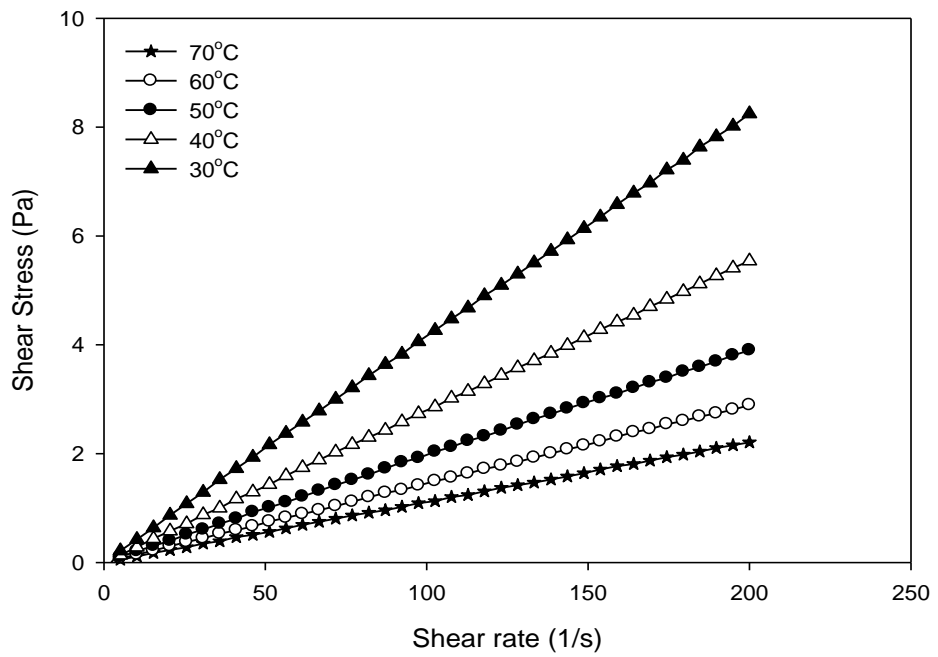


Figure 4.29. Flow curve of summer milk fat

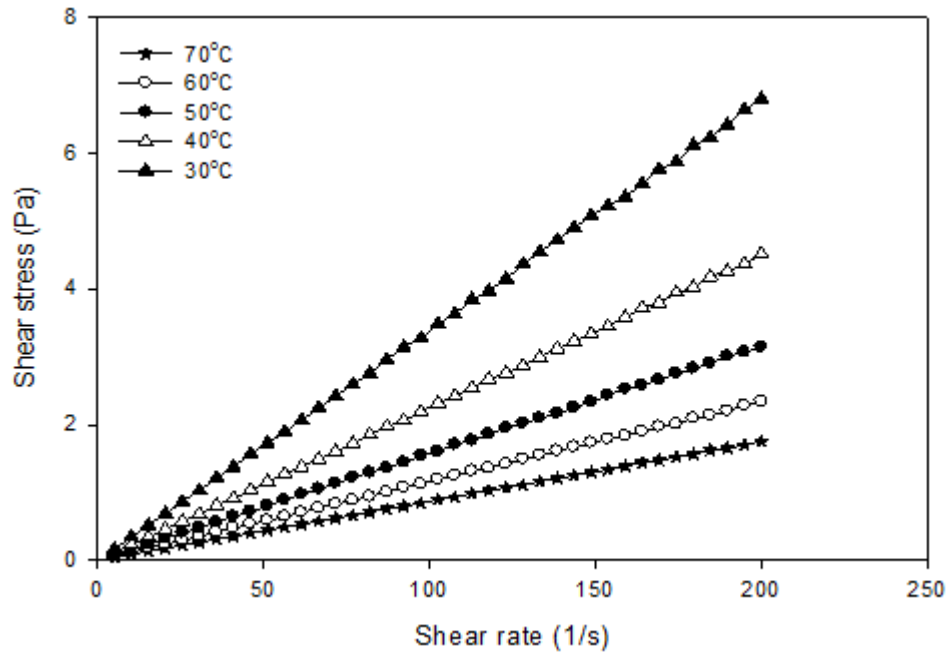


Figure 4.30. Flow curve of autumn milk fat

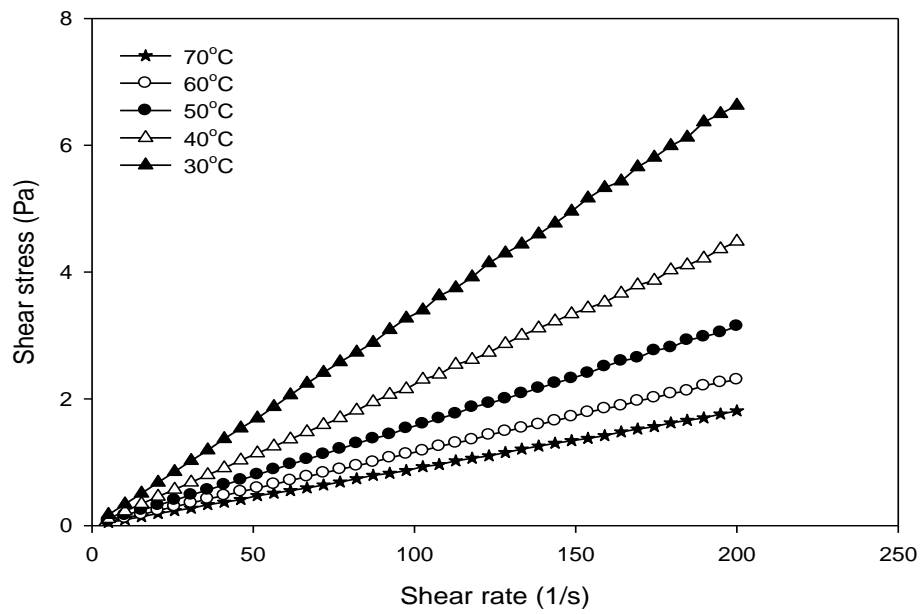


Figure 4.31. Flow curve of winter milk fat

Table 4.6. Viscosity and activation energy values of milk fats

Milk fat sample	Temperature (°C)	Viscosity (mPa.s)	r ²	Ea (kJ/mol)	r ²
Spring milk fat	30	35.98	0.9998	28.69±0.66	0.998
	40	24.11	0.9992		
	50	16.95	0.9996		
	60	12.56	1.0000		
	70	9.52	0.9972		
Summer milk fat	30	41.38	0.9998	28.46±0.69	0.998
	40	27.83	0.9994		
	50	19.62	0.9992		
	60	14.50	0.9990		
	70	11.10	0.9942		
Autumn milk fat	30	33.92	0.9998	29.22±0.67	0.998
	40	22.52	0.9998		
	50	15.77	0.9996		
	60	11.63	0.9988		
	70	8.74	0.9964		
Winter milk fat	30	33.35	0.9998	28.41±0.86	0.997
	40	22.33	0.9994		
	50	15.71	0.9992		
	60	11.57	0.9950		
	70	9.00	0.9970		

4.5. XRD Measurements

4.5.1. Isothermal Crystallization

Isothermal crystallization at 20, 17, 14, 10 and 5°C after cooled from 70°C at rapid (10°C/min) and slow cooling (2°C/min) like DSC was also monitored at wide angle XRD. While small-angle patterns give information on longitudinal stacking of TAG molecules generally in double or triple layers (as 2L and 3L), the wide-angle patterns gives the lateral packing of chains in these layers and their subcells (Lopez et al., 2002). Figure 4.32, 4.33, 4.34 and 4.35 shows the XRD compare plot and 3D plot of autumn milk fat respectively isothermal crystallization at 5°C at slow and rapid cooling. As shown in Figure 4.32, two different crystallization forms were formed. The first diffraction peak formed at $q = 4.13 \text{ \AA}$ which was correspond to α form. After 35 minutes the height of α peak began to smaller. In the figures, each line indicates the scans. Instrument measured the intensity by time frames of 7 minutes. Figure 4.32 showed that new two peaks started to form at 35 minute isothermal time. These new peaks appeared at $q = 3.8 \text{ \AA}$ and $q = 4.2 \text{ \AA}$ which were characteristic d-

spacing of the β' form. These results were supported with a few studies in literature. Lopez et al. (2002) studied the similar procedure and obtained XRD pattern of isothermal crystallization at 4°C at wide angle. They found the same polymorphic form at the same d-spacing. Same results were obtained at 5°C by Fredrick et al. (2011).

According to the figures, it was clear that cooling rate had not an effect on type of polymorphic form and time of peak formation. Patterns of isothermal crystallization after slow and rapid cooling included the same peak with same polymorphic forms. Also these properties were not affected by season. XRD patterns of each season at the same temperature were the same. All β' were existed at $q = 3.8 \text{ \AA}$ and $q = 4.2 \text{ \AA}$ where α form differed from 4.10 \AA to 4.15 \AA . Others XRD patterns showed in Appendix A.

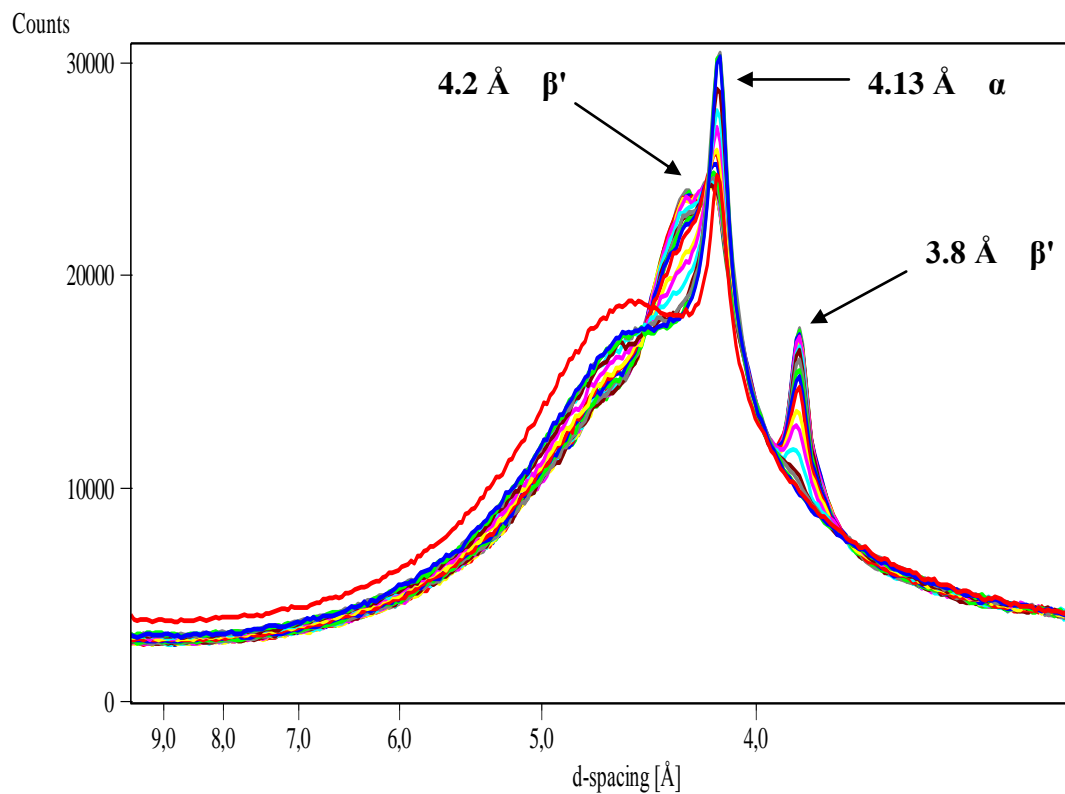


Figure 4.32. Wide angle XRD pattern of the isothermal crystallization after rapid cooling (10°C/min) of the autumn milk fat from 70 to 5°C

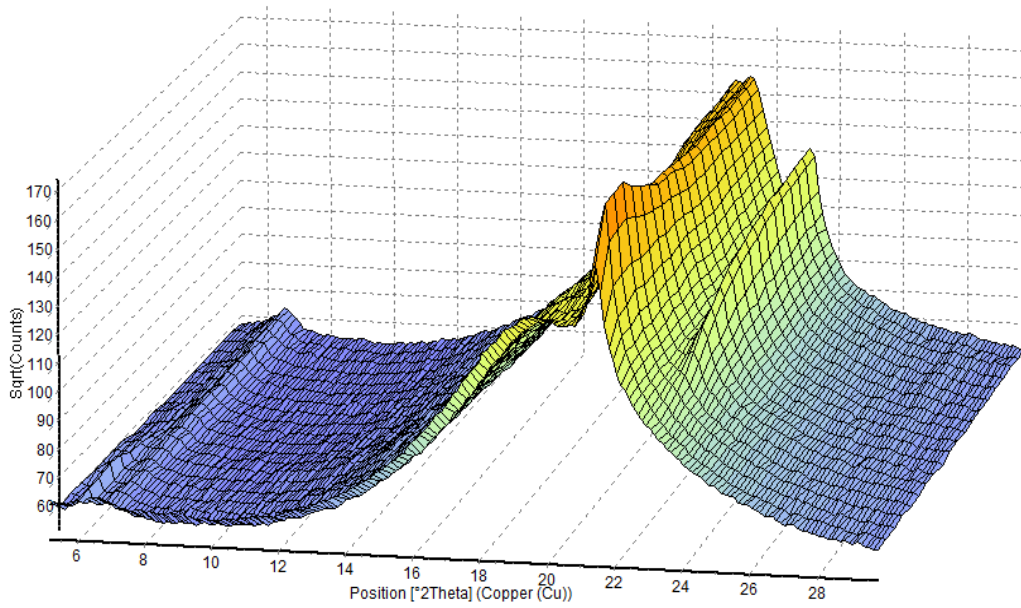


Figure 4.33. 3D plots of XRD pattern of of the isothermal crystallization after rapid cooling (10°C/min) of the autumn milk fat from 70 to 5°C

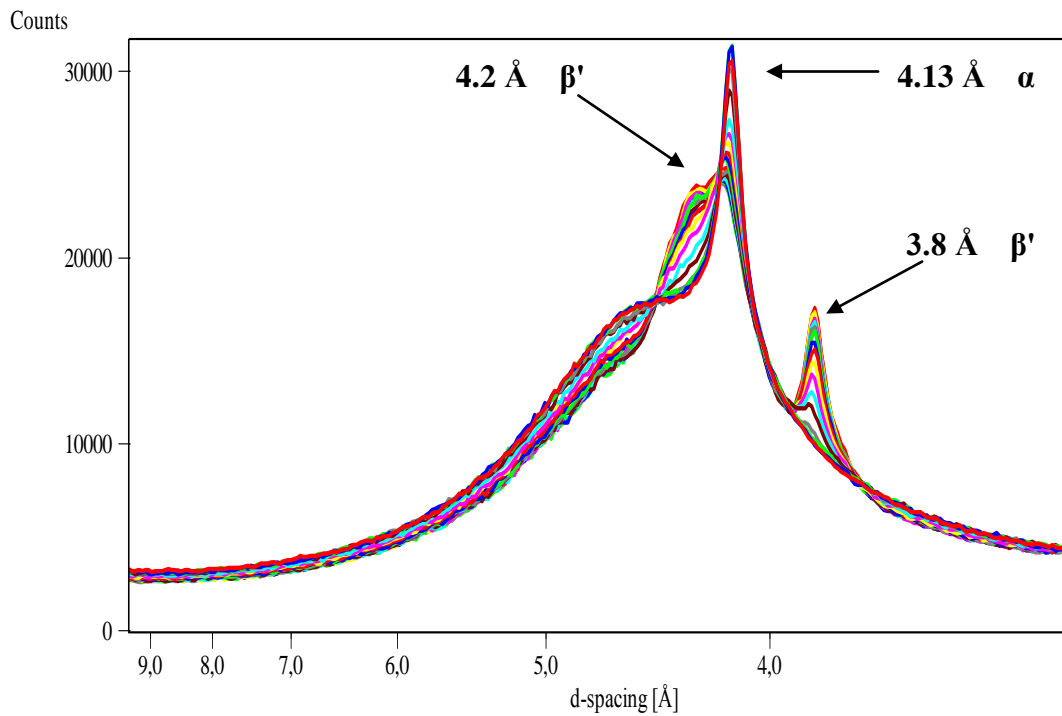


Figure 4.34. Wide angle XRD pattern of the isothermal crystallization after slow cooling (2°C/min) of the autumn milk fat from 70 to 5°C

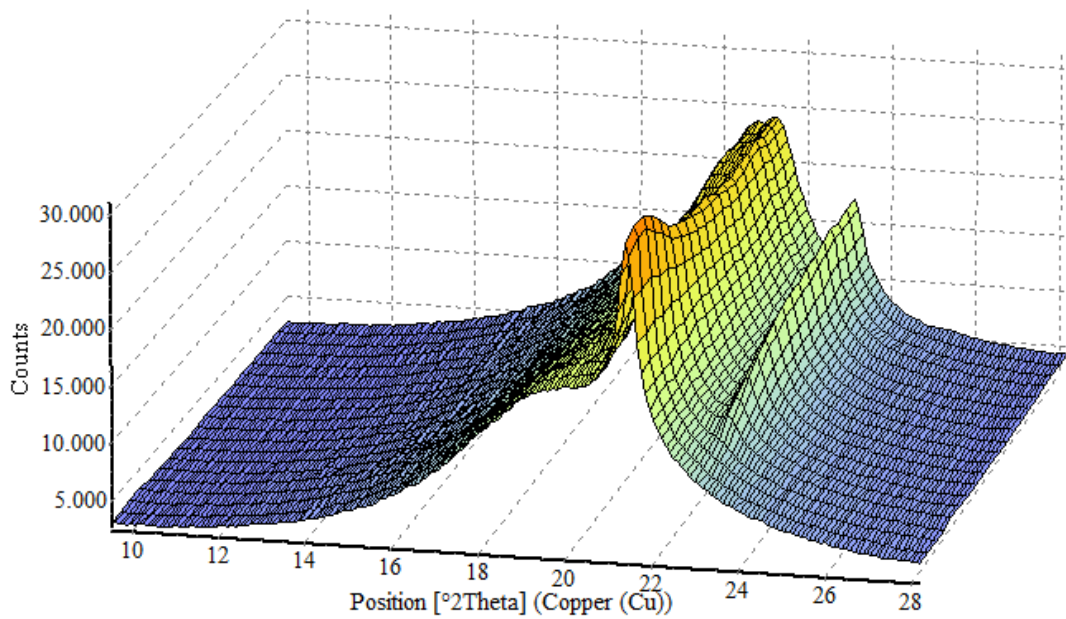


Figure 4.35. 3D plots of XRD pattern of of the isothermal crystallization after slow cooling (2°C/min) of the autumn milk fat from 70 to 5°C

Isothermal crystallization at 20°C was interesting and different from other temperatures (Figure 4.36 and 4.37). At 20°C, α form was not observed. Only β' crystals were formed at $q = 3.8 \text{ \AA}$ and $q = 4.3 \text{ \AA}$ at 14 minute isothermal time. High final crystallization temperature of milk fat causes initial β' crystallization (Lopez et al., 2005; Mazzanti et al., 2004). One of the other differences was time of the β' occurrence. At 20°C, both of the β' formed at 14 minutes.

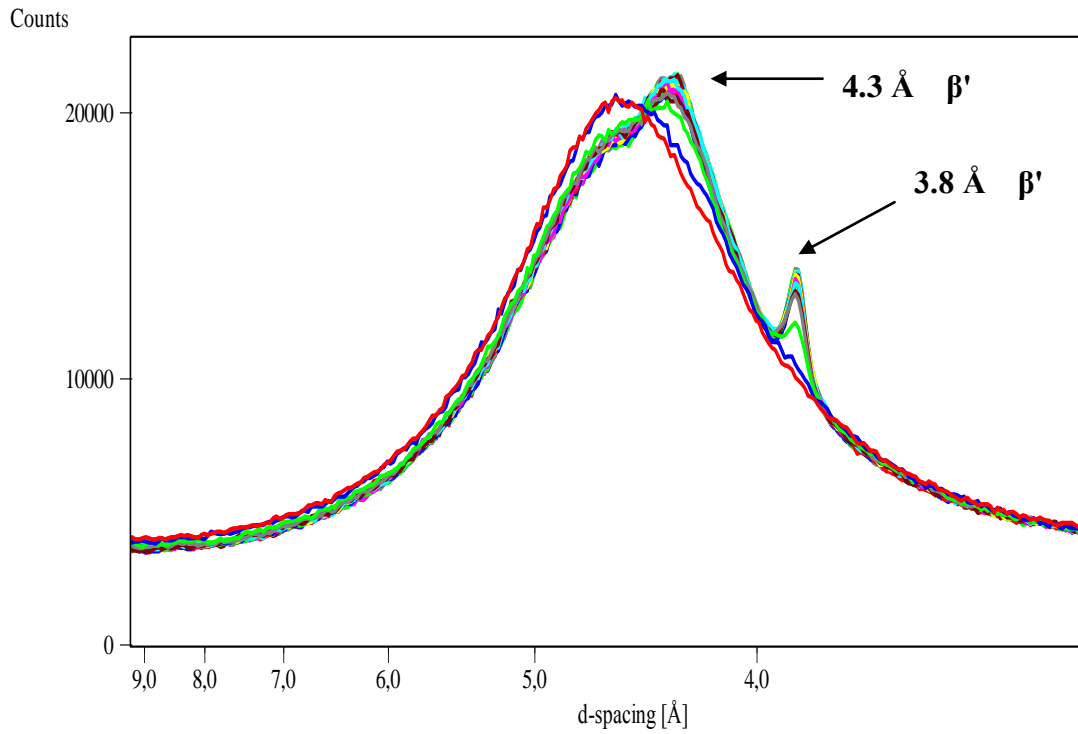


Figure 4.36. Wide angle XRD pattern of the isothermal crystallization after rapid cooling (10°C/min) of the autumn milk fat from 70 to 20°C

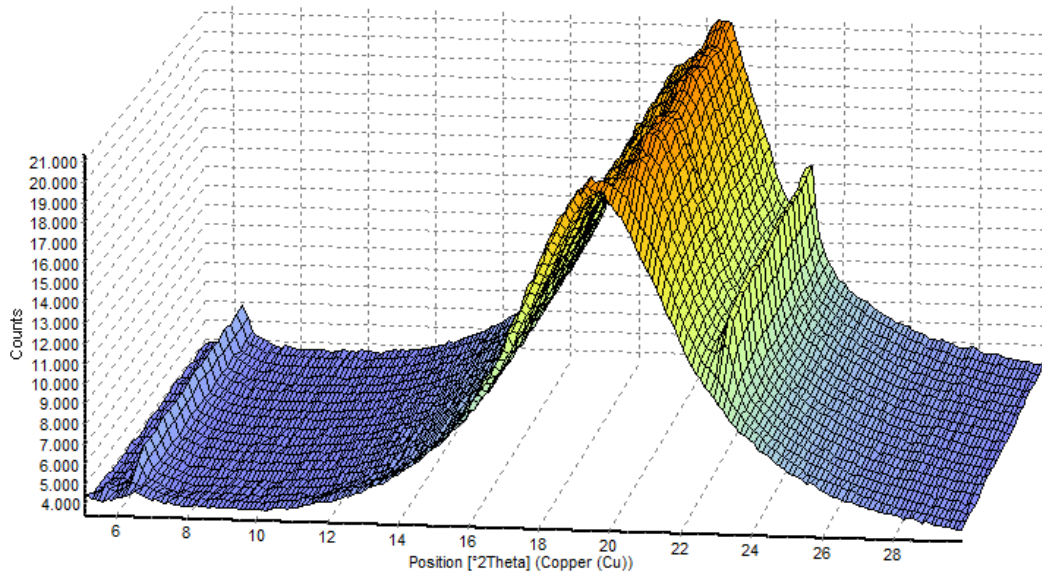


Figure 4.37. 3D plots of XRD pattern of of the isothermal crystallization after rapid cooling (10°C/min) of the autumn milk fat from 70 to 20°C

4.6. Solid Fat Content Determination

Solid fat content of milk fat at eight temperatures from 0°C to 35°C were measured by NMR method. SFC curves also obtained from DSC melting curves. Figure 4.38 shows the solid fat contents measured by NMR of milk fat samples for each season as a function temperature. At 0°C, autumn milk fat had highest SFC and it was 56 %. At the same temperature lowest SFC contents belonged to winter and spring milk fat and the values were 45.5 % and 46 % respectively. SFC of summer milk fat was 51 %.

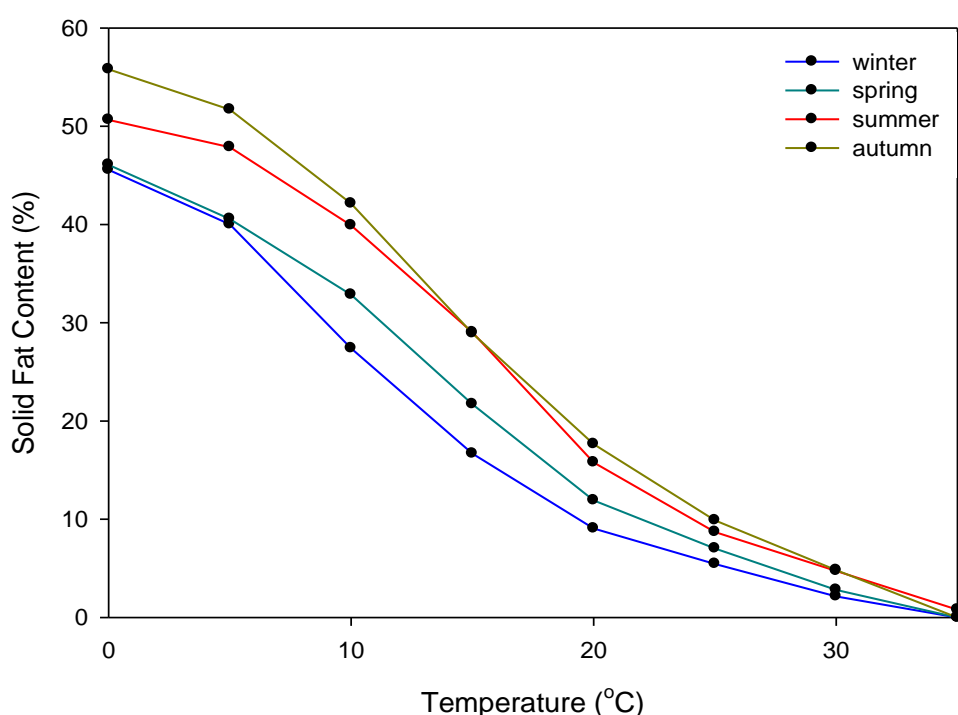


Figure 4.38. Solid fat content profile of milk fat samples by NMR

Figure 4.39 and 4.40 show the solid fat content vs. temperature of milk fat samples calculated by integrating directly DSC melting curves recorded on heating at 2°C/min and 10°C/min after cooling at same rates. Fast crystallization result in a higher SFC level (Campos et.al., 2002; Herrera and Hartel, 2000; de Man, 1964; Wright et al., 2001). Our results were confirmed by these studies. SFC of milk fats at a rate 2°C/min varied from 72 to 78%. On the other hand, SFC range of milk fats cooled rapidly was between 75 and 84%. Campos et al. (2002) observed the similar results. Boudreau and Saint Amant (1985) reported that when butter was cooled

rapidly, more liquid fat was adsorbed to the crystal surfaces, thus less liquid fat presented in phase and SFC was higher.

In general all of the milk fat samples showed the similar trends but the SFC values were closer between summer-autumn and winter-spring milk fat. All milk fats were totally melted approximately at 35°C.

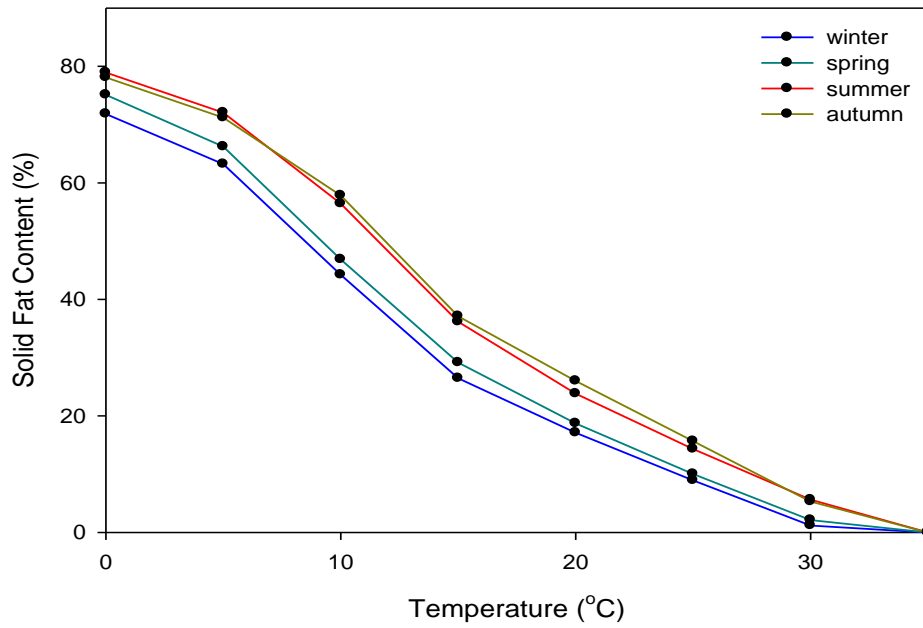


Figure 4.39. SFC curves of milk fat sample heating at 2°C/min by DSC

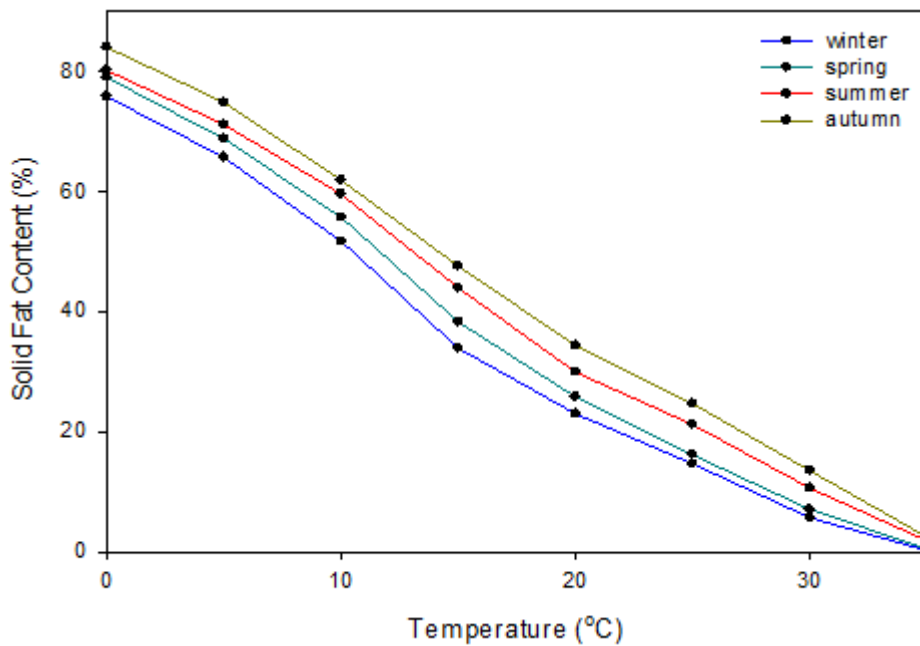


Figure 4.40. SFC curves of milk fat sample heating at 10°C/min by DSC

4.7. Polarized Light Microscopy

Macroscopic rheological properties of a fat system are affected by the microstructural level (Shahidi, 2005; deMan and Beers, 1987; Heertje et al., 1987; Narine and Marangoni, 1999). In this study, polarised light microscopy was used to image the microstructure of milk fat crystals. Milk fat samples were cooled from 50°C to different crystallization temperatures at rates of 0.1, 2 and 10°C/min using 10x objective.

Polarised microscopy has been used to visually observe the onset of nucleation (Widlak et al., 2001; D'Souza et al., 1992; Zeitoun et al., 1993). In our study, crystallization began at 25°C for milk fat cooled at 0.1°C/min. At 25°C, sporadic nucleation began, and in progresses of time, these early nuclei intermittently grew outward in a radial shape as the temperature decreases. Between the temperatures of 25°C and 22°C, there was a separate and continuous growth region where the microstructures increase considerably in size as a function of time. Until 10.6°C there was no significant growth. From approximately 10°C to 5°C, minor space filling crystal growth occurred. Onset temperature of crystallization for milk fat cooled at 2°C/min and 10°C/min were 20.3 and 20.4 respectively.

Figure 4.41 also showed that different cooling rates resulted in different size and morphology of the milk fat crystals (Wiking et al., 2009). The microstructure of milk fat crystallized rapidly exhibited a granul morphology composed of large number of small crystals. On the other hand, for slow crystallization process, a spherulitic microstructural texture was observed. Similar results were reported by other research groups for milk fat (Wright et al., 2001; DeMan, 1961, 1964; Herrera and Hartel, 2000a, 2000b; Van Aken and Visser, 2000; Campos et al., 2002).

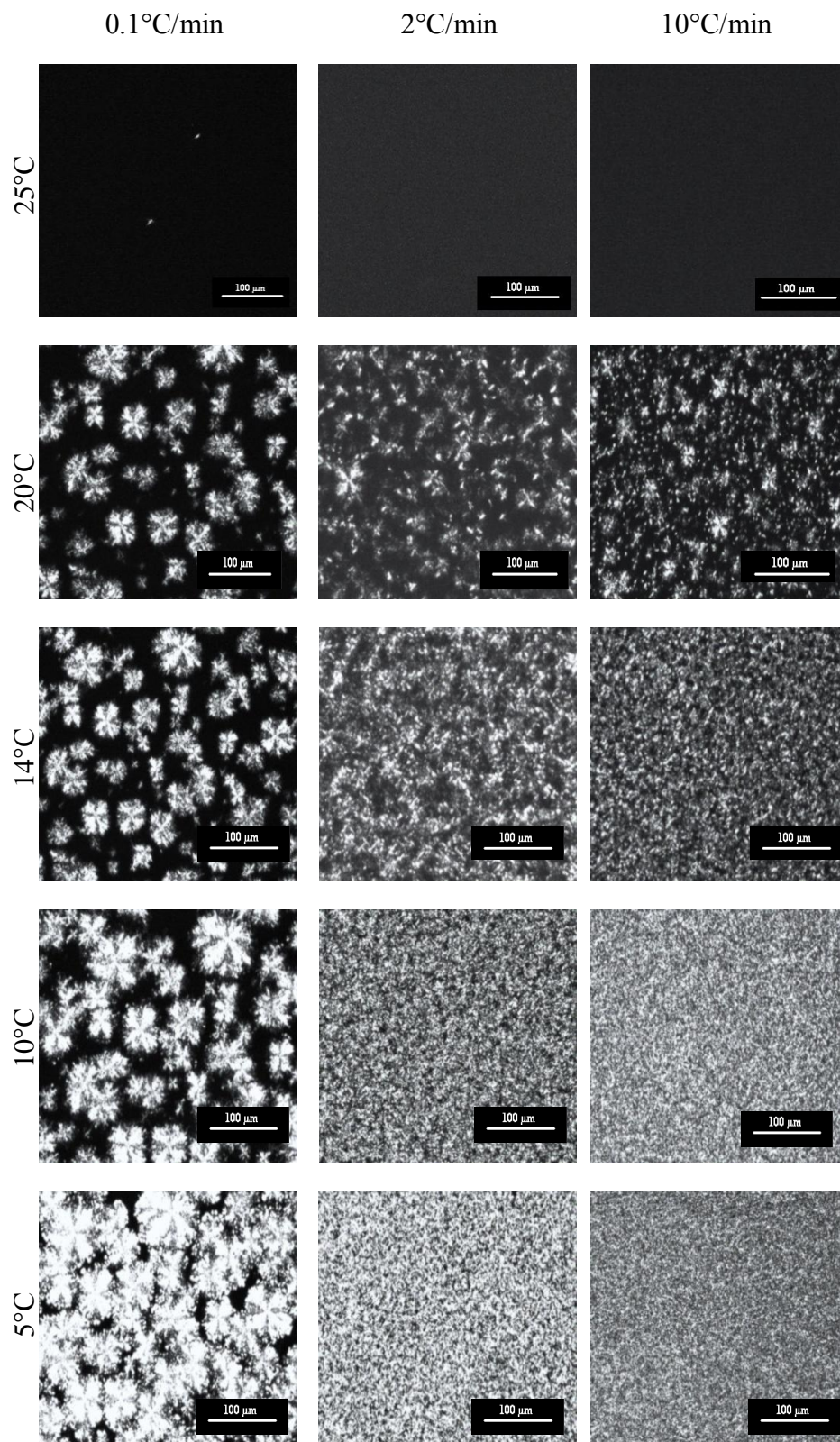


Figure 4.41. Images of milk fat crystals at different temperatures and cooling rates

CHAPTER V

CONCLUSION

Seasonal differences had significant effect on the color and fatty acid composition of milk fat.

All milk fats showed three endothermic peaks during heating and two exothermic peaks during cooling.

Cooling rate affected the crystallization and melting behavior, enthalpy of crystallization (ΔH) and the temperature at which the milk fat started to crystallize (onset temperature).

In isothermal crystallization curve, the clearest peak appeared for autumn milk fat. Melting points of milk fats showed a change from 25 to 35°C. The highest melting point belonged to summer milk fat for slow cooling and autumn milk fat for rapid cooling.

Autumn milk fat had highest viscosity in contrast to winter milk fat. Viscosities decreased with increasing shear rate for slow and rapid cooling. At above crystallization temperature, milk fats flowed as Newtonian. Activation energies of milk fats calculated from Arrhenius equation were not different significantly.

Two polymorphic forms (β' and α) were observed. Cooling rate and seasonal differences had not an effect on type of polymorph and time of peak formation.

At 0°C, autumn milk fat had highest solid fat content (SFC) and lowest SFC belonged to winter milk fat. Cooling rates affected the size and morphology of the milk fat crystals.

REFERENCES

- Alonso, L., Brana, J., Bada, J.C. (2004). Seasonal and regional influences on the fatty acid composition of cow's milk fat from Asturias, Spain. *Grasas y Aceites*, **55**, 169-173.
- AOCS. American Oil Chemists' Society. (1989). Solid fat content (SFC) by low-resolution nuclear magnetic resonance- The indirect method. Cd 16-81.
- Boudreau, A., Saint Amant, L. (1985). Butter. In dairy science and technology: principles and applications. (J.P. Julien, J.P. Nadeau, R. Dummais Eds.). Canada: Presses Université Laval.
- Breitschuh, B., Windhab, E.J. (1996). Direct Measurement of thermal fat crystal properties for milk fat fractionation. *Journal of the American Oil Chemists' Society*, **73**, 1603-1610.
- Breitschuh, B., Windhab, E.J. (1998). Parameters influencing cocrystallization and polymorphism in milk fat. *Journal of the American Oil Chemists' Society*, **75**, 897-904.
- Bylund, G. 2003. Dairy Processing Handbook. Sweden: Tetra Pak Processing Systems AB.
- Campos, R., Narine, S.S., Marangoni, A.G. (2002). Effect of cooling rate on the structure and mechanical properties of milk fat and lard. *Food Research International*, **35**, 971-981.
- Deffense, E. (1993). Milk fat fractionation today: A review. *Journal of the American Oil Chemists' Society*, **70**, 1193-1201.

DeMan, J. M. (1961). Physical properties of milk fat: II. some factors influencing crystallization. *Journal of Dairy Research*, **28**, 117–122.

DeMan J.M. (1963). The rheology of plastic fats. *Food in Canada*, **23**, 27-29.

DeMan, J. M. (1964). Effect of cooling procedures on consistency, crystal structure and solid fat content of milk fat. *Dairy Industries*, **29**, 244–246.

DeMan, J.M., Beers, A.M. (1987). Review: Fat crystal networks: Structure and rheological properties. *Journal of Texture Studies*, **18**, 303-318.

D'Souza, V., DeMan, J.M., deMan, L. (1992). Chemical and physical properties of the solid fat in commercial margarines. *Journal of the American Oil Chemists' Society*, **69**, 1198-1205.

Fatouh, A.E., Singh, R.K., Koehler, P.E., Mahran, G.A., El-Ghandour, M.A., Metwally, A.E. (2003). Chemical and thermal characteristic of buffalo butter oil fractions obtained by multi-step dry fractionation. *LWT-Food Science and Technology*, **36**, 483-496.

Fox P.F., McSweeney P.L.H. (1998). Dairy chemistry and biochemistry. London: Blackie Academic & Professional.

Foubert, I., Fredrick, E., Vereecken, J., Sichien, M., Dewettinck, K. (2008). Stop-and-return DSC method to study fat crystallization. *Thermochimica Acta*, **471**, 7-13.

Fox P.F, McSweeney P.L.H. (2006). Advanced dairy chemistry Volume 2 Lipids. Ireland: Springer Science.

Fredrick, E., Van de Walle, D., Walstra, P., Zijtveld, J.H., Fischer, S., Van der Meeren, P., Dewettinck, K. (2011). Isothermal crystallization behavior of milk fat in bulk and emulsified state. *International Dairy Journal*, **21**, 685-695.

Frelich, J., Šlachta, M., Hanuš, O., Špička, J., Samková, E. (2009). Fatty acid composition of cow milk fat produced on low-input mountain farms. *Czech Journal of Animal Science*, **2009**, 532-539.

Garti, N., Sato, K. (eds) (2001). Crystallization process in fats and lipid systems. New York: Marcel-Dekker.

Grall, D.S., Hartel, R.W. (1992). Kinetics of butterfat crystallization. *Journal of the American Oil Chemists' Society*, **8**, 741-747.

Heertje, I., Leunis, M., van Zeyl, W. J. M., Berends, E. (1987). Product microscopy of fatty products. *Food Microstructure*, **6**, 1-8.

Herrera, M.L., Hartel, R.W. (2000a). Effect of processing conditions on physical properties of a milk fat model system: micro-structure. *Journal of the American Oil Chemists' Society*, **77**, 1197–1204.

Herrera, M.L., Hartel, R.W. (2000b). Effect of processing conditions on physical properties of a milk fat model system: rheology. *Journal of the American Oil Chemists' Society*, **77**, 1189–1195.

Heyen, G., Alleman, X., Kalitventzeff, B., Dalemans, D. (1999). Modelling the butterfat crystallization process. *Computers & Chemical Engineering*, **23**, 819-822.

Hui Y.H. (2007). Handbook of food product manufacturing. Canada: Wiley-Interscience.

ISO. International Organization of Standardization. 2000. ISO 5509:2000. Animal and vegetable fats and oils – Preparation of methyl esters of fatty acids.

Kaylegian, K.E., and Lindsay, R.C. (eds.) (1995). Handbook of milk fat fractionation technology and applications. Champaign: AOCS Press.

Lopez, C., Lavigne, F., Lesieur, P., Keller, G., Ollivon, M. (2001). Thermal and structural behavior of anhydrous milk fat.2. Crystalline forms obtained by slow cooling. *Journal of Dairy Science*, **84**, 2402-2412.

Lopez, C., Bourgaux, C., Leiseur, P., Ollivon, M. (2002). Crystalline structures formed in cream and anhydrous milk fat at 4°C. *Lait*, **82**, 317-335.

Lopez, C., Lesieur, P., Bourgaux, C., Ollivon, M. (2005). Thermal and structural behavior of anhydrous milk fat.3.Influence of cooling rate. *Journal of Dairy Science*, **88**, 511-526.

Lopez, C., Bourgaux, C., Leiseur, P., Riaublanc, A., Ollivon, M. (2006). Milk fat and primary fractions obtained by dry fractionation 1. Chemical composition and crystallization properties. *Chemistry and Physics of Lipids*, **144**, 17-33.

Lopez, C., Ollivon, M. (2009). Triglycerides obtained by dry fractionation of milk fat 2. Thermal properties and polymorphic evolutions on heating. *Chemistry and Physics of Lipids*, **159**, 1-12.

Lopez, C., Bourgaux, C., Leiseur, P., Ollivon, M. (2007). Coupling of time-resolved synchrotron X-ray diffraction and DSC to elucidate the crystallisation properties and polymorphism of triglycerides in milk fat globules. *Lait*, **87**, 459–480.

Månsson, H. (2008). Fatty acids in bovine milk fat. *Food and Nutrition Research*, **52**, 13.

Marangoni, A.G. (2002). The nature of fractality in fat crystal networks. *Trends in Food Science and Technology*, **13**, 37-47.

Mazzanti, G., Guthrie, S., Sirota, E.B., Marangoni, A.G., Idzial, H.J. (2004). Effect of minor components and temperature profiles on polymorphism in milk fat. *Crystal Growth and Design*, **4**, 1303–1309.

Mazzanti, G., Marangoni, A. G., Idziak, S. H. J. (2009). Synchrotron study on crystallization kinetics of milk fat under shear flow. *Food Research International*, **42**, 5-6.

McGauley, S.E. (2001). *The relationship between polymorphism, crystallization kinetics and microstructure of statically crystallized cocoa butter*. The Faculty of Graduate Studies, The University of Guelph, Canada.

Narine, S.S., Marangoni, A.G. (1999). Relating structure of fat crystal networks to mechanical properties: A review. *Food Research International*, **32**, 227-248.

Narine, S. S., Marangoni, A. G. (1999). Fractal Nature of Fat Crystal Networks. *Physical Review E*, **59**, 1908-1920.

Oldörp, K. (2007). What happens when rheological properties change? Looking into rheological properties with simultaneous collection of microscopic images. *Annual Transactions of the Nordic Rheology Society*, **15**.

Ozbayram, O. (2000). *Stability of butter oils*. Graduate School of Natural and Applied Sciences, University of Gaziantep, Turkey.

Parkinson, C., Sherman, P., Matsumoto, S. (1970). Fat crystals and the flow rheology of butter and margarine. *Journal of Texture Studies*, **1**, 206-213.

Ranken, M.D. 1988. *Food Industrial Manual*. Blackie.

Shahidi, F. (edt) 2005. *Bailey's Industrial Oil and Fat Products*. Wiley-Interscience.

Shi, Y., Smith, C.M., Hartel, R.W. (2001). Compositional effects on milk fat crystallization. *Journal of dairy science*, **84**, 2392-2401.

Smet, K., Coudijzer, K., Fredrick, E., De Campeneere, S., De Block, J., Wouters, J., Raes, K., Dewettinck, K. (2010). Crystallization behavior of milk fat obtained from linseed-fed cows. *Journal of Dairy Science*, **93**, 495-505.

Sri K, Vishweshwar J.L. (2005). *Quality control of milk and processing*. India: Telugu Academi Publication.

Ten Grotenhuis, E., van Aken, G.A., van Malssen, K.F., Schenk, H. (1999). Polymorphism of milk fat studied by differential scanning calorimeter and real-time X-ray powder diffraction. *Journal of the American Oil Chemists' Society*, **76**, 1031-1039.

Timms, R.E. (1980). The phase behaviour and polymorphism of milk fat, milk fat fractions and fully hardened milk fat. *The Australian journal of dairy technology*, **35**,47-53.

Timms, R.E. (1994). Physical chemistry of fats. In: Moran, D.P.J. and Rajah, K.K. (edt.). *Fats in food products*. Blackie Academic and Professional.

Van Aken, G.A., Ten Grotenhuis, E., Van Langevelde, A.J., Schenk, H. (1999). Composition and crystallization of milk fat fractions. *Journal of the American Oil Chemists' Society*, **76**, 1323-1331.

Van Aken, G.A., Visser, K.A. (2000). Firmness and crystallization of milk fat in relation to processing conditions. *Journal of Dairy Science*, **83**, 1919–1932.

Vanhoutte, B. (2002). *Milk fat crystallization: Fractionation and texturation*. Graduate School of Applied Biological Sciences: Chemistry, Ghent University, Belgium.

Varnam, A., Sutherland, J.P. 2001. *Milk and milk products: Technology, chemistry and microbiology*. USA: An Aspen Publication.

Walstra, P. and Jenness, R. (eds) (1984). *Dairy chemistry and physics*. 5 Lipids. New York: . JohnWiley and Sons.

Widlak, N., Hartel, R., Narine, S. (eds). 2001. *Crystallization and solidification properties of lipids*. USA: AOCS Press.

Wiking, L., Graef, V.D., Rasmussen, M., Dewettinck, K. (2009). Relations between crystallisation mechanisms and microstructure of milk fat. *International Dairy Journal*, **19**, 424-430.

Woodrow, I.L., deMan, J.M. (1968). Polymorphism in milk fat shown by X-ray diffraction and infrared spectroscopy. *Journal of Dairy Science*, **51**, 996-1000.

Wright, A.J., Hartel, R.W., Narine, S.S., Marangoni, A.G. (2000). The effect of minor components on milk fat crystallization. *Journal of the American Oil Chemists' Society*, **77**, 463-475.

Wright, A.J., Scanlon, M.G., Hartel, R.W., Marangoni, A.G. (2001). Rheological properties of milkfat and butter. *Concise Reviews and Hypotheses in Food Science*, **66**, 1056-1071.

Zeitoun, N.A.M., Neff, W.E., List, G.R., Mounts, T.L. (1993). Physical properties of interesterified fat blends. . *Journal of the American Oil Chemists' Society*, **70**, 467-471.

APPENDIX A

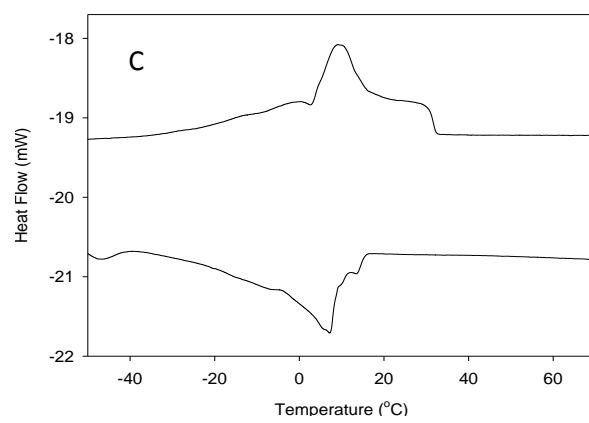
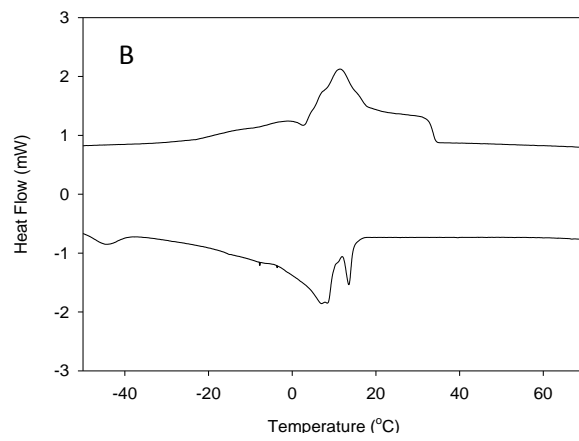
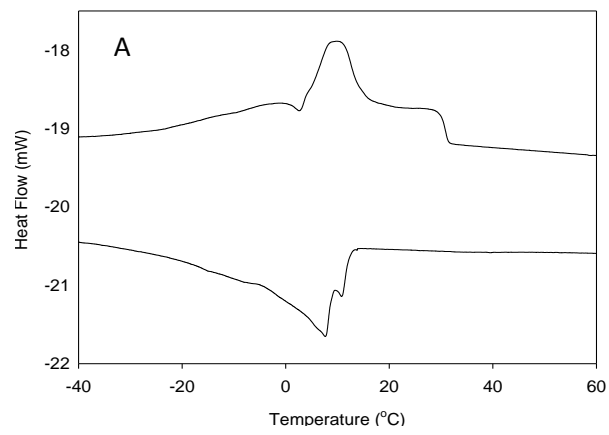


Figure A.1. Melting profile of milk fat samples cooling at 2°C/min (A) winter milk fat, (B) summer milk fat, (C) spring milk fat

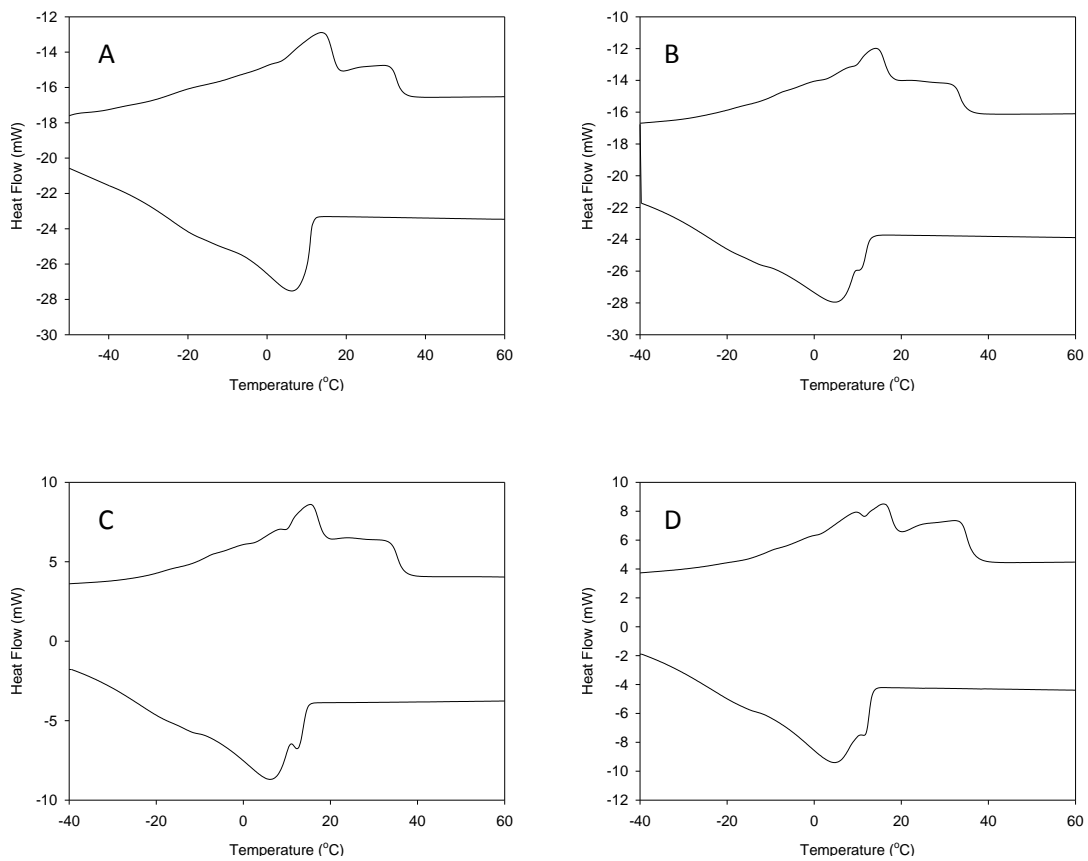


Figure A.2. Melting profile of milk fat samples cooling at 10°C/min (A) winter milk fat, (B) spring milk fat, (C) summer milk fat, (D) autumn milk fat

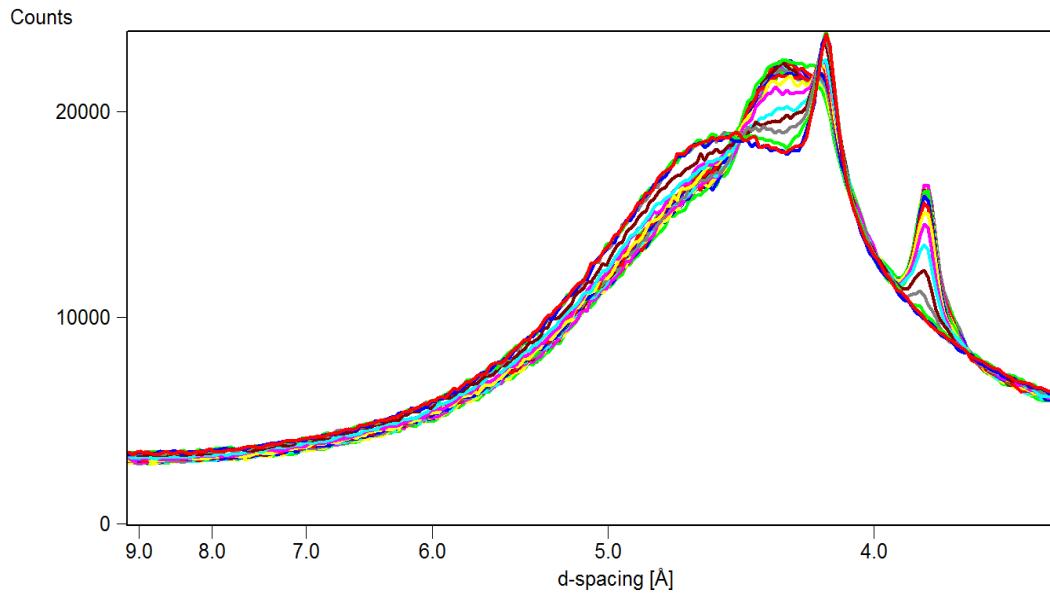


Figure A.3. Wide angle X-ray diffraction pattern of the isothermal crystallization after slow cooling (2°C/min) of the autumn milk fat from 70 to 10°C

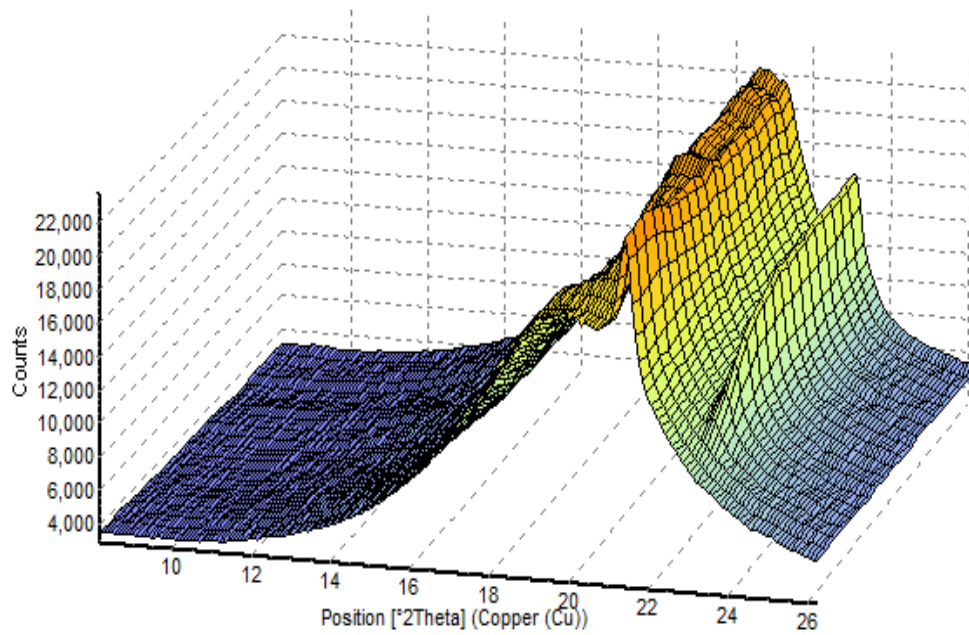


Figure A.4. 3D plots of X-ray diffraction pattern of the isothermal crystallization after slow cooling (2°C/min) of the autumn milk fat from 70 to 10°C

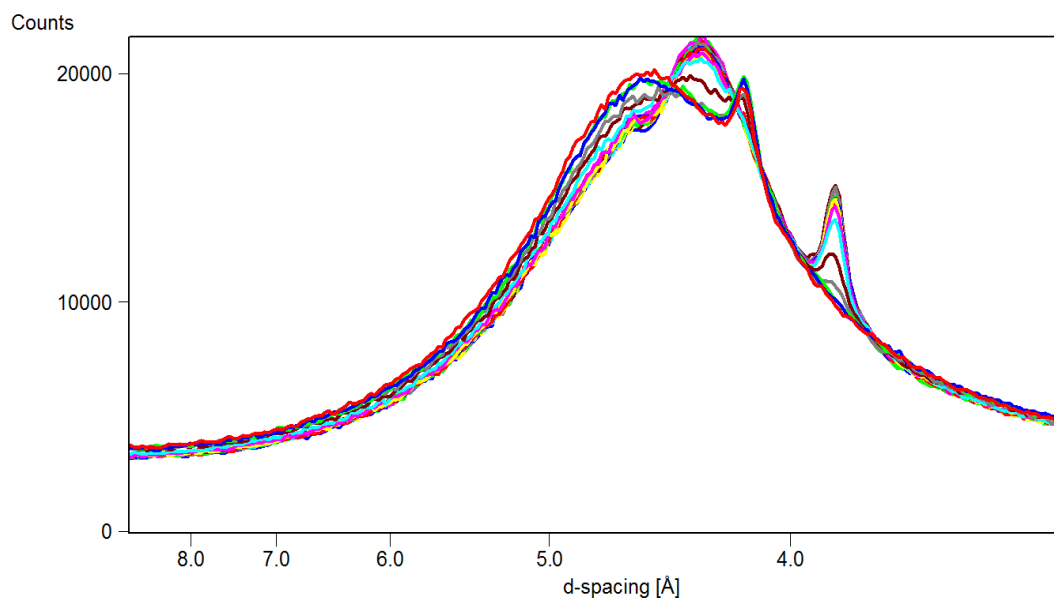


Figure A.5. Wide angle X-ray diffraction pattern of the isothermal crystallization after slow cooling (2°C/min) of the autumn milk fat from 70 to 14°C

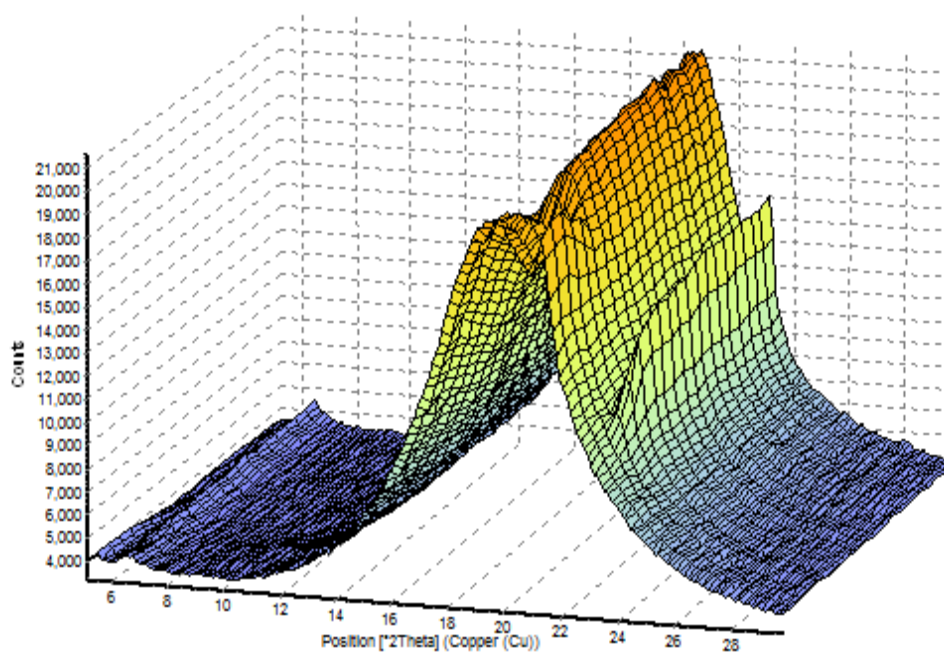


Figure A.6. 3D plots of X-ray diffraction pattern of of the isothermal crystallization after slow cooling (2°C/min) of the autumn milk fat from 70 to 14°C

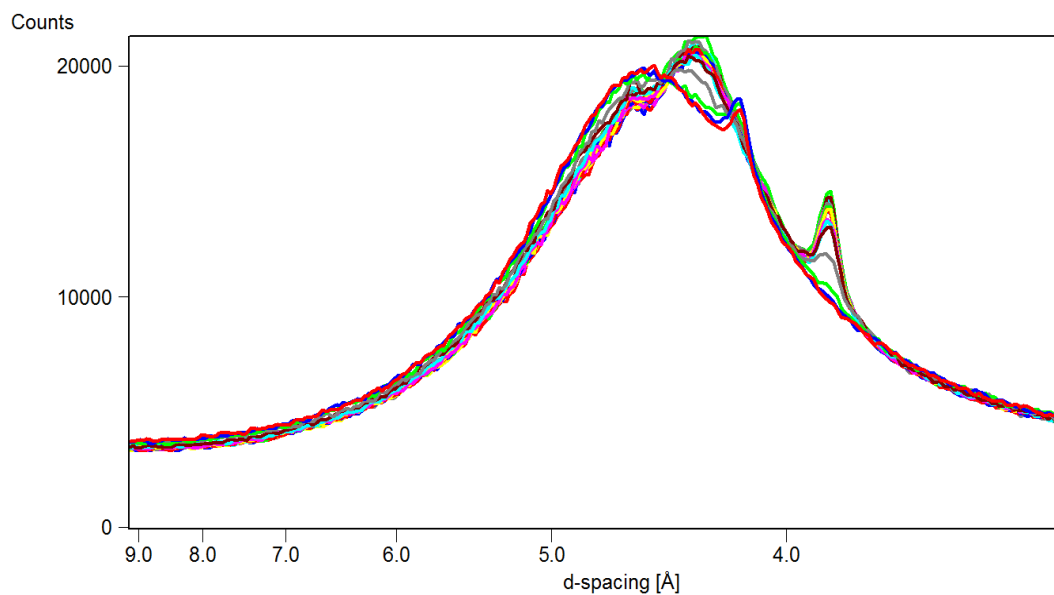


Figure A.7. Wide angle X-ray diffraction pattern of the isothermal crystallization after slow cooling (2°C/min) of the autumn milk fat from 70 to 17°C

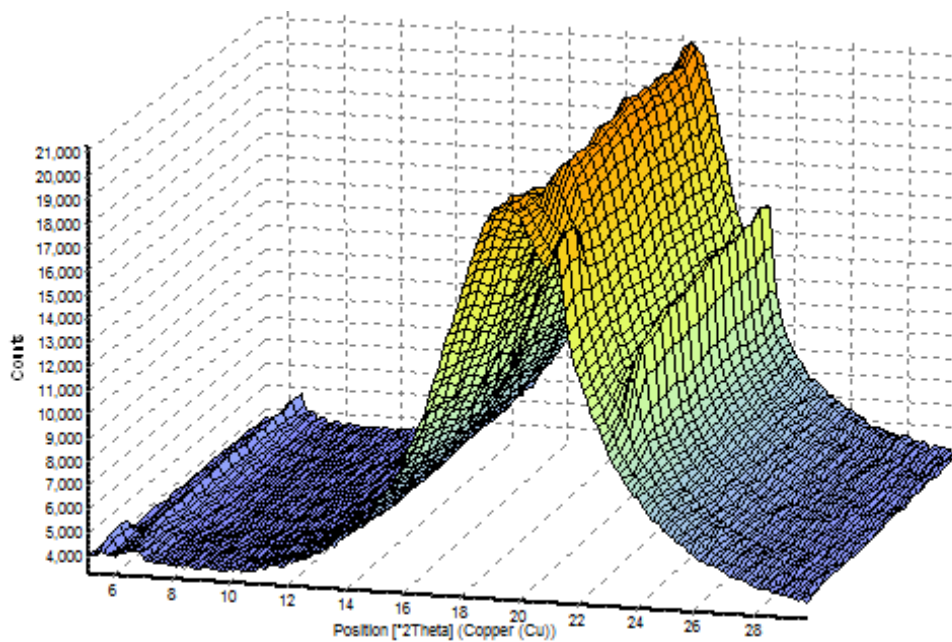


Figure A.8. 3D plots of X-ray diffraction pattern of of the isothermal crystallization after slow cooling (2°C/min) of the autumn milk fat from 70 to 17°C

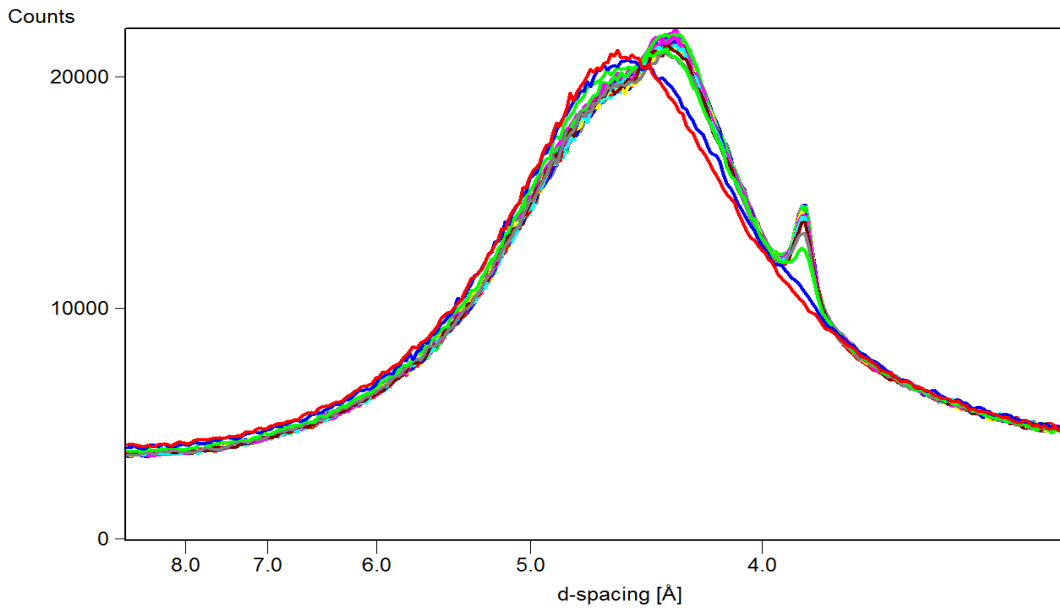


Figure A.9. Wide angle X-ray diffraction pattern of the isothermal crystallization after slow cooling (2°C/min) of the autumn milk fat from 70 to 20°C

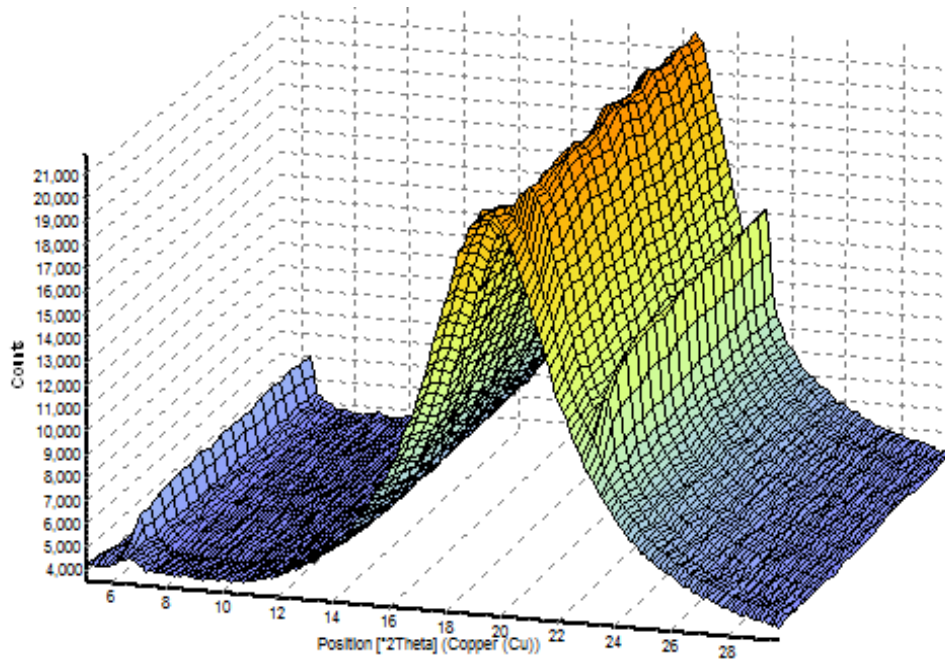


Figure A.10. 3D plots of X-ray diffraction pattern of of the isothermal crystallization after slow cooling (2°C/min) of the autumn milk fat from 70 to 20°C

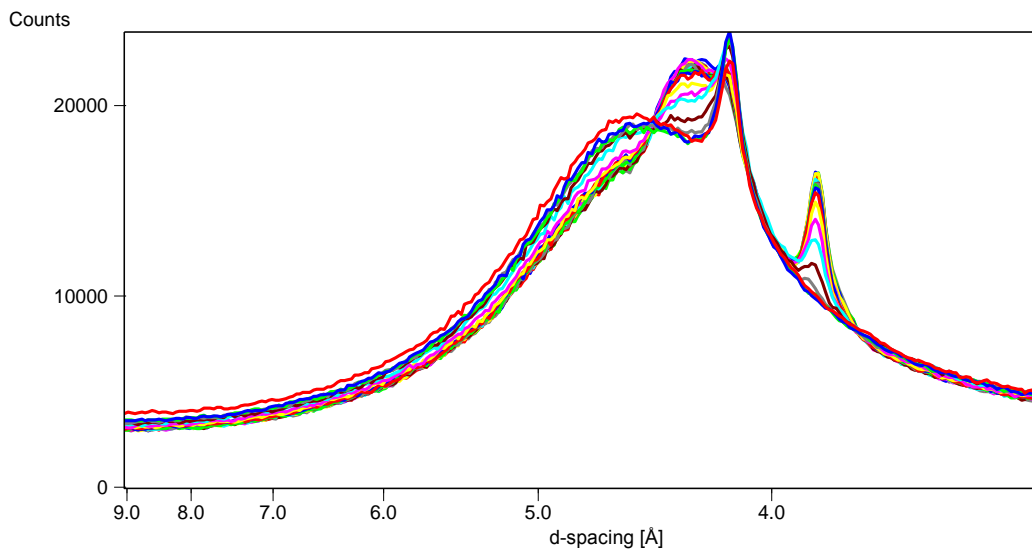


Figure A.11. Wide angle X-ray diffraction pattern of the isothermal crystallization after fast cooling ($10^{\circ}\text{C}/\text{min}$) of the autumn milk fat from 70 to 10°C

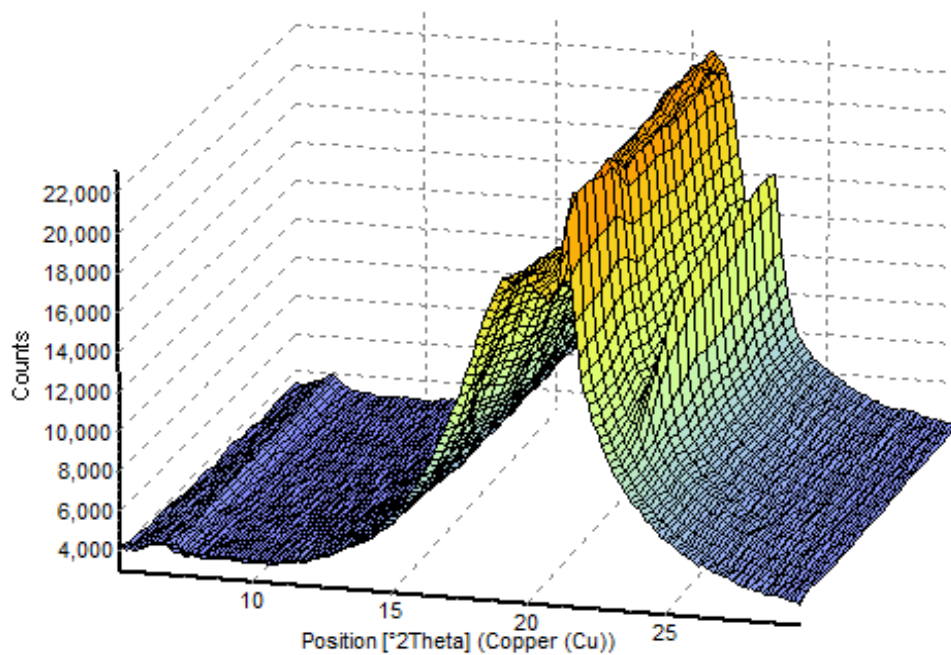


Figure A.12. 3D plots of X-ray diffraction pattern of of the isothermal crystallization after fast cooling ($10^{\circ}\text{C}/\text{min}$) of the autumn milk fat from 70 to 10°C

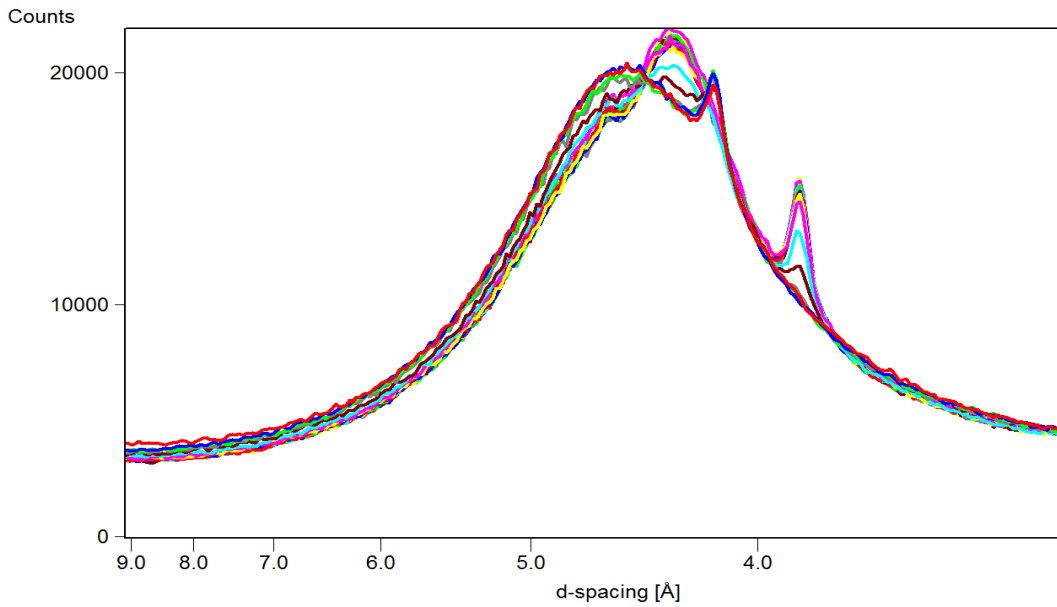


Figure A.13. Wide angle X-ray diffraction pattern of the isothermal crystallization after fast cooling (10°C/min) of the autumn milk fat from 70 to 14°C

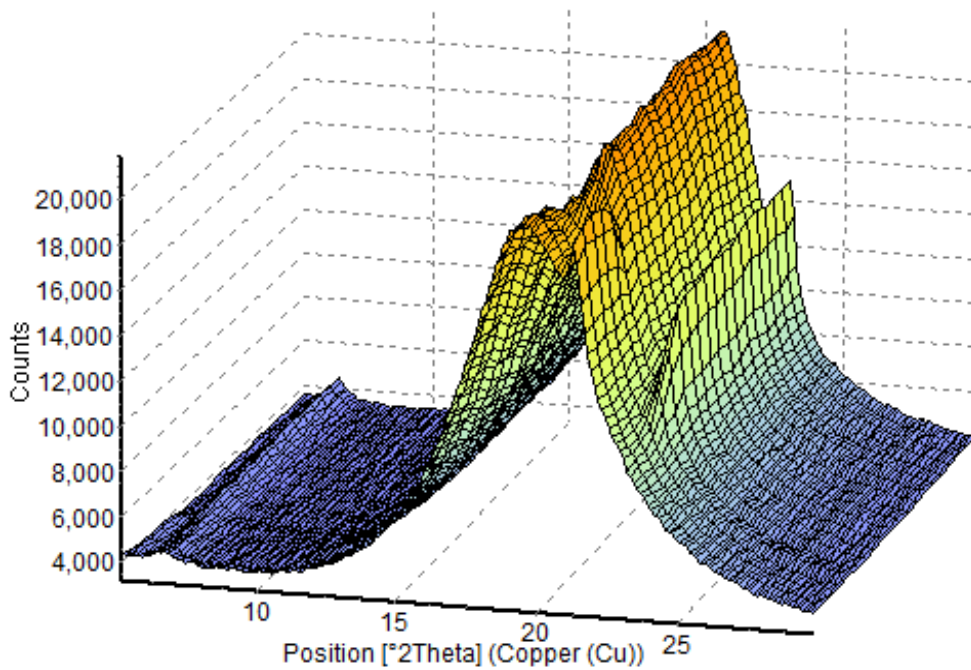


Figure A.14. 3D plots of X-ray diffraction pattern of of the isothermal crystallization after fast cooling (10°C/min) of the autumn milk fat from 70 to 14°C

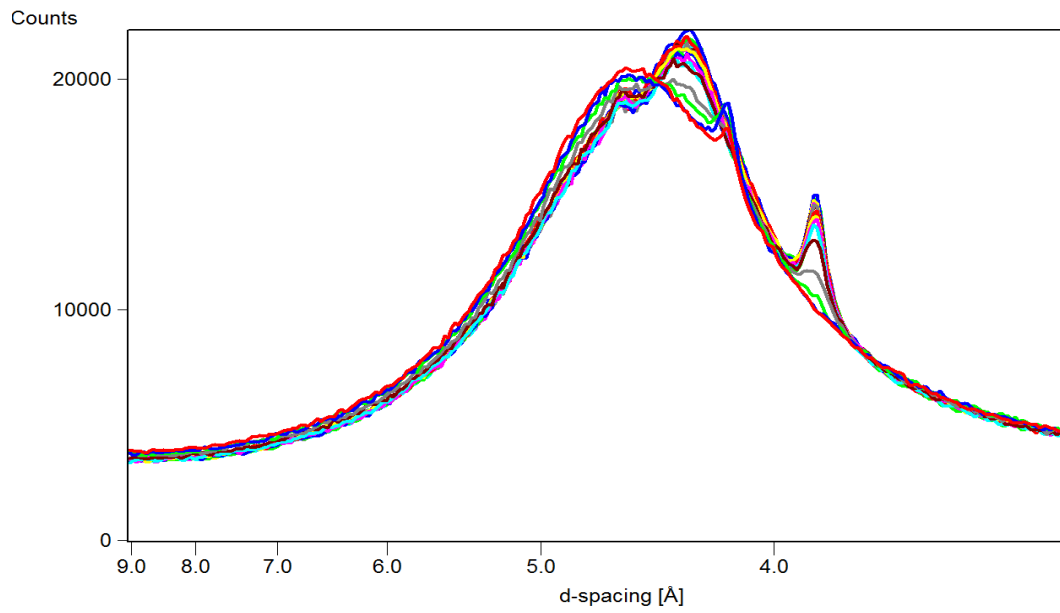


Figure A.15. Wide angle X-ray diffraction pattern of the isothermal crystallization after fast cooling (10°C/min) of the autumn milk fat from 70 to 17°C

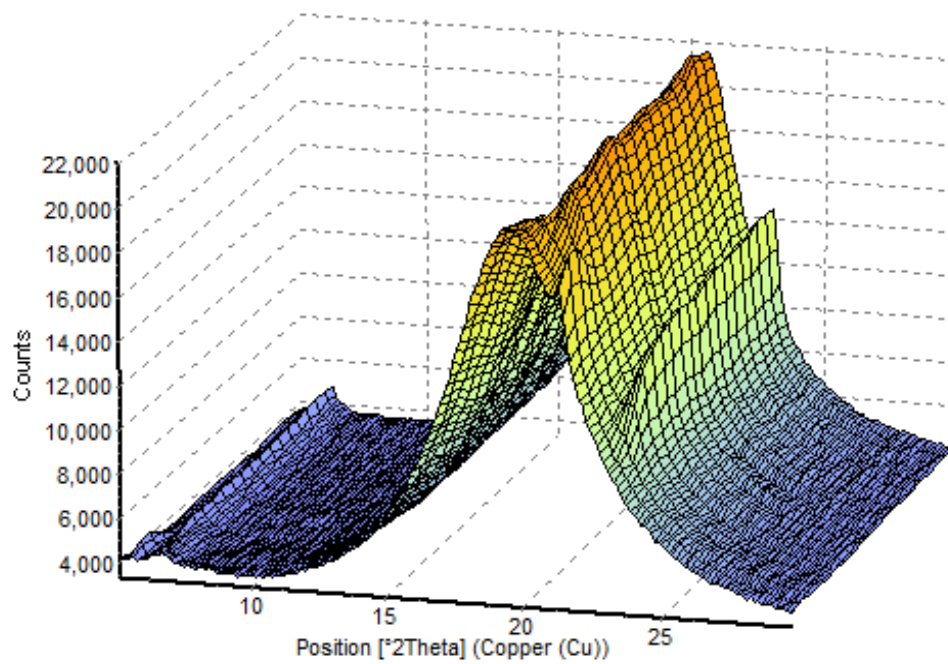


Figure A.16. 3D plots of X-ray diffraction pattern of of the isothermal crystallization after fast cooling (10°C/min) of the autumn milk fat from 70 to 17°C

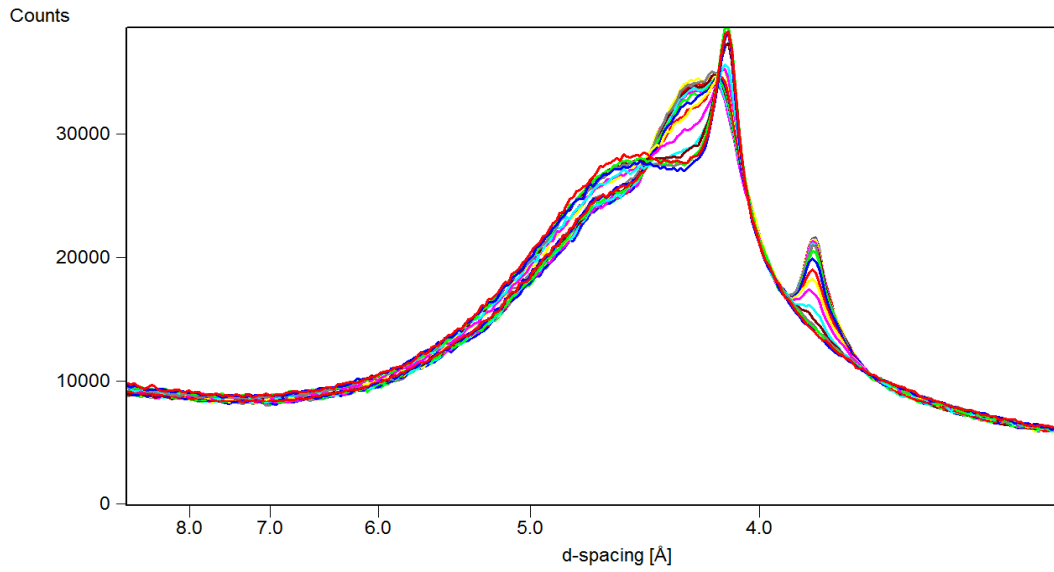


Figure A.17. Wide angle X-ray diffraction pattern of the isothermal crystallization after slow cooling (2°C/min) of the winter milk fat from 70 to 5°C

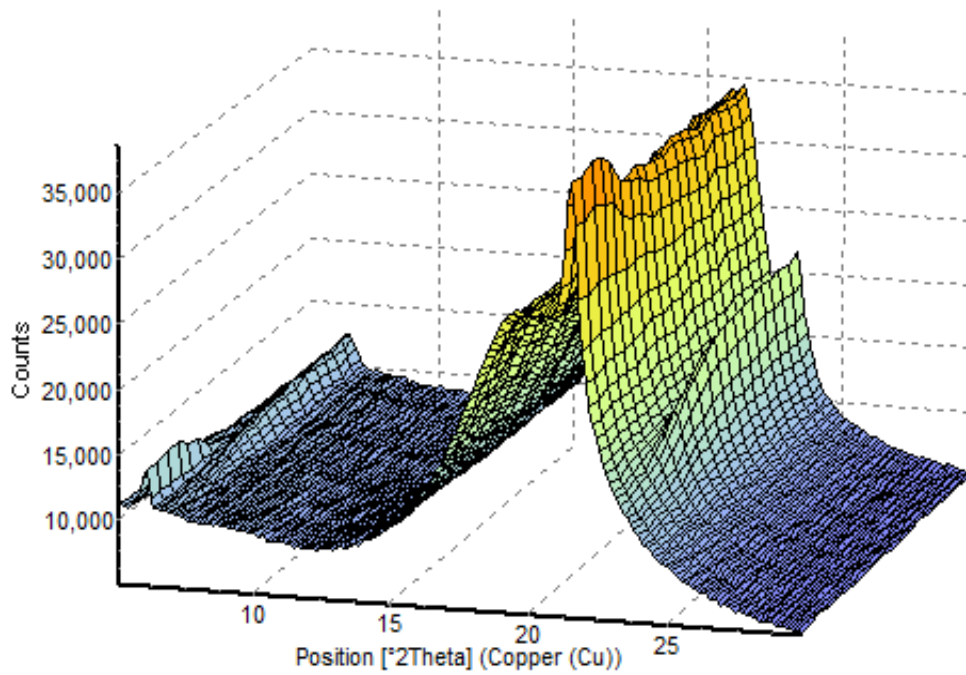


Figure A.18. 3D plots of X-ray diffraction pattern of of the isothermal crystallization after slow cooling (2°C/min) of the winter milk fat from 70 to 5°C

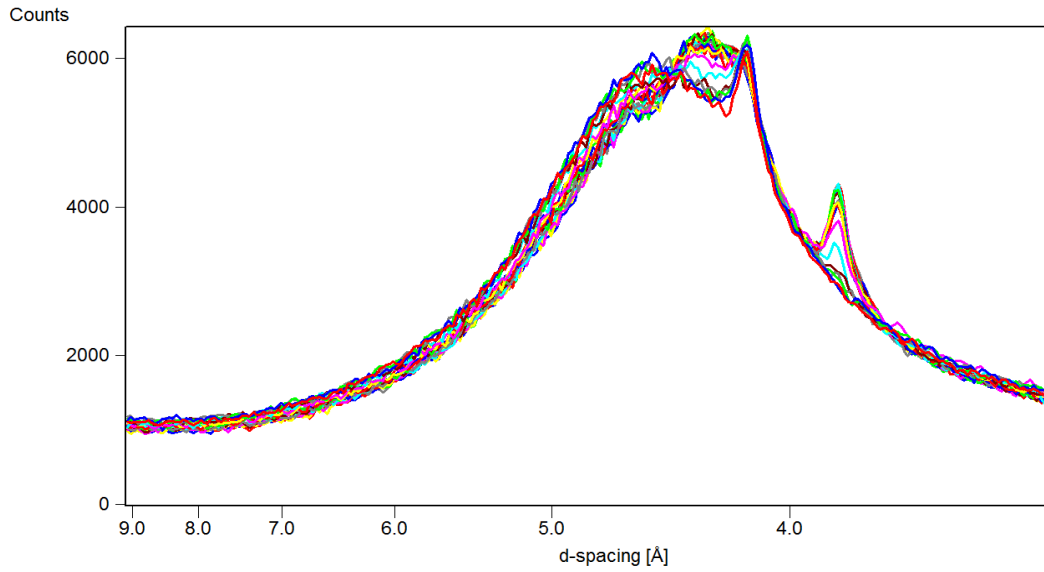


Figure A.19. Wide angle X-ray diffraction pattern of the isothermal crystallization after slow cooling (2°C/min) of the winter milk fat from 70 to 10°C

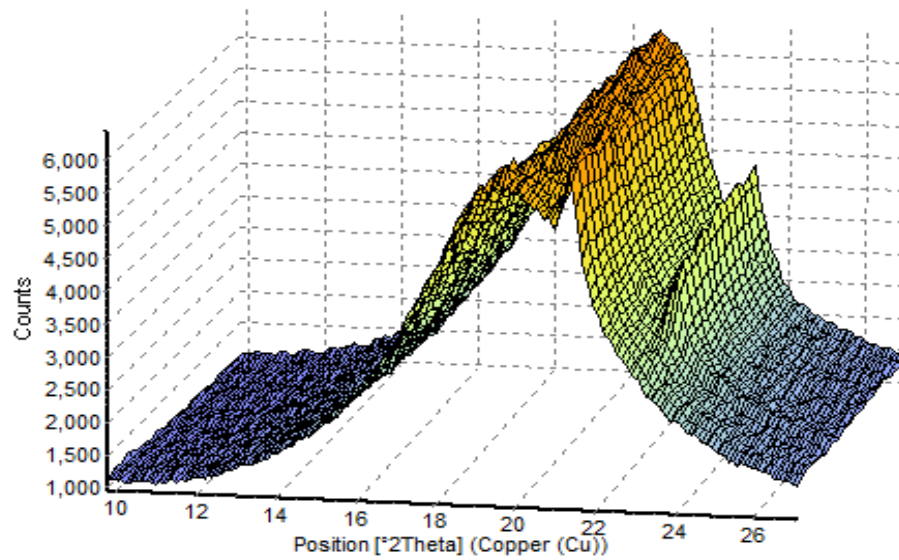


Figure A.20. 3D plots of X-ray diffraction pattern of of the isothermal crystallization after slow cooling (2°C/min) of the winter milk fat from 70 to 10°C

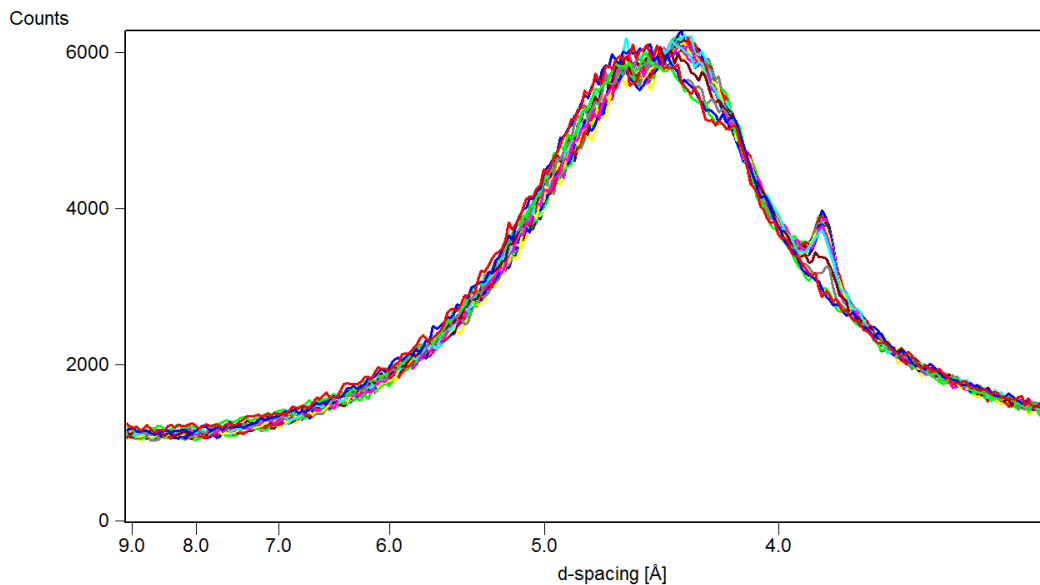


Figure A.21. Wide angle X-ray diffraction pattern of the isothermal crystallization after slow cooling (2°C/min) of the winter milk fat from 70 to 14°C

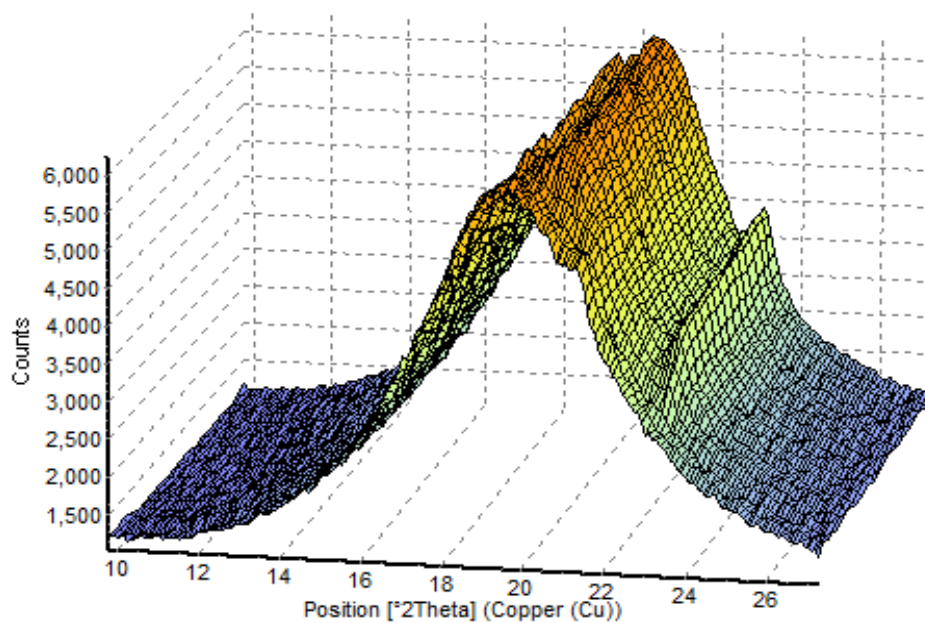


Figure A.22. 3D plots of X-ray diffraction pattern of of the isothermal crystallization after slow cooling (2°C/min) of the winter milk fat from 70 to 14°C

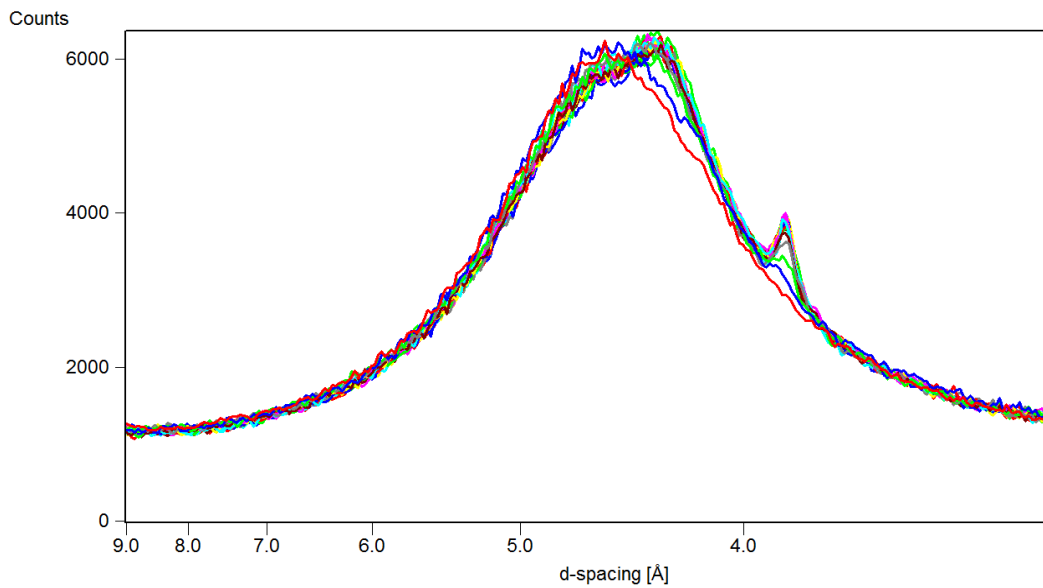


Figure A.23. Wide angle X-ray diffraction pattern of the isothermal crystallization after slow cooling (2°C/min) of the winter milk fat from 70 to 17°C

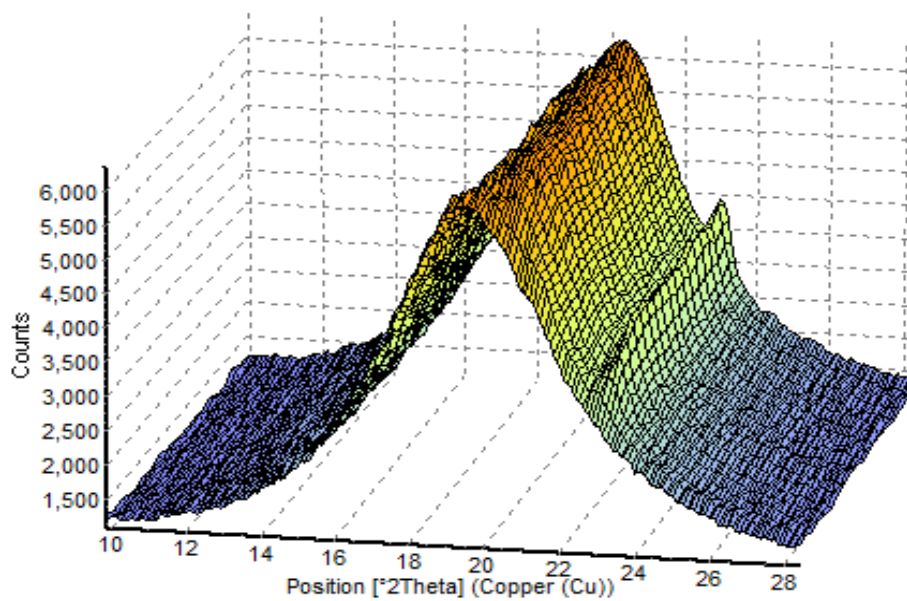


Figure A.24. 3D plots of X-ray diffraction pattern of of the isothermal crystallization after slow cooling (2°C/min) of the winter milk fat from 70 to 17°C

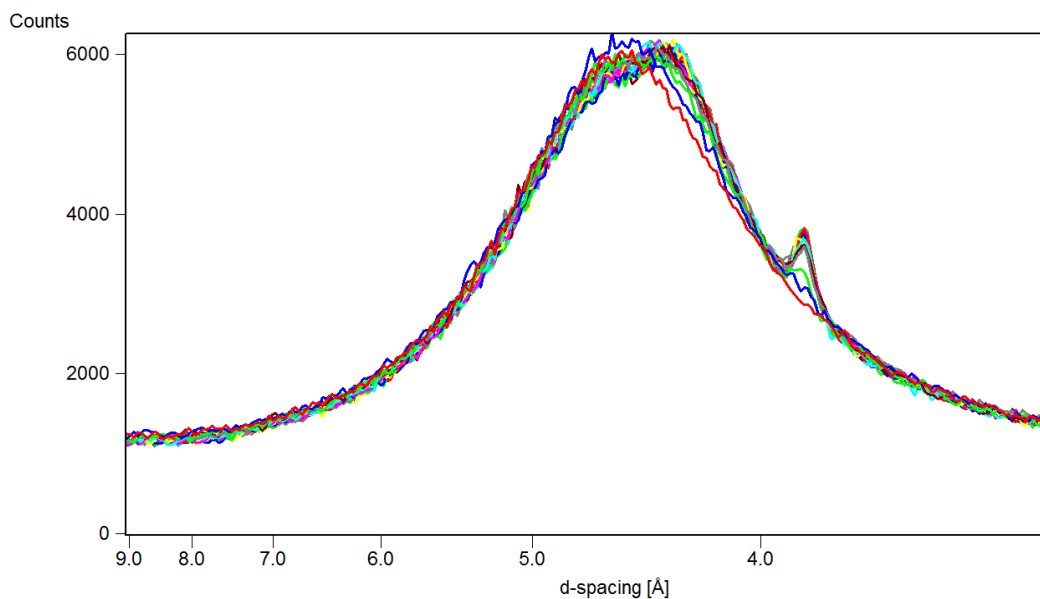


Figure A.25. Wide angle X-ray diffraction pattern of the isothermal crystallization after slow cooling (2°C/min) of the winter milk fat from 70 to 20°C

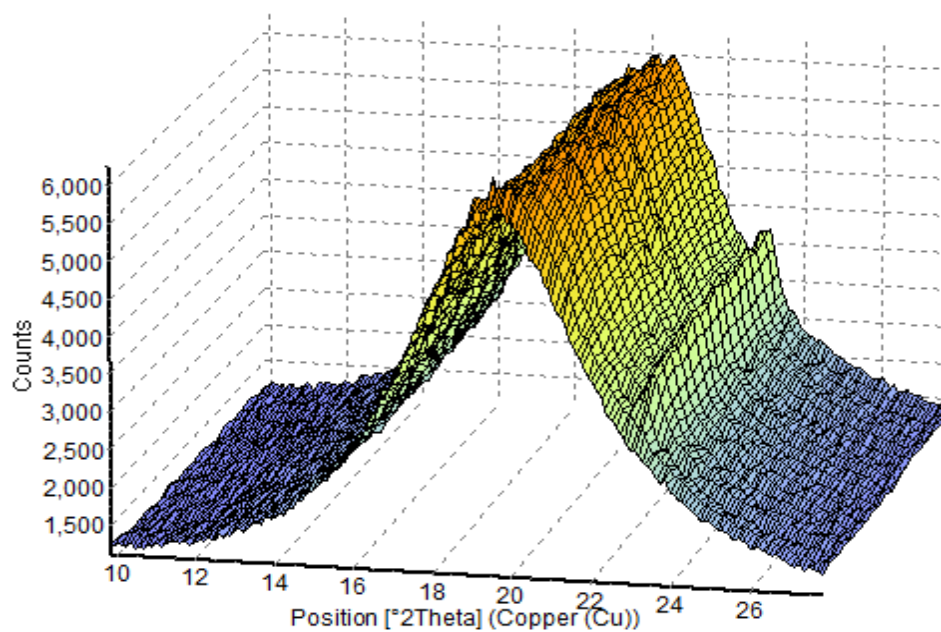


Figure A.26. 3D plots of X-ray diffraction pattern of of the isothermal crystallization after slow cooling (2°C/min) of the winter milk fat from 70 to 20°C

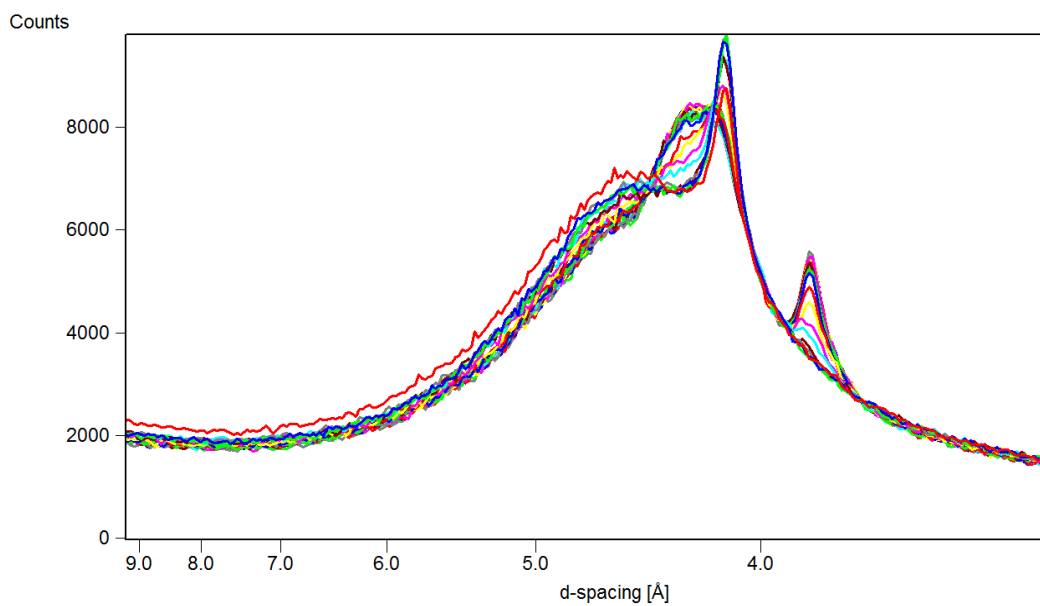


Figure A.27. Wide angle X-ray diffraction pattern of the isothermal crystallization after fast cooling (10°C/min) of the winter milk fat from 70 to 5°C

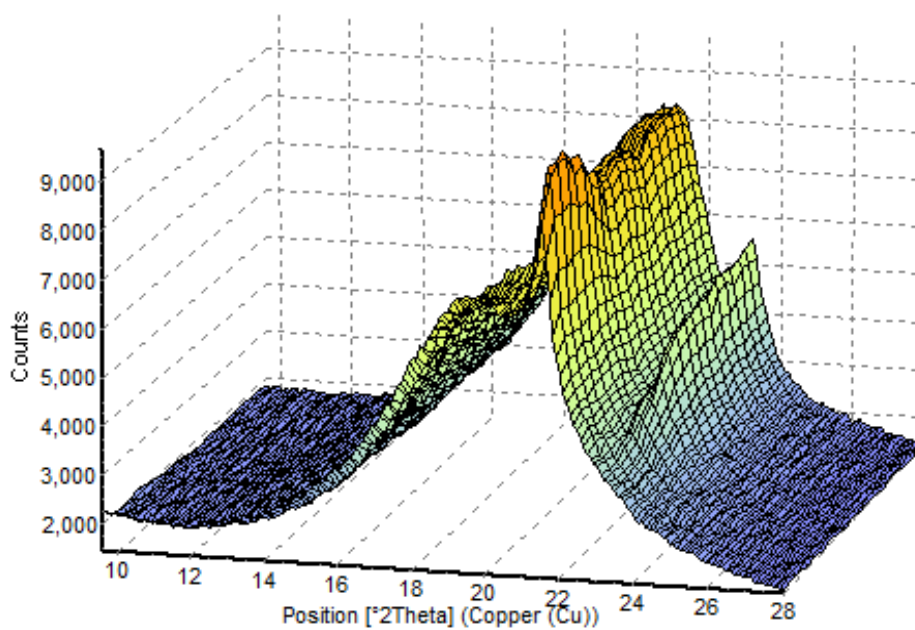


Figure A.28. 3D plots of X-ray diffraction pattern of of the isothermal crystallization after fast cooling (10°C/min) of the winter milk fat from 70 to 5°C

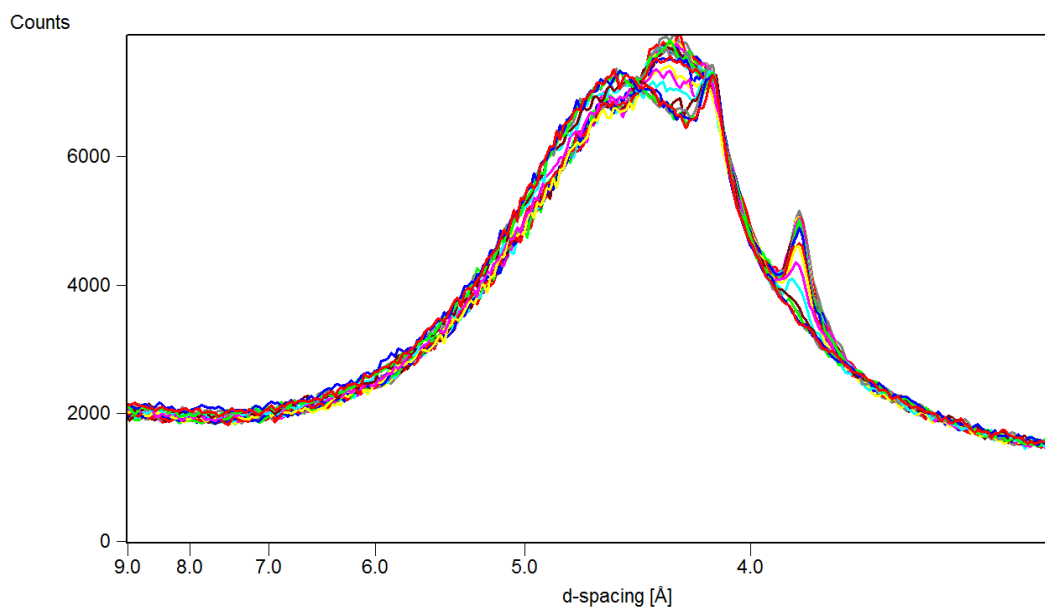


Figure A.29. Wide angle X-ray diffraction pattern of the isothermal crystallization after fast cooling (10°C/min) of the winter milk fat from 70 to 10°C

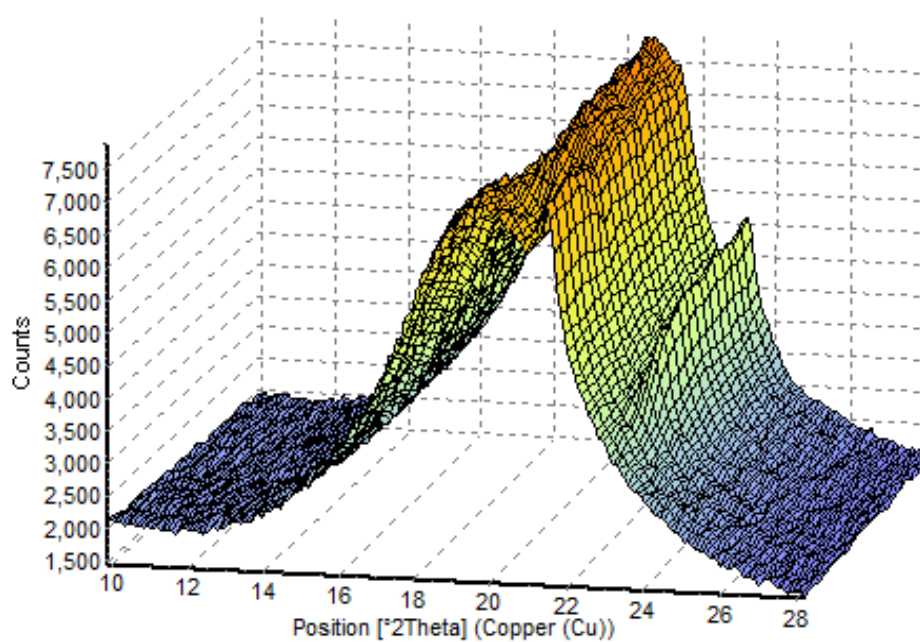


Figure A.30. 3D plots of X-ray diffraction pattern of of the isothermal crystallization after fast cooling (10°C/min) of the winter milk fat from 70 to 10°C

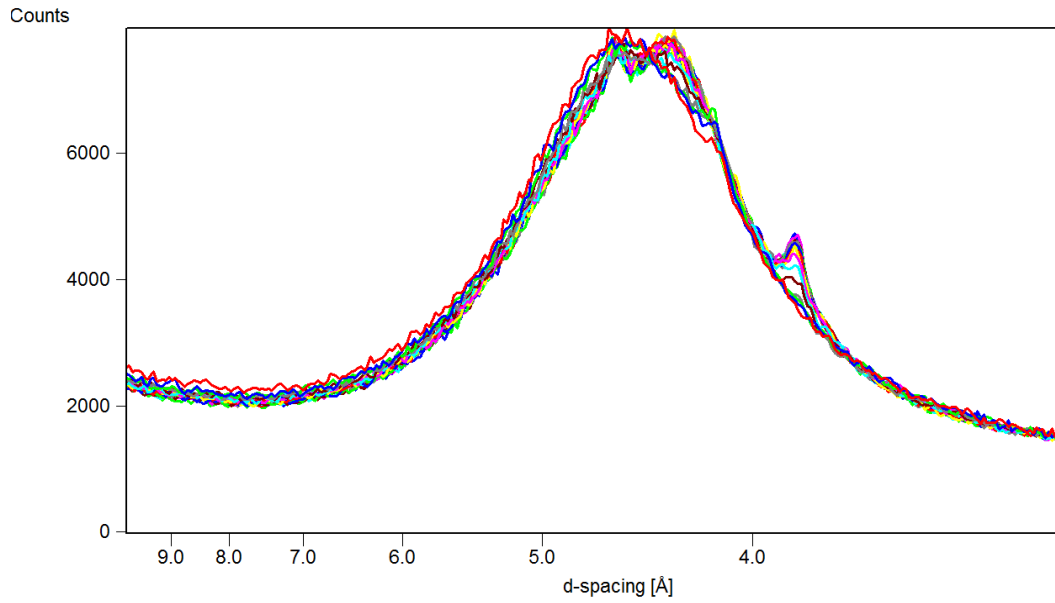


Figure A.31. Wide angle X-ray diffraction pattern of the isothermal crystallization after fast cooling (10°C/min) of the winter milk fat from 70 to 14°C

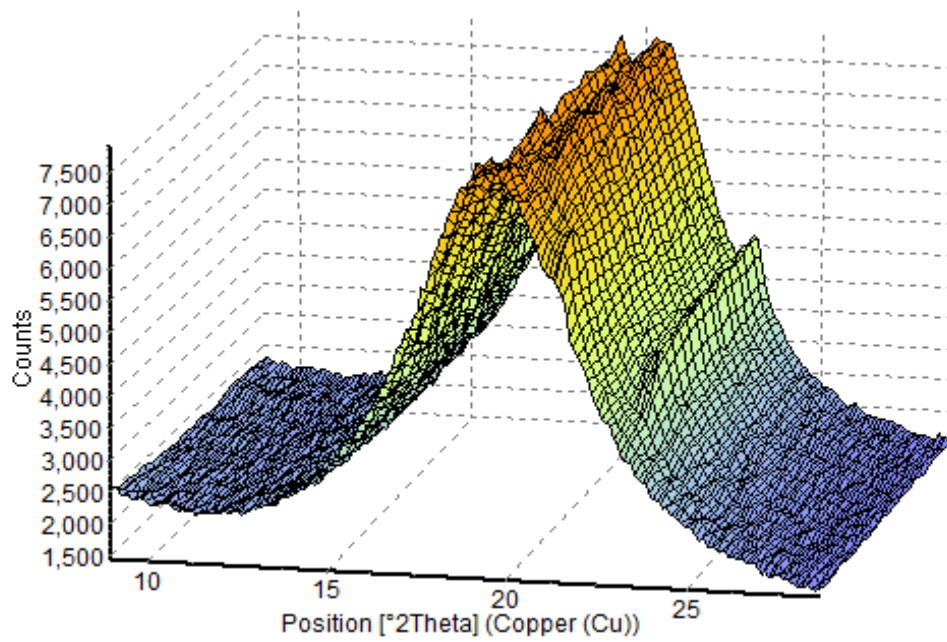


Figure A.32. 3D plots of X-ray diffraction pattern of of the isothermal crystallization after fast cooling (10°C/min) of the winter milk fat from 70 to 14°C

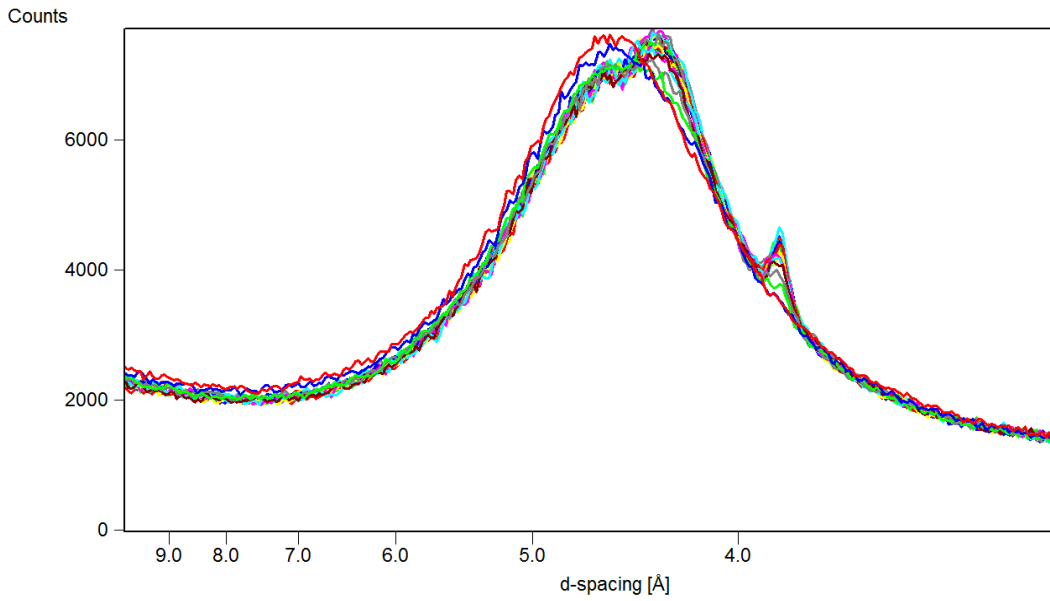


Figure A.33. Wide angle X-ray diffraction pattern of the isothermal crystallization after fast cooling (10°C/min) of the winter milk fat from 70 to 17°C

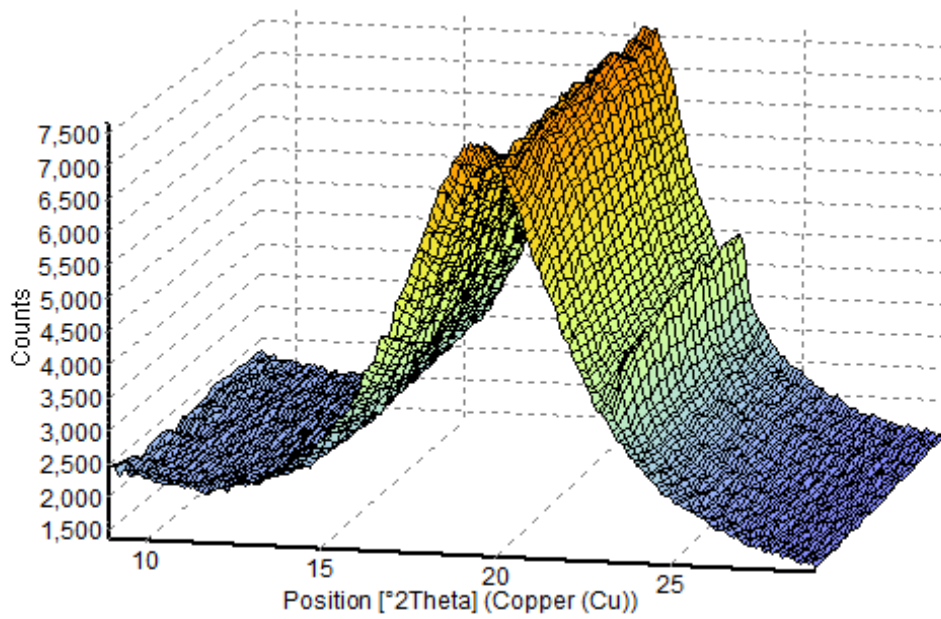


Figure A.34. 3D plots of X-ray diffraction pattern of of the isothermal crystallization after fast cooling (10°C/min) of the winter milk fat from 70 to 17°C

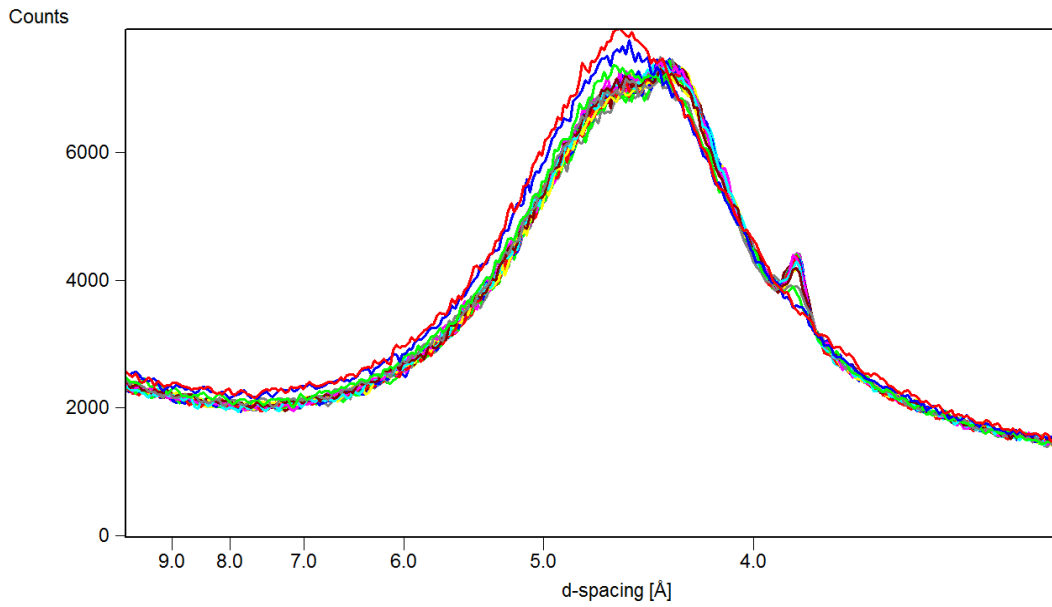


Figure A.35. Wide angle X-ray diffraction pattern of the isothermal crystallization after fast cooling (10°C/min) of the winter milk fat from 70 to 20°C

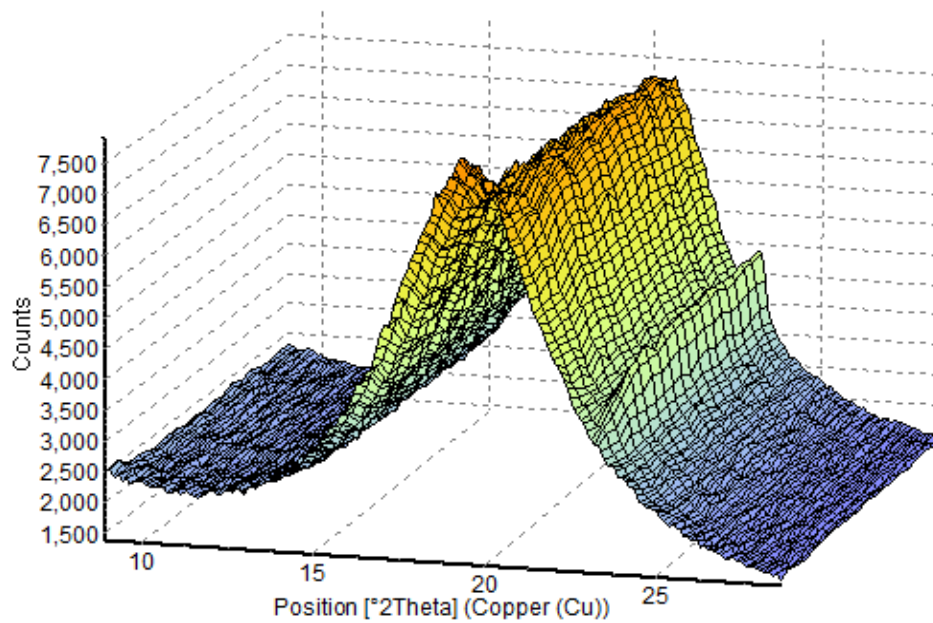


Figure A.36. 3D plots of X-ray diffraction pattern of of the isothermal crystallization after fast cooling (10°C/min) of the winter milk fat from 70 to 20°C

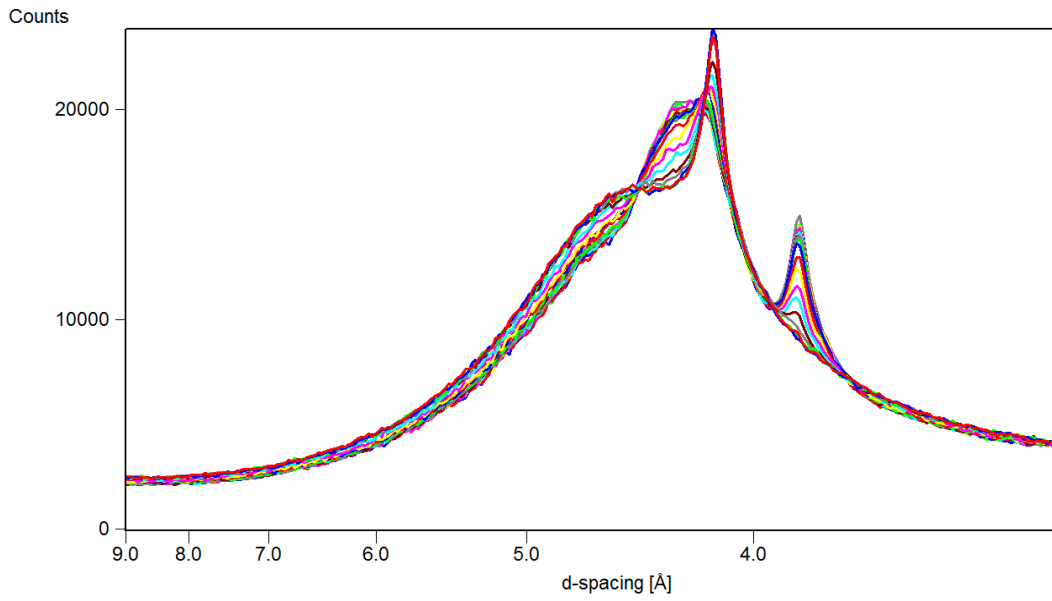


Figure A.37. Wide angle X-ray diffraction pattern of the isothermal crystallization after slow cooling (2°C/min) of the spring milk fat from 70 to 5°C

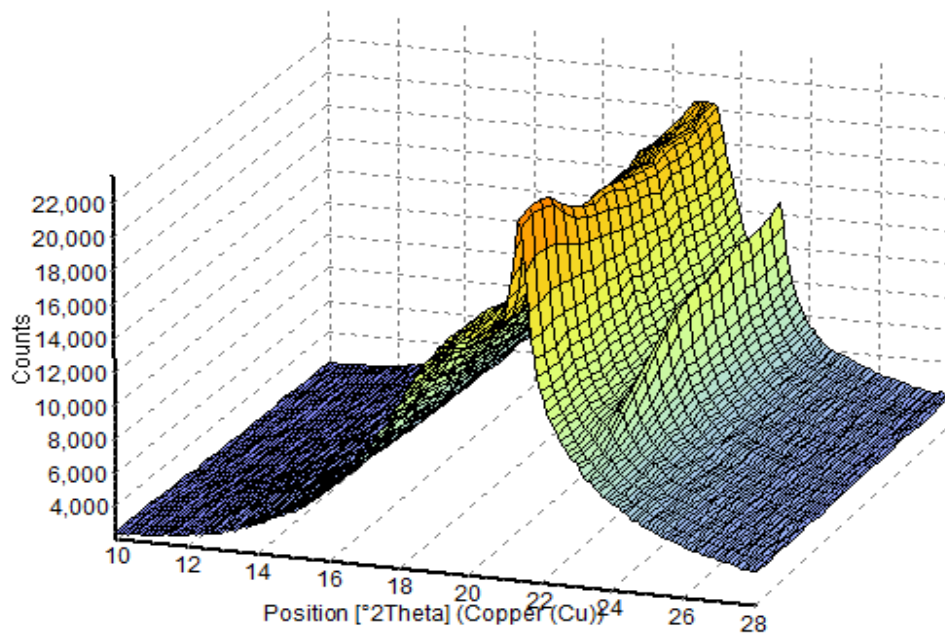


Figure A.38. 3D plots of X-ray diffraction pattern of of the isothermal crystallization after slow cooling (2°C/min) of the spring milk fat from 70 to 5°C

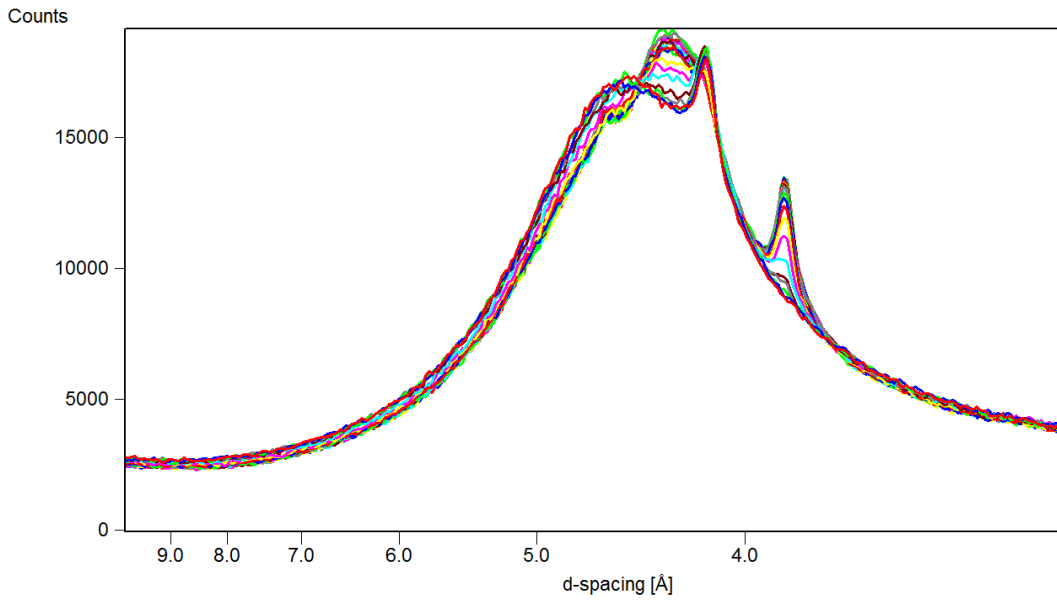


Figure A.39. Wide angle X-ray diffraction pattern of the isothermal crystallization after slow cooling (2°C/min) of the spring milk fat from 70 to 10°C

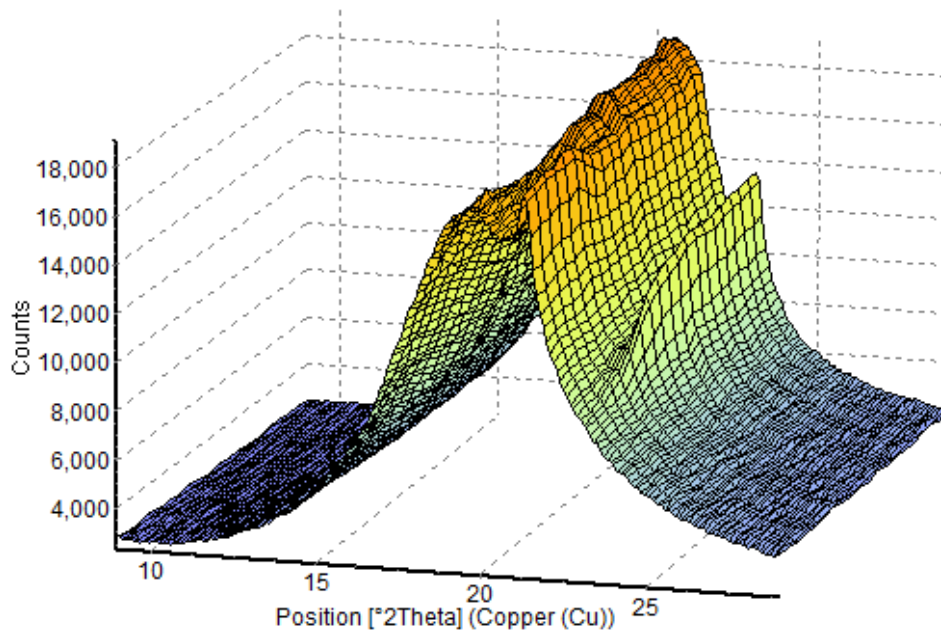


Figure A.40. 3D plots of X-ray diffraction pattern of of the isothermal crystallization after slow cooling (2°C/min) of the spring milk fat from 70 to 10°C

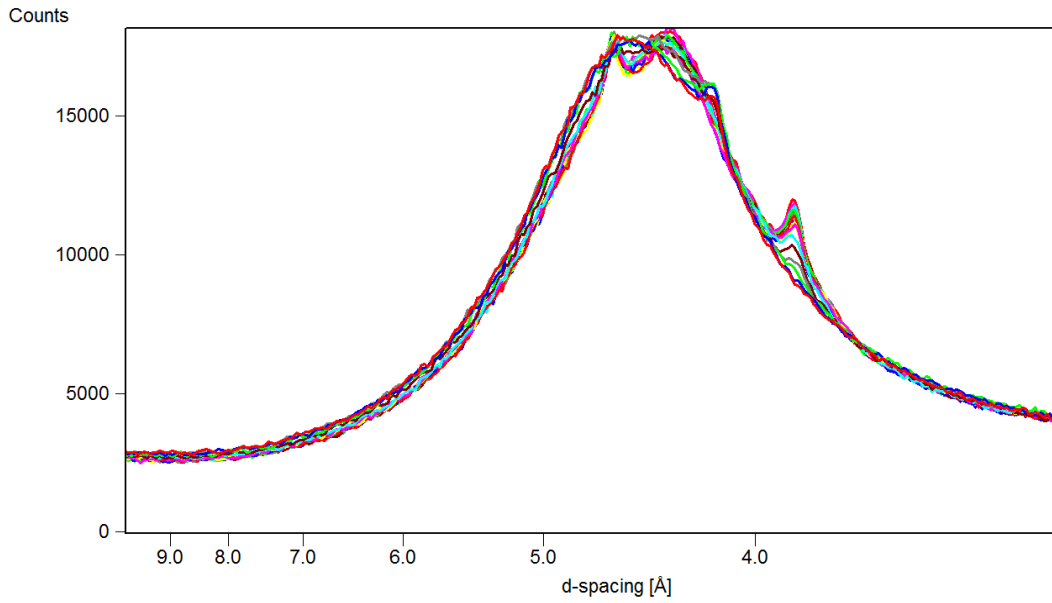


Figure A.41. Wide angle X-ray diffraction pattern of the isothermal crystallization after slow cooling (2°C/min) of the spring milk fat from 70 to 14°C

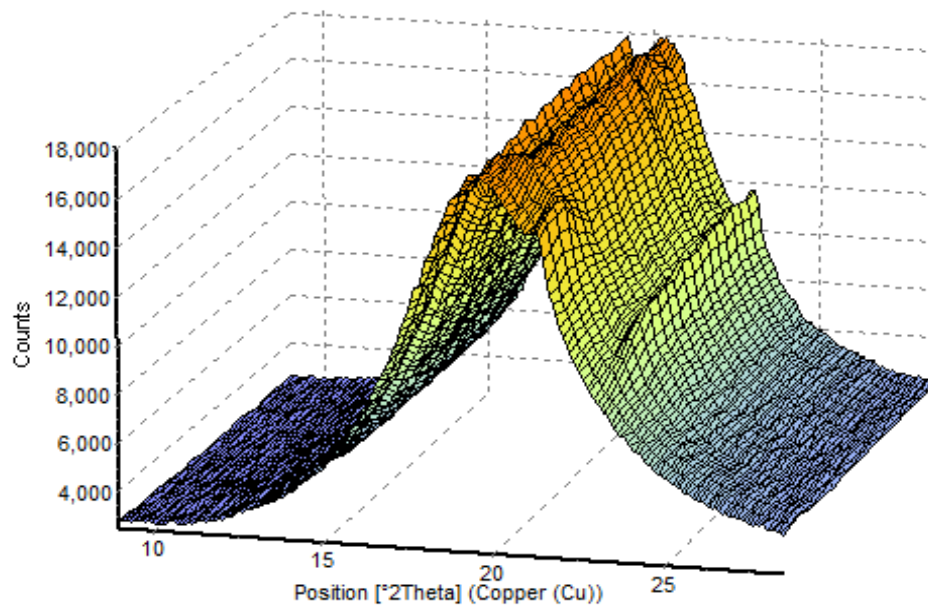


Figure A.42. 3D plots of X-ray diffraction pattern of of the isothermal crystallization after slow cooling (2°C/min) of the spring milk fat from 70 to 14°C

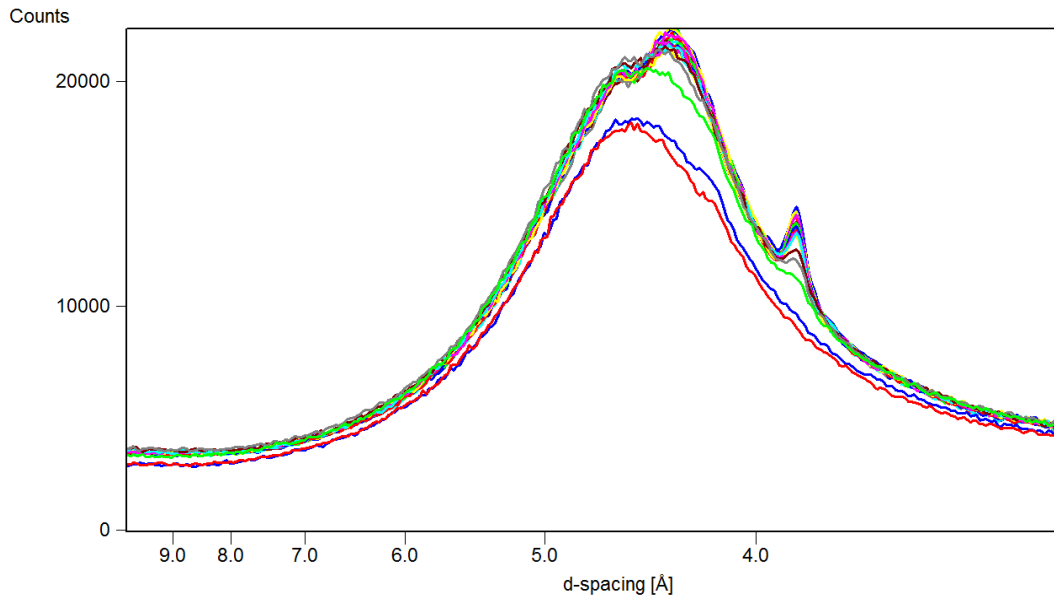


Figure A.43. Wide angle X-ray diffraction pattern of the isothermal crystallization after slow cooling (2°C/min) of the spring milk fat from 70 to 17°C

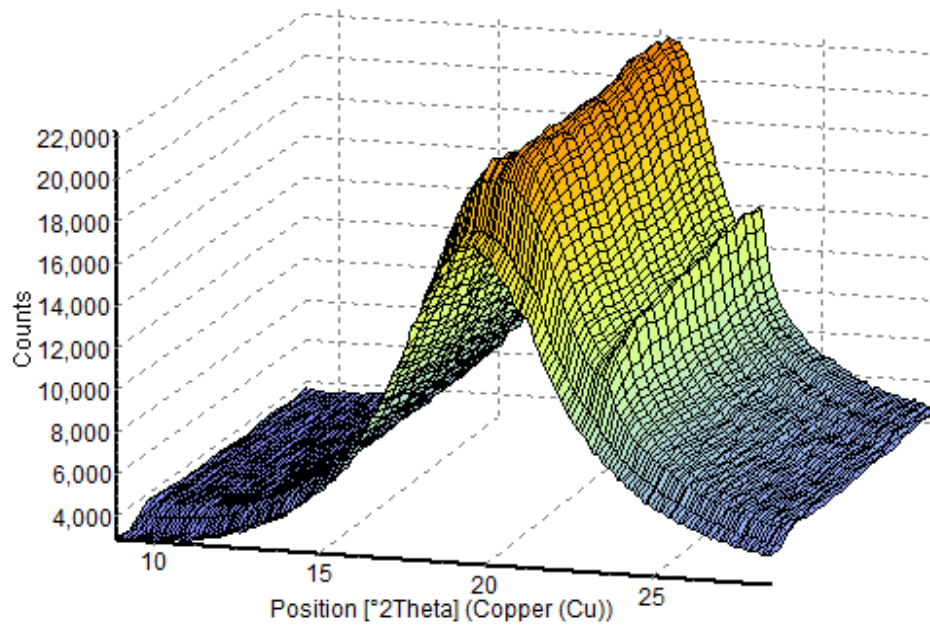


Figure A.44. 3D plots of X-ray diffraction pattern of of the isothermal crystallization after slow cooling (2°C/min) of the spring milk fat from 70 to 17°C

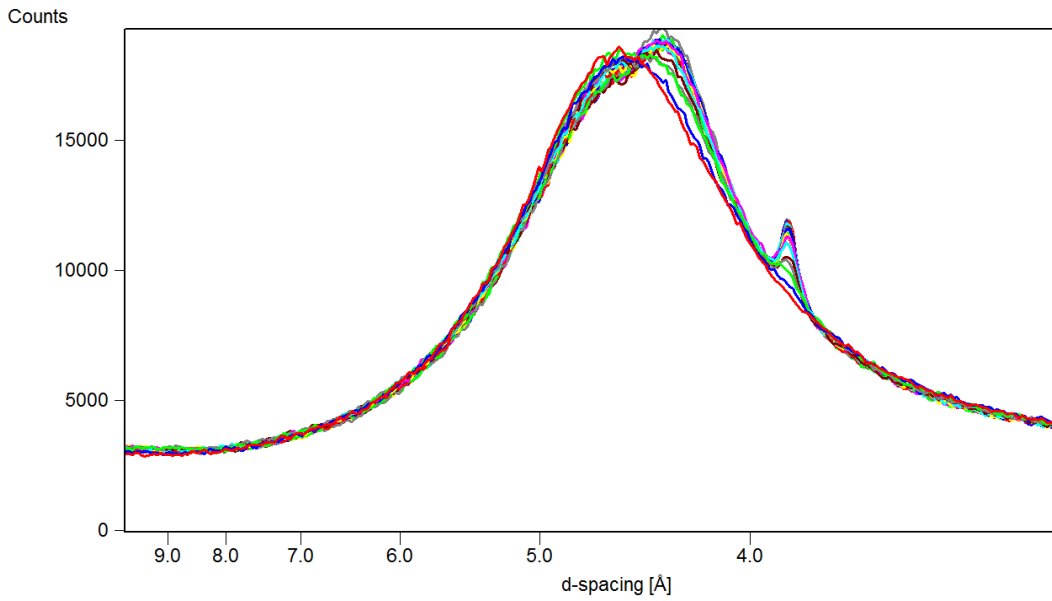


Figure A.45. Wide angle X-ray diffraction pattern of the isothermal crystallization after slow cooling (2°C/min) of the spring milk fat from 70 to 20°C

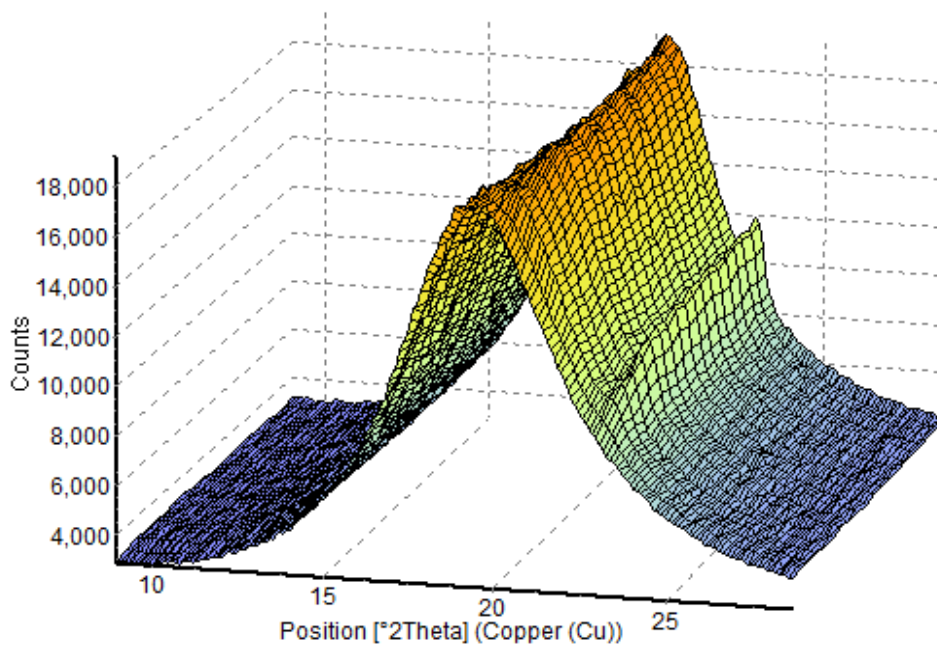


Figure A.46. 3D plots of X-ray diffraction pattern of of the isothermal crystallization after slow cooling (2°C/min) of the spring milk fat from 70 to 20°C

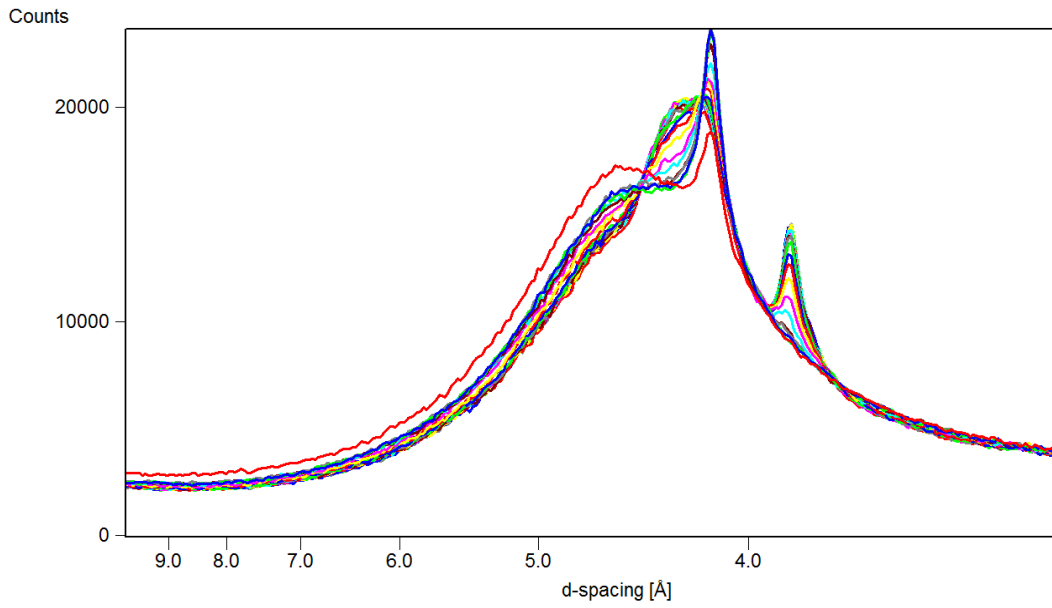


Figure A.47. Wide angle X-ray diffraction pattern of the isothermal crystallization after fast cooling (10°C/min) of the spring milk fat from 70 to 5°C

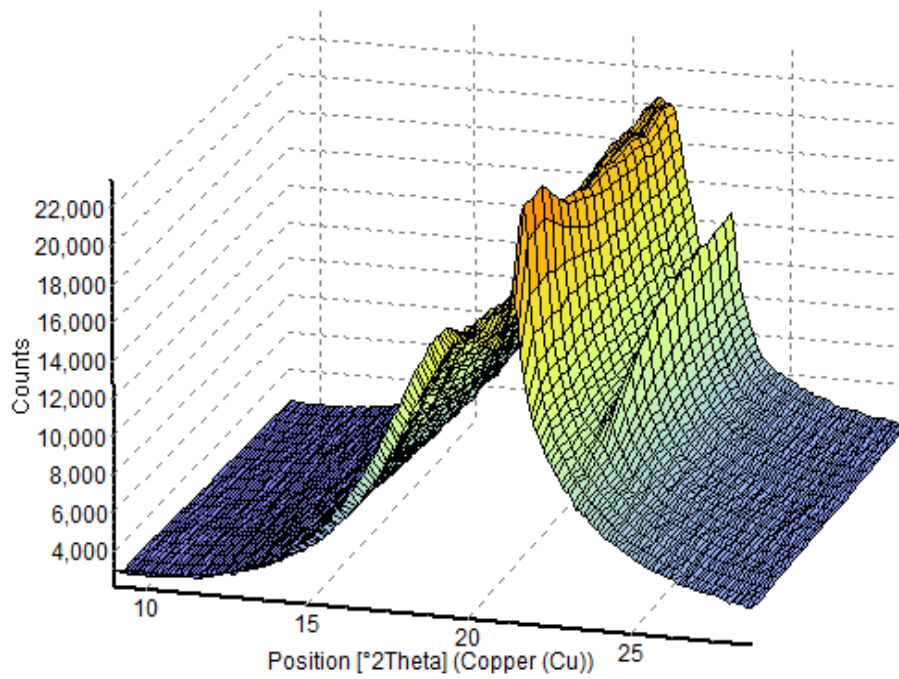


Figure A.48. 3D plots of X-ray diffraction pattern of of the isothermal crystallization after fast cooling (10°C/min) of the spring milk fat from 70 to 5°C

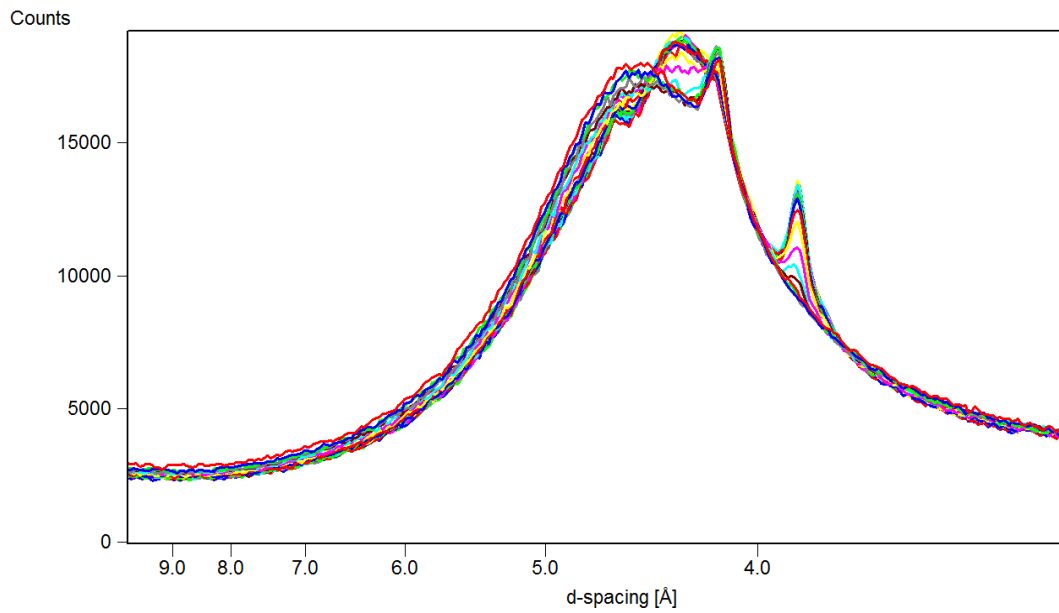


Figure A.49. Wide angle X-ray diffraction pattern of the isothermal crystallization after fast cooling (10°C/min) of the spring milk fat from 70 to 10°C

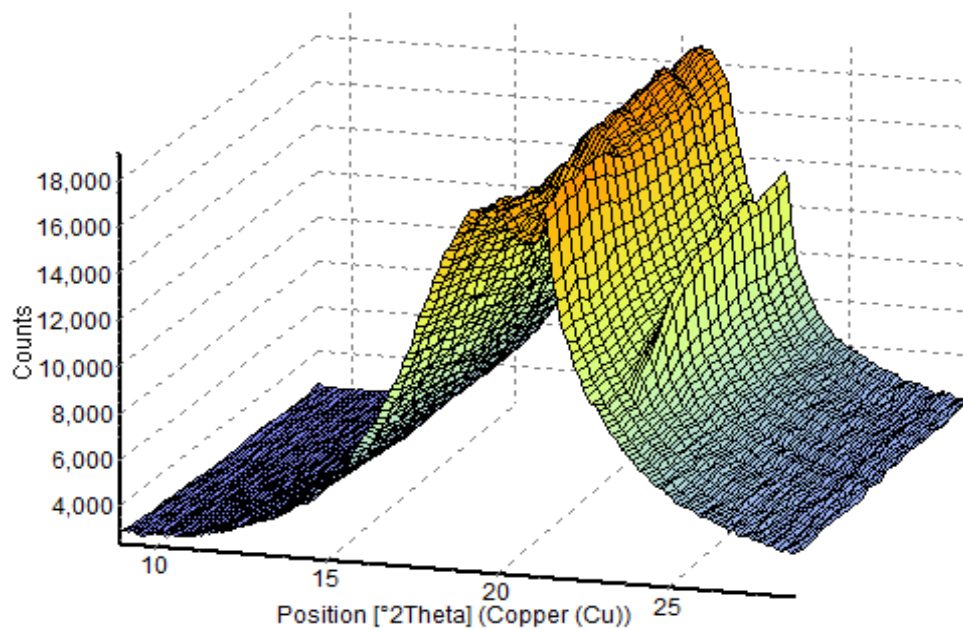


Figure A.50. 3D plots of X-ray diffraction pattern of of the isothermal crystallization after fast cooling (10°C/min) of the spring milk fat from 70 to 10°C

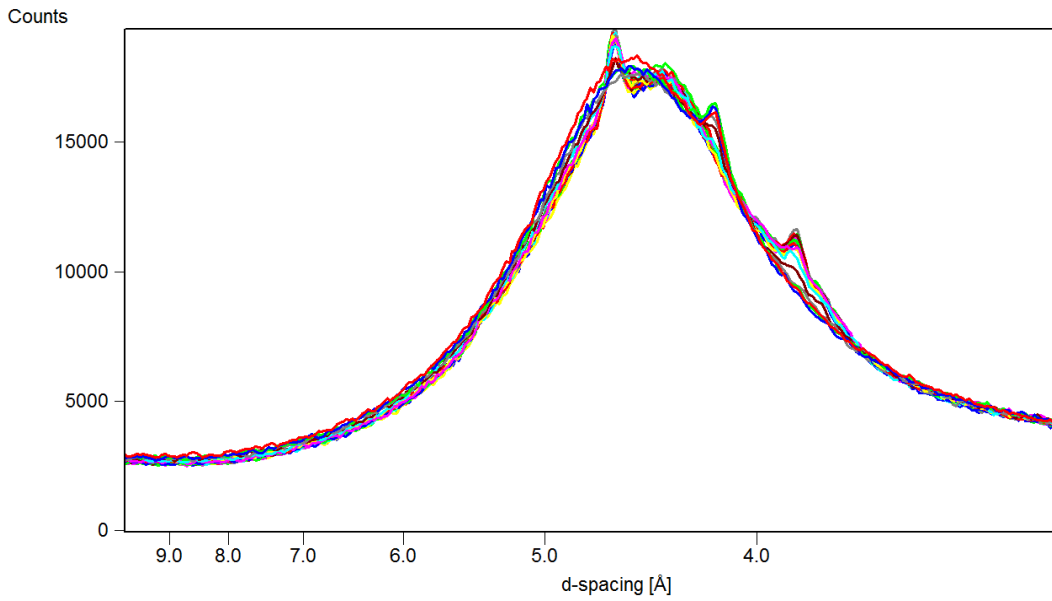


Figure A.51. Wide angle X-ray diffraction pattern of the isothermal crystallization after fast cooling (10°C/min) of the spring milk fat from 70 to 14°C

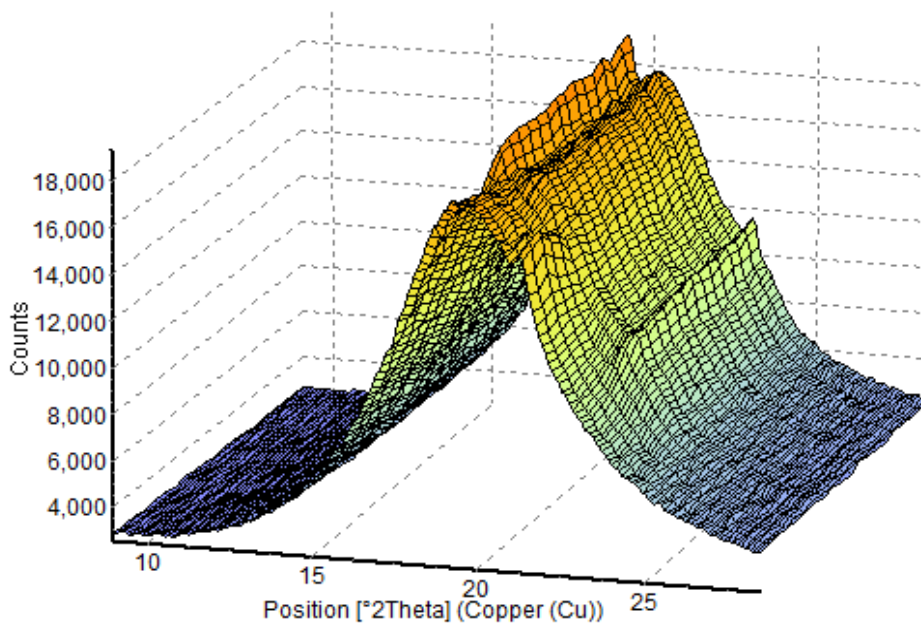


Figure A.52. 3D plots of X-ray diffraction pattern of of the isothermal crystallization after fast cooling (10°C/min) of the spring milk fat from 70 to 14°C

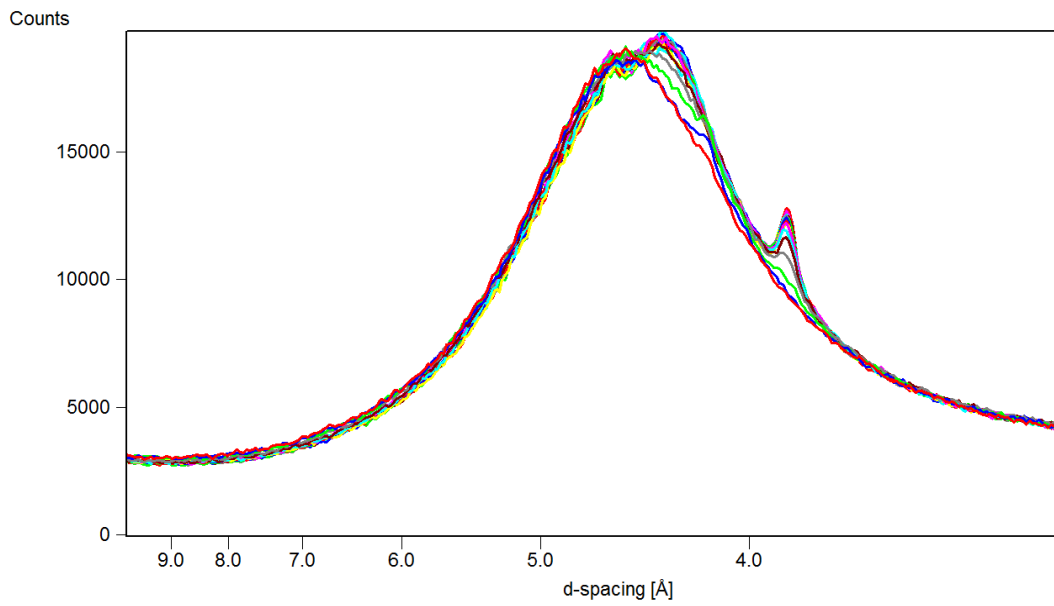


Figure A.53. Wide angle X-ray diffraction pattern of the isothermal crystallization after fast cooling (10°C/min) of the spring milk fat from 70 to 17°C

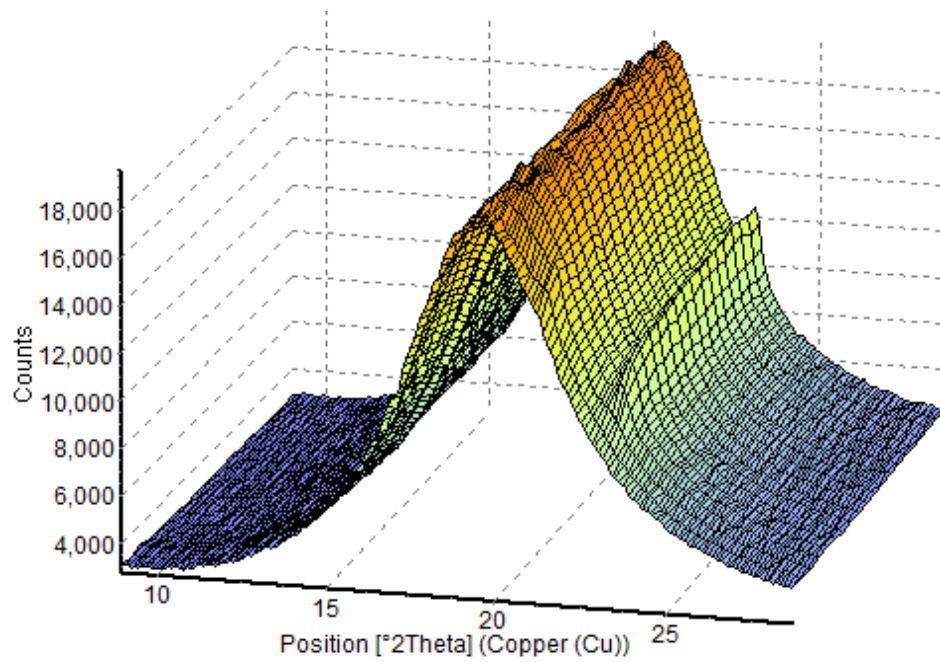


Figure A.54. 3D plots of X-ray diffraction pattern of of the isothermal crystallization after fast cooling (10°C/min) of the spring milk fat from 70 to 17°C

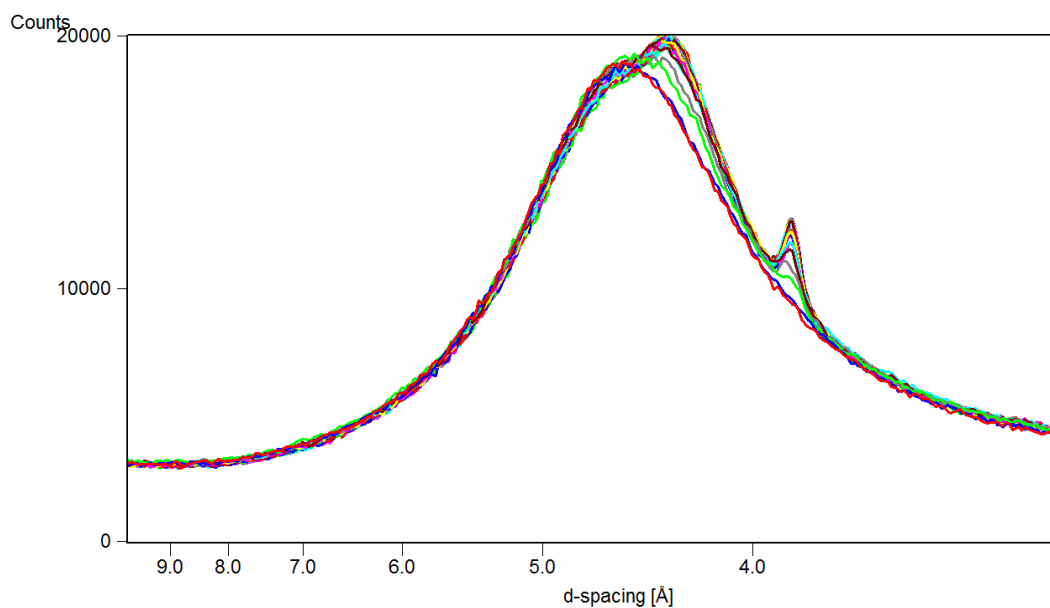


Figure A.55. Wide angle X-ray diffraction pattern of the isothermal crystallization after fast cooling (10°C/min) of the spring milk fat from 70 to 20°C

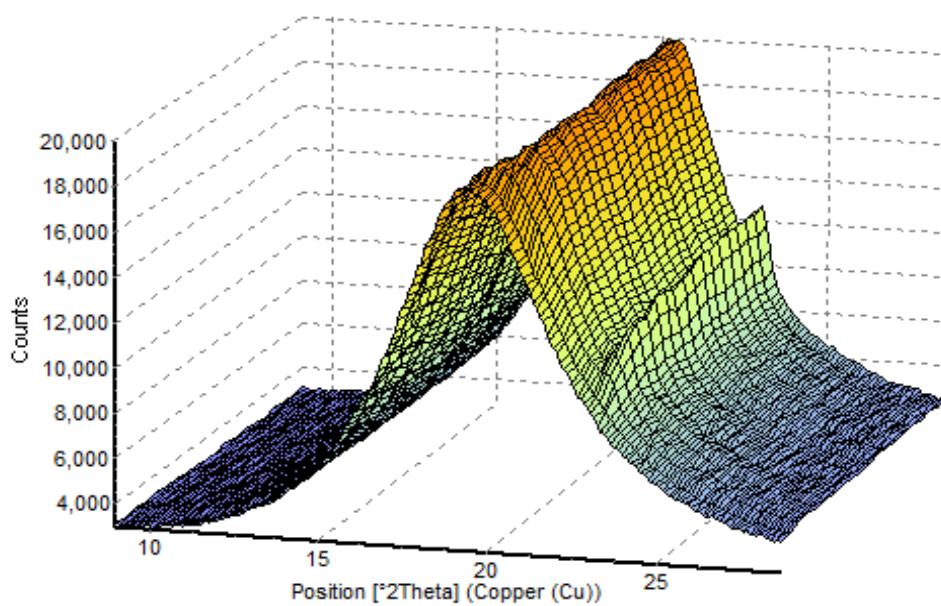


Figure A.56. 3D plots of X-ray diffraction pattern of of the isothermal crystallization after fast cooling (10°C/min) of the spring milk fat from 70 to 20°C

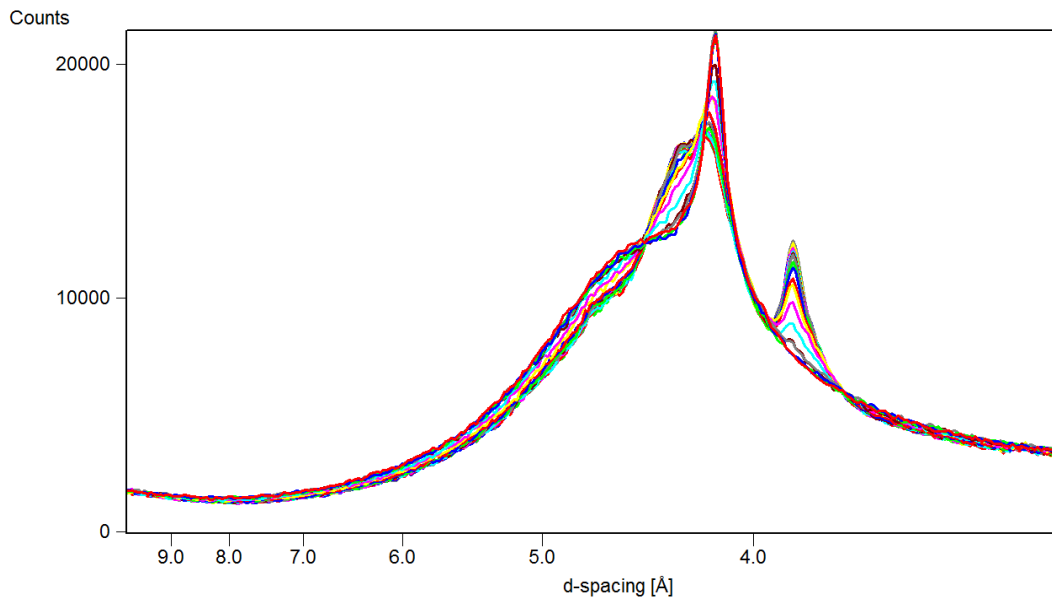


Figure A.57. Wide angle X-ray diffraction pattern of the isothermal crystallization after slow cooling (2°C/min) of the summer milk fat from 70 to 5°C

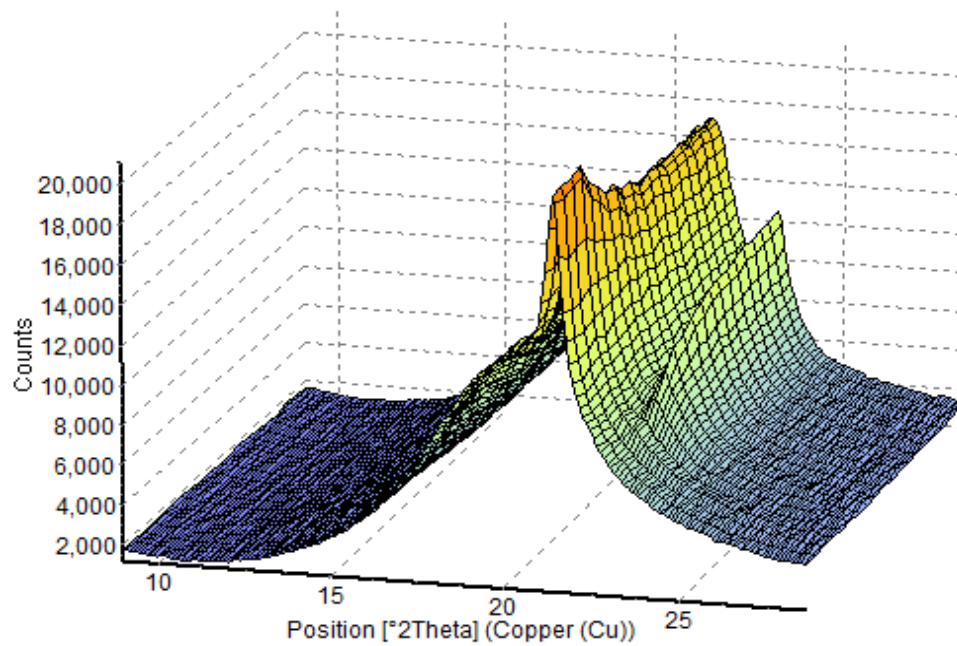


Figure A.58. 3D plots of X-ray diffraction pattern of of the isothermal crystallization after slow cooling (2°C/min) of the summer milk fat from 70 to 5°C

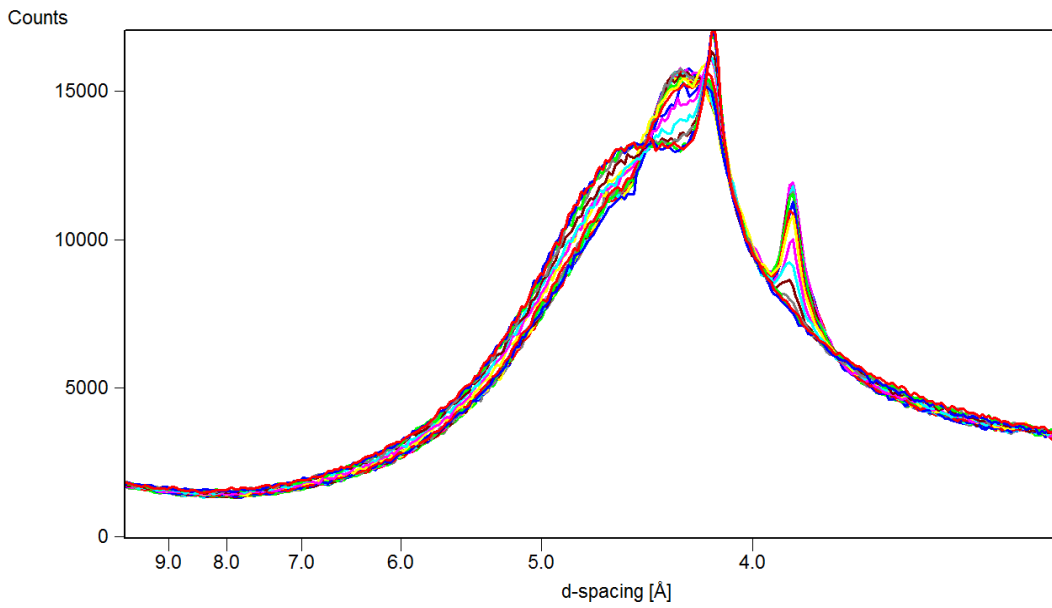


Figure A.59. Wide angle X-ray diffraction pattern of the isothermal crystallization after slow cooling (2°C/min) of the summer milk fat from 70 to 10°C

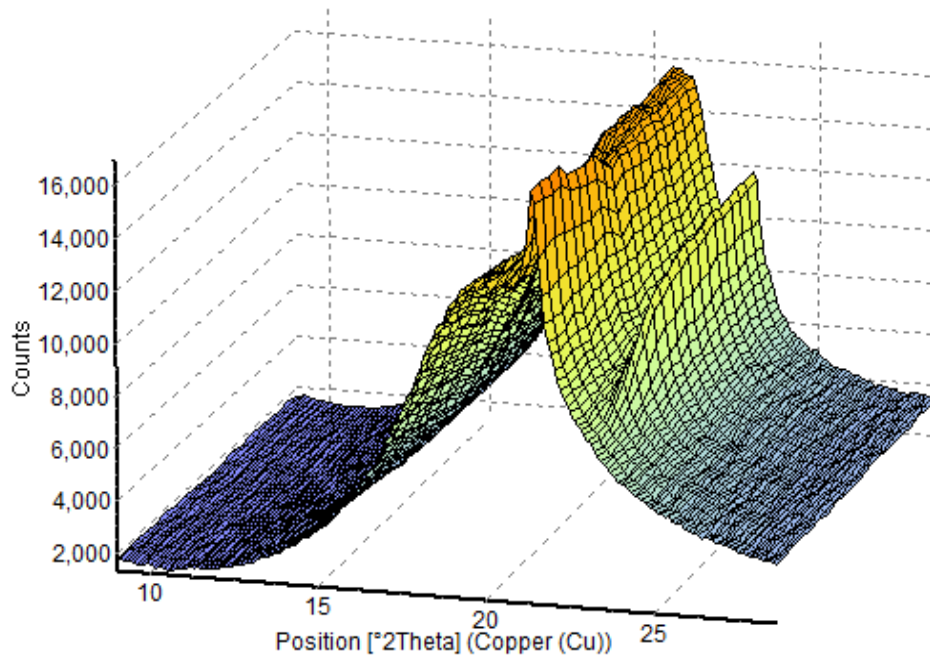


Figure A.60. 3D plots of X-ray diffraction pattern of of the isothermal crystallization after slow cooling (2°C/min) of the summer milk fat from 70 to 10°C

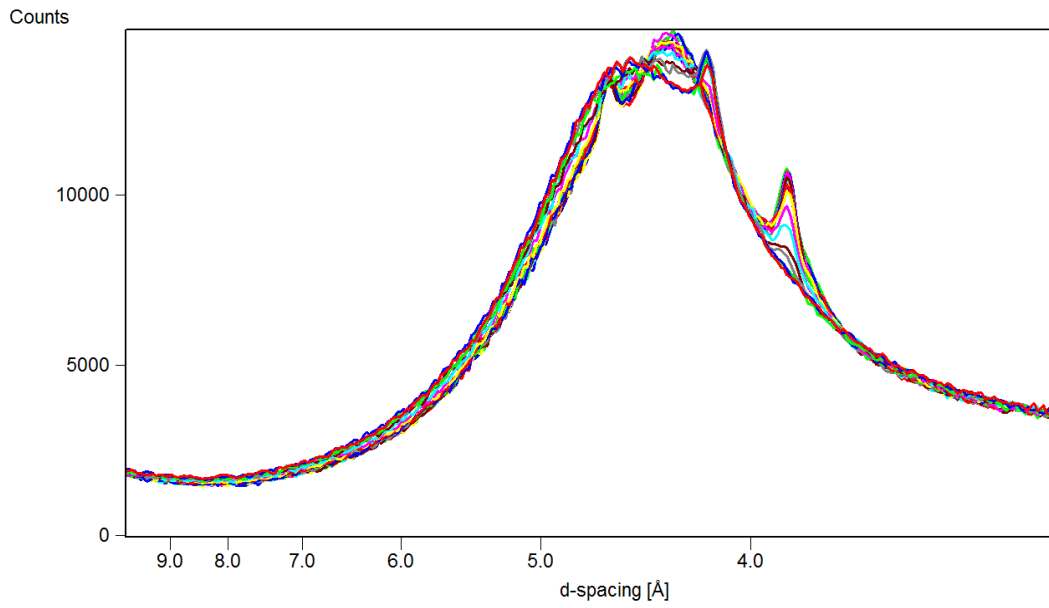


Figure A.61. Wide angle X-ray diffraction pattern of the isothermal crystallization after slow cooling (2°C/min) of the summer milk fat from 70 to 14°C

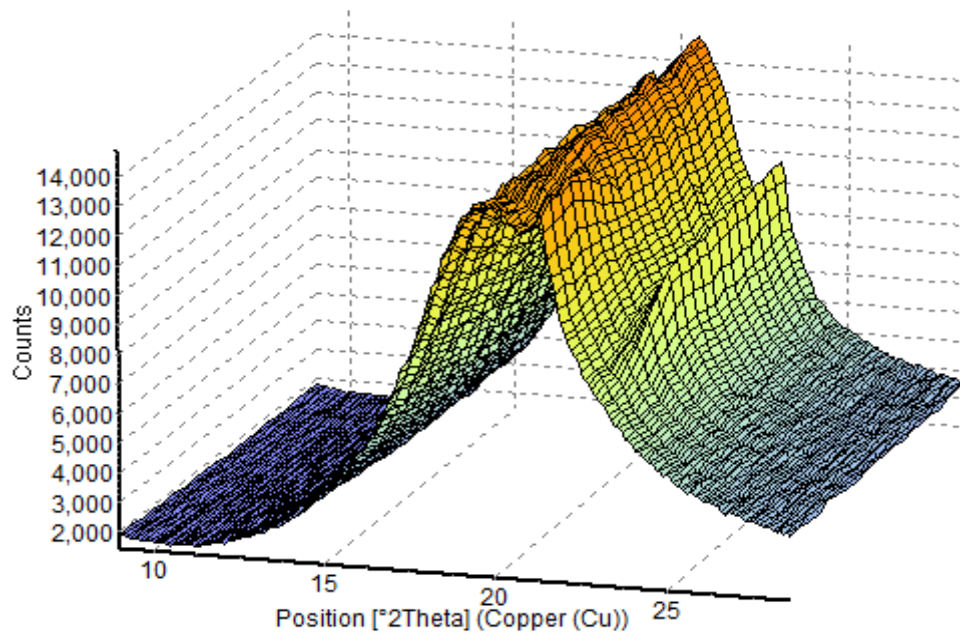


Figure A.62. 3D plots of X-ray diffraction pattern of of the isothermal crystallization after slow cooling (2°C/min) of the summer milk fat from 70 to 14°C

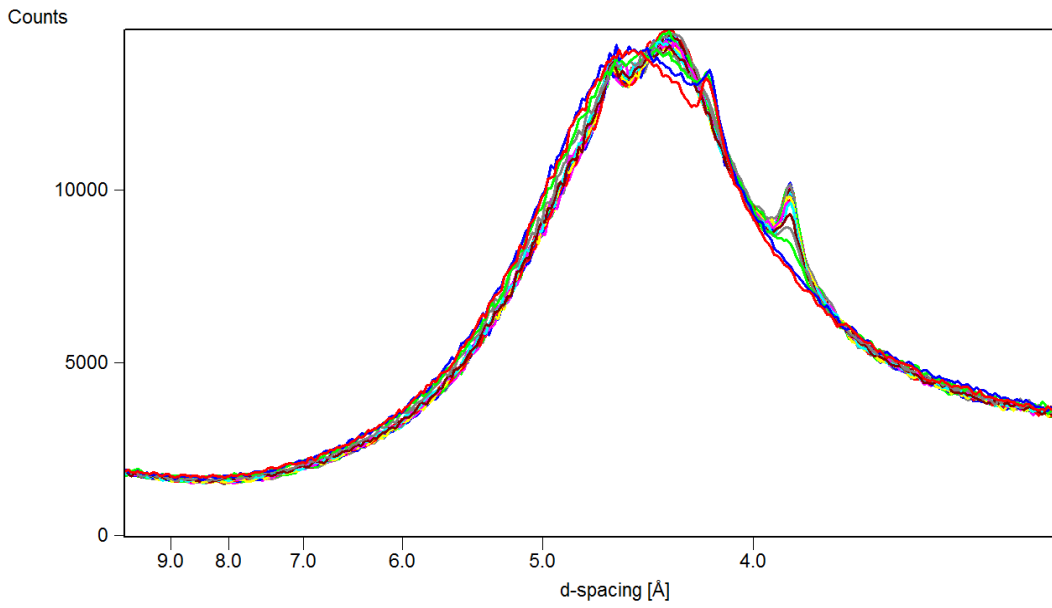


Figure A.63. Wide angle X-ray diffraction pattern of the isothermal crystallization after slow cooling (2°C/min) of the summer milk fat from 70 to 17°C

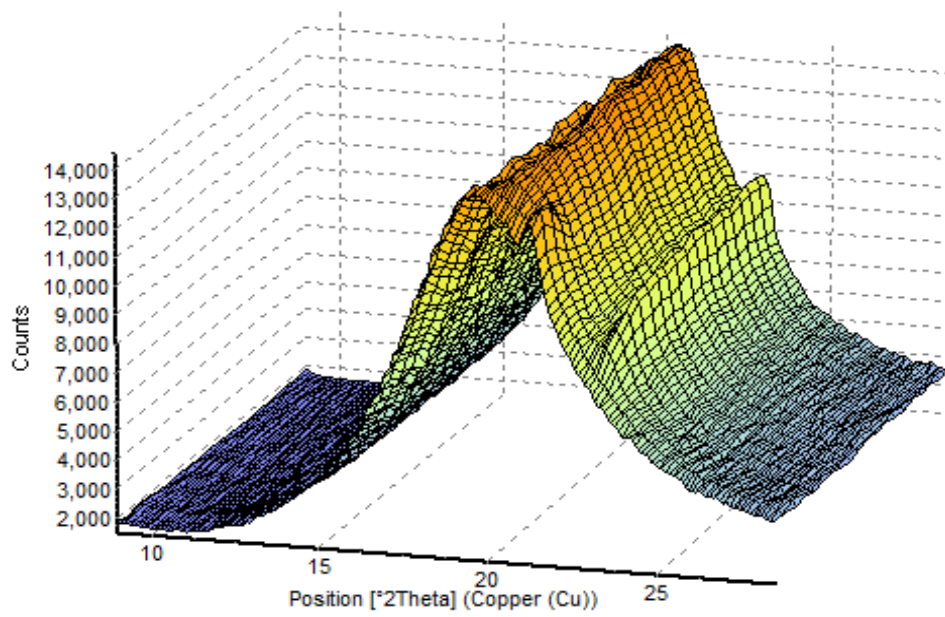


Figure A.64. 3D plots of X-ray diffraction pattern of of the isothermal crystallization after slow cooling (2°C/min) of the summer milk fat from 70 to 17°C

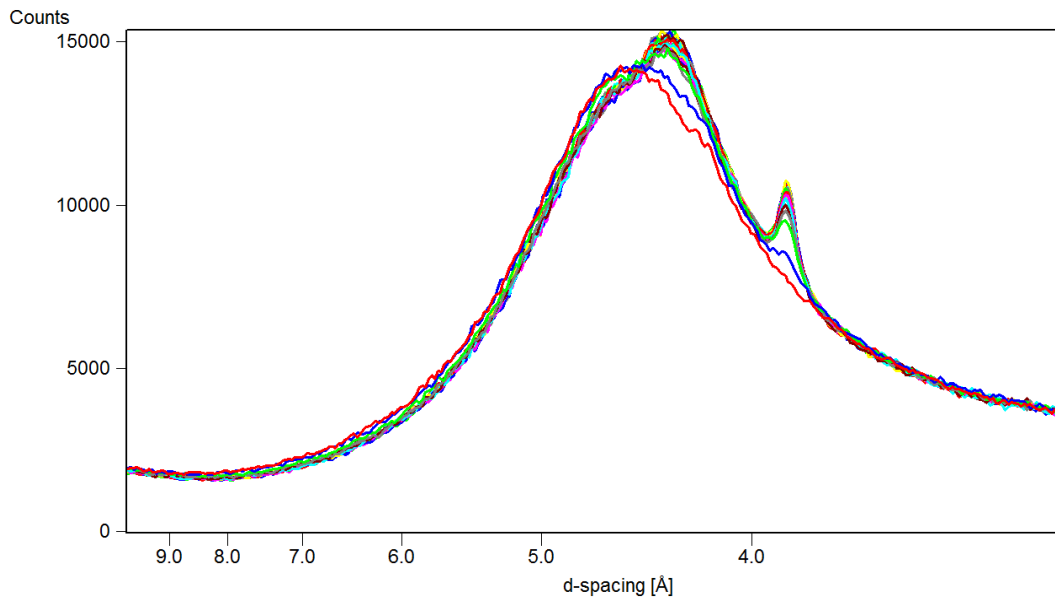


Figure A.65. Wide angle X-ray diffraction pattern of the isothermal crystallization after slow cooling (2°C/min) of the summer milk fat from 70 to 20°C

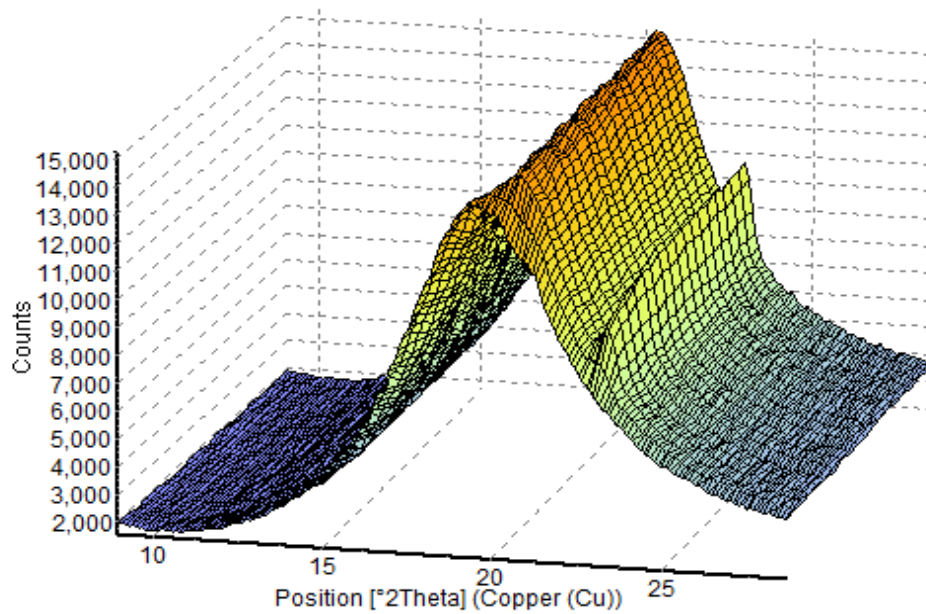


Figure A.66. 3D plots of X-ray diffraction pattern of of the isothermal crystallization after slow cooling (2°C/min) of the summer milk fat from 70 to 20°C

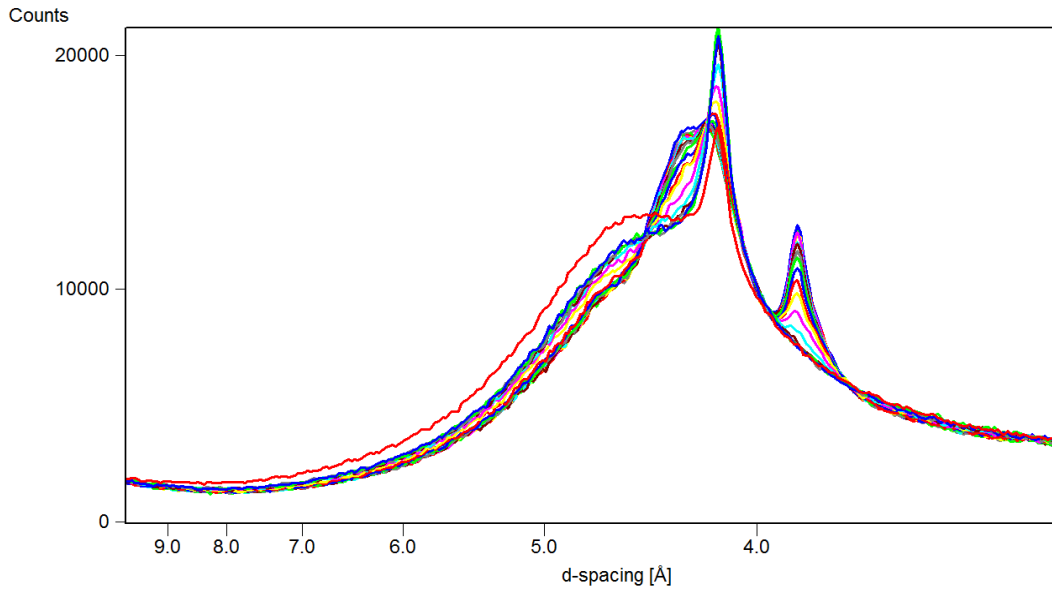


Figure A.67. Wide angle X-ray diffraction pattern of the isothermal crystallization after fast cooling (10°C/min) of the summer milk fat from 70 to 5°C

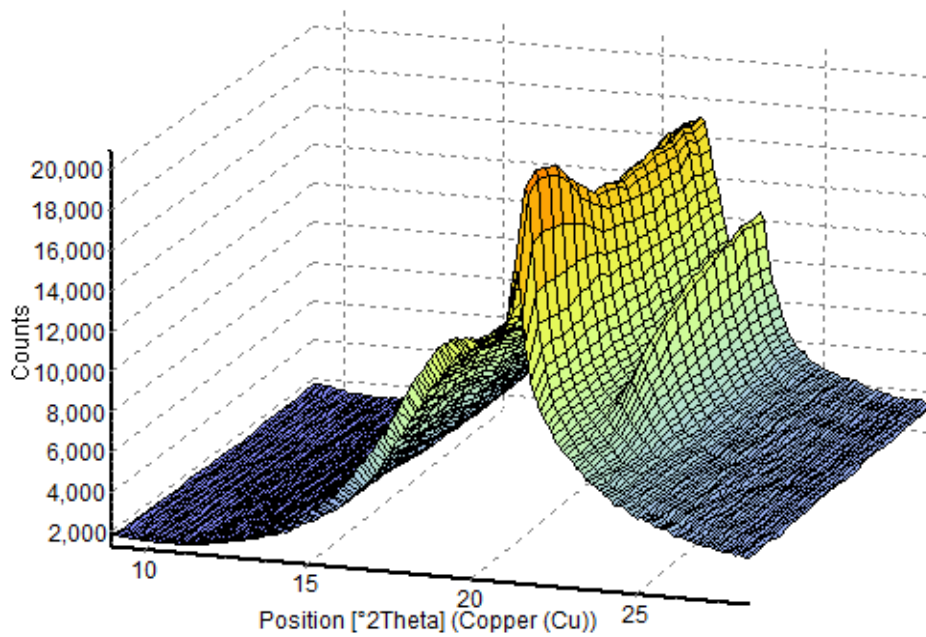


Figure A.68. 3D plots of X-ray diffraction pattern of of the isothermal crystallization after fast cooling (10°C/min) of the summer milk fat from 70 to 5°C

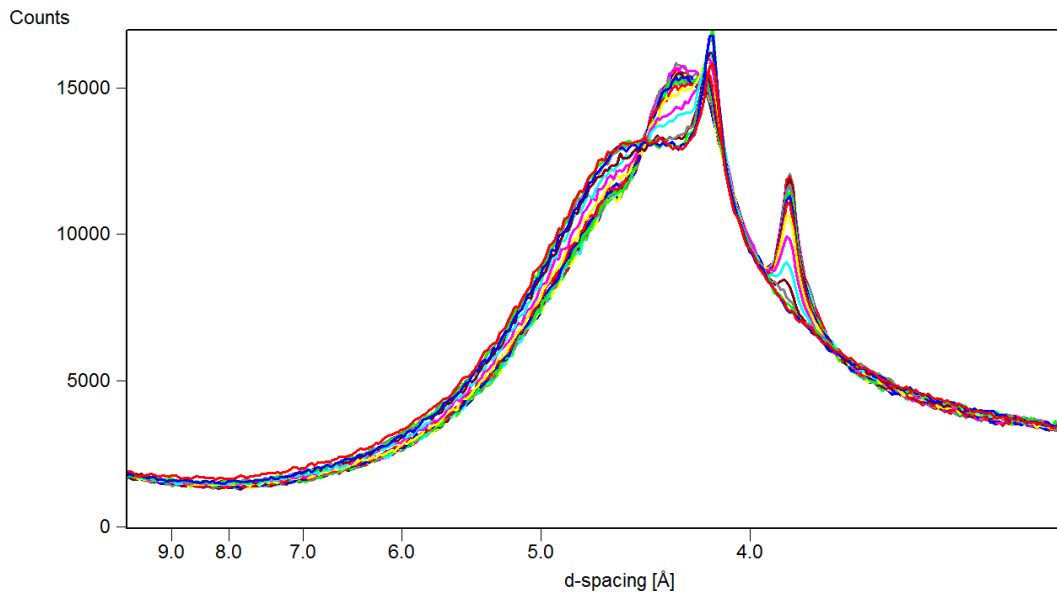


Figure A.69. Wide angle X-ray diffraction pattern of the isothermal crystallization after fast cooling ($10^{\circ}\text{C}/\text{min}$) of the summer milk fat from 70 to 10°C

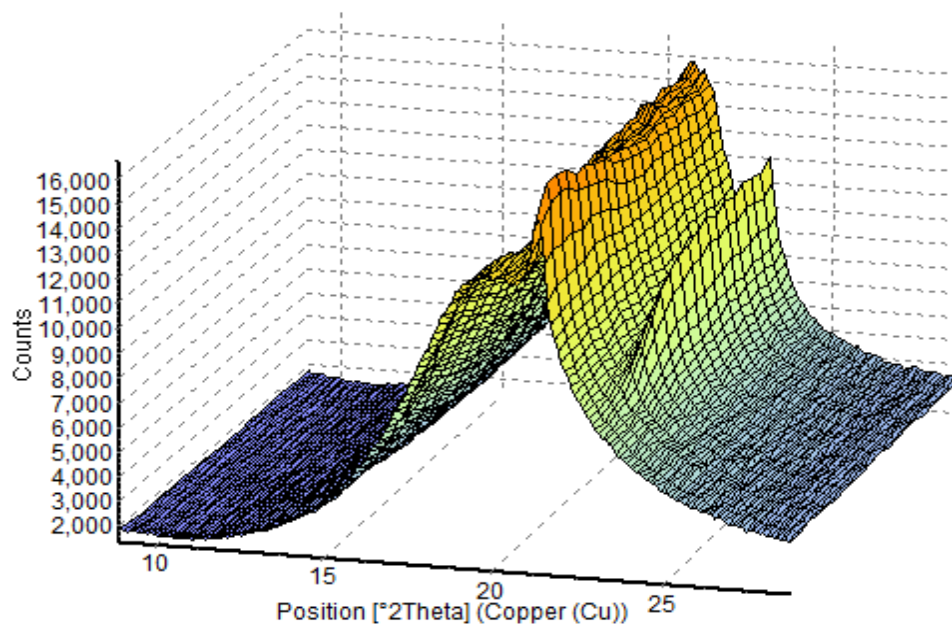


Figure A.70. 3D plots of X-ray diffraction pattern of of the isothermal crystallization after fast cooling ($10^{\circ}\text{C}/\text{min}$) of the summer milk fat from 70 to 10°C

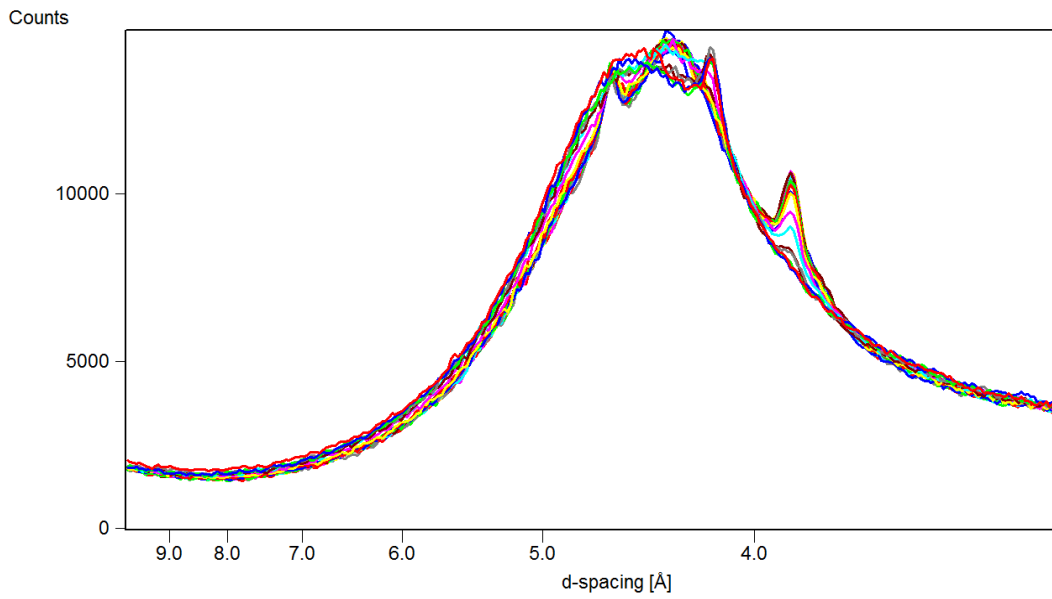


Figure A.71. Wide angle X-ray diffraction pattern of the isothermal crystallization after fast cooling (10°C/min) of the summer milk fat from 70 to 14°C

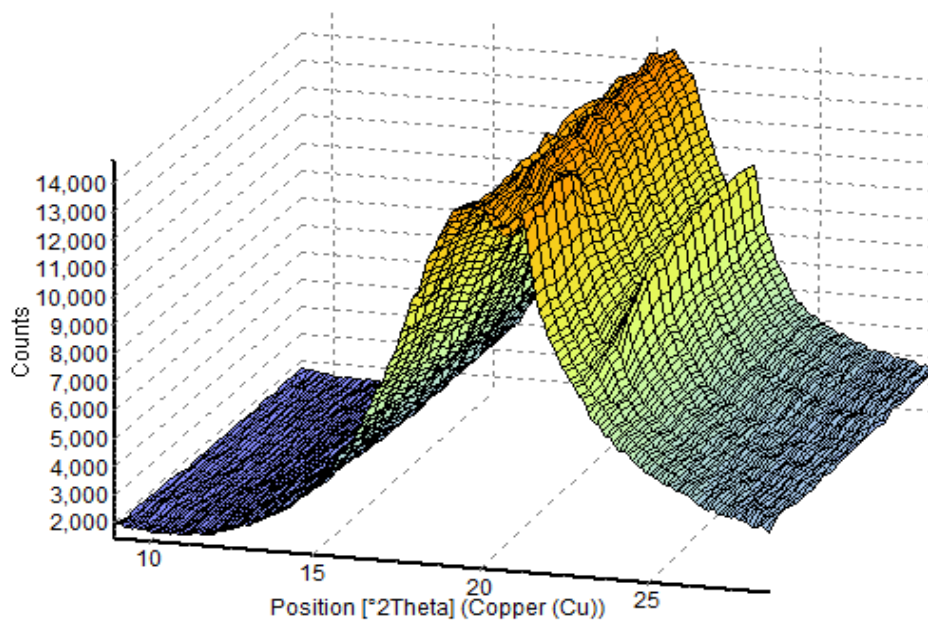


Figure A.72. 3D plots of X-ray diffraction pattern of of the isothermal crystallization after fast cooling (10°C/min) of the summer milk fat from 70 to 14°C

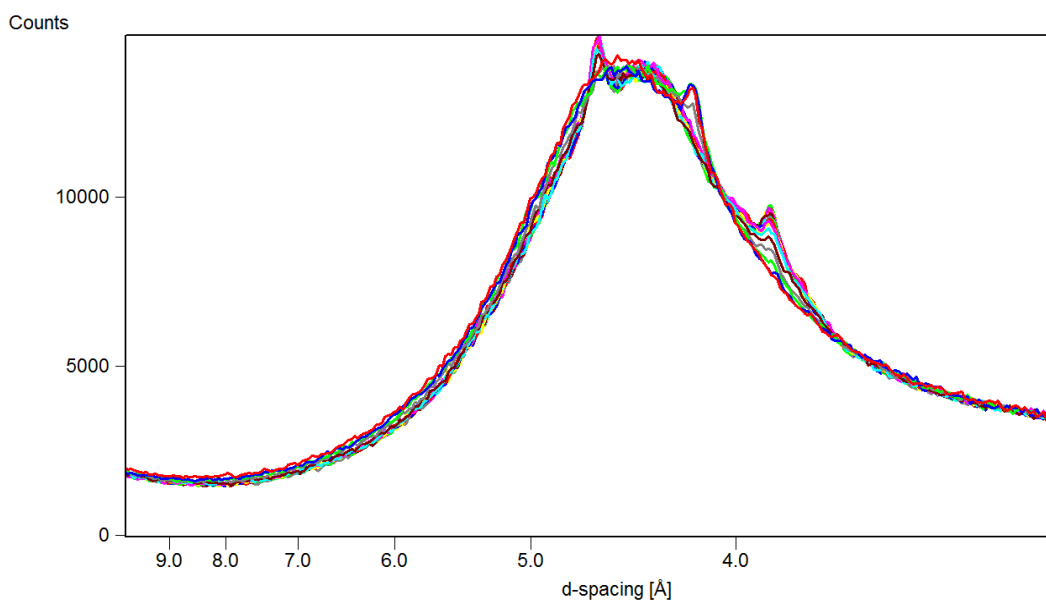


Figure A.73. Wide angle X-ray diffraction pattern of the isothermal crystallization after fast cooling ($10^{\circ}\text{C}/\text{min}$) of the summer milk fat from 70 to 17°C

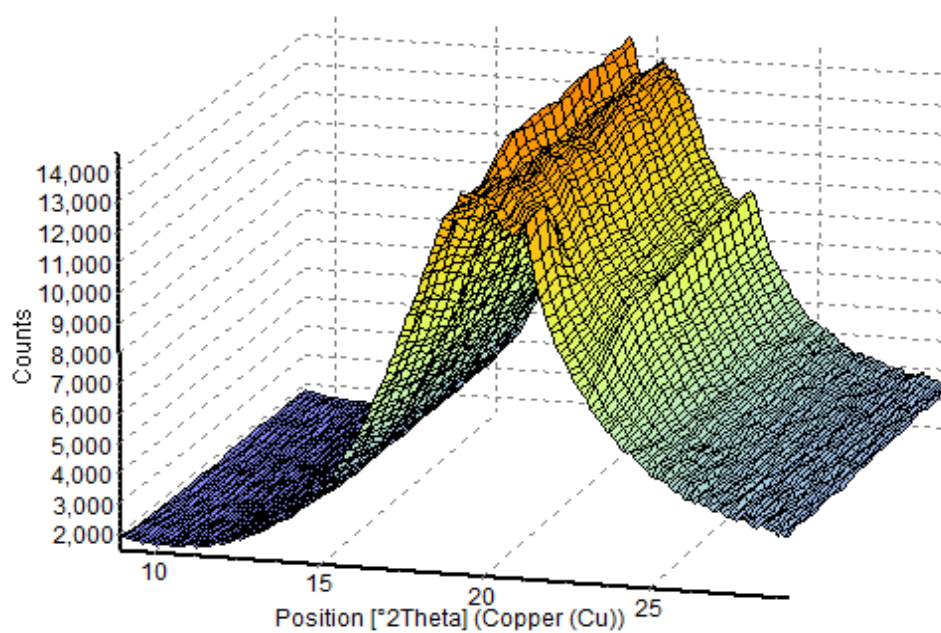


Figure A.74. 3D plots of X-ray diffraction pattern of of the isothermal crystallization after fast cooling ($10^{\circ}\text{C}/\text{min}$) of the summer milk fat from 70 to 17°C

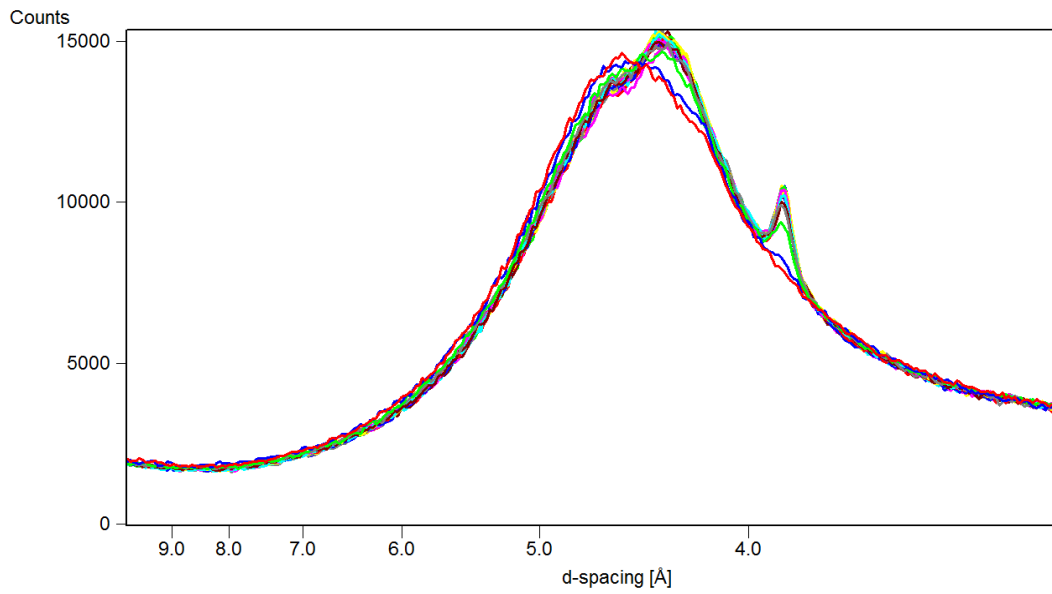


Figure A.75. Wide angle X-ray diffraction pattern of the isothermal crystallization after fast cooling (10°C/min) of the summer milk fat from 70 to 20°C

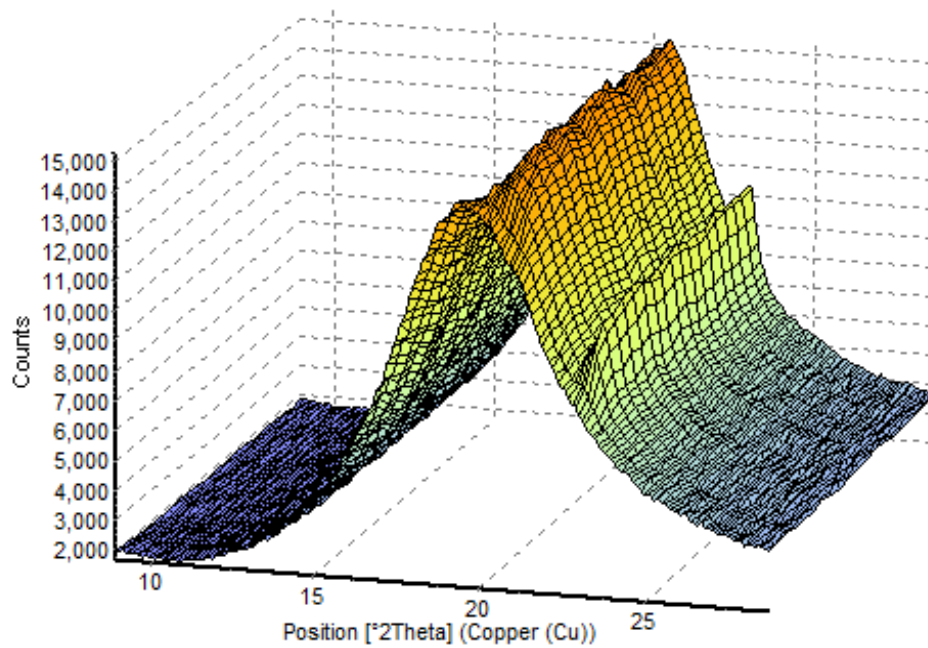


Figure A.76. 3D plots of X-ray diffraction pattern of of the isothermal crystallization after fast cooling (10°C/min) of the summer milk fat from 70 to 20°C

APPENDIX B

Table B.1. ANOVA results of myristic acid content of milk fat by seasons

Myristic acid	Sum of Squares	df	Mean Square	F	Sig.
Between Groups	13.815	3	4.605	43.158	0.002
Within Groups	0.427	4	0.107		
Total	14.242	7			

Table B.2. ANOVA results of palmitic acid content of milk fat by seasons

Palmitic acid	Sum of Squares	df	Mean Square	F	Sig.
Between Groups	64.855	3	21.618	1.081E3	0.000
Within Groups	0.080	4	0.020		
Total	64.935	7			

Table B.3. ANOVA results of stearic acid content of milk fat by seasons

Stearic acid	Sum of Squares	df	Mean Square	F	Sig.
Between Groups	15.895	3	5.298	264.917	0.000
Within Groups	0.080	4	0.020		
Total	15.975	7			

Table B.4. ANOVA results of oleic acid content of milk fat by seasons

Oleic acid	Sum of Squares	df	Mean Square	F	Sig.
Between Groups	57.200	3	19.067	953.333	0.000
Within Groups	0.080	4	0.020		
Total	57.280	7			

Table B.5. ANOVA results of L* value of milk fats by seasons

L*	Sum of Squares	df	Mean Square	F	Sig.
Between Groups	10.085	3	3.362	18.436	0.008
Within Groups	0.729	4	0.182		
Total	10.815	7			

Table B.6. ANOVA results of a* value of milk fats by seasons

a*	Sum of Squares	df	Mean Square	F	Sig.
Between Groups	1.060	3	0.353	15.516	0.011
Within Groups	0.091	4	0.023		
Total	1.151	7			

Table B.7. ANOVA results of b* value of milk fats by seasons

b*	Sum of Squares	df	Mean Square	F	Sig.
Between Groups	870.348	3	290.116	215.776	0.000
Within Groups	5.378	4	1.345		
Total	875.727	7			

Table B.8. ANOVA results of yellowness index of milk fats by seasons

Yellowness index	Sum of Squares	df	Mean Square	F	Sig.
Between Groups	2797.553	3	932.518	265.987	0.000
Within Groups	14.023	4	3.506		
Total	2811.577	7			

Table B.9. ANOVA results of activation energies of milk fats by seasons

Activation Energy	Sum of Squares	df	Mean Square	F	Sig.
Between Groups	1.236	3	0.412	0.785	0.535
Within Groups	4.200	8	0.525		
Total	5.437	11			